The Study of Friction Variation with Temperature in A Harmonic Drive System – Modeling and Control

Zhao Zhongyu

A Thesis
In The Department of
Mechanical and Industrial Engineering

Presented in Partial Fulfillment of the Requirements
For the Degree of Master of Applied Science at
Concordia University
Montreal, Quebec, Canada

August, 2006

Your file Votre référence
ISBN: 978-0-494-20770-3
Our file Notre référence
ISBN: 978-0-494-20770-3

Abstract

The Study of Friction Variation with Temperature in A Harmonic Drive System – Modeling and Control

Zhao Zhongyu

This thesis studies the effects of temperature in friction modeling for a harmonic drive. A mathematic model of how friction varies with temperature change is built based on the exponential friction model. The mathematic model is then used in building the nonlinear dynamic model of the harmonic drive. A Cascaded Fuzzy Model of friction with temperature is proposed so that the friction experienced in the harmonic drive can be modeled as a fuzzy combination of linear models at different operating temperature and velocity. The fuzzy model is then integrated to the dynamic model of the harmonic drive to build the fuzzy TS model which is used in the controller design.

The parameters in both mathematic model and the fuzzy model are estimated. The estimation is formed into an optimization problem of minimizing the quadratic cost function of estimation errors. Since the cost function is highly nonlinear, a new algorithm of Evolutionary Parallel Gradient Search is applied to help the search escaping from local minima.

The optimal controller for fuzzy TS system is proposed in the form of LMI based optimization with new constraints and applied to the harmonic drive. In simulation, the closed loop system shows the capability of accurately tracking large range of reference signals even when the temperature is changing, either continuously or drastically.

Acknowledgments

I would like to take this opportunity to thank my supervisor, Dr. Wen-Fang, Xie, for her help and support in the past two years. Without her patient supervision and guide, this research will never be done.

I would like to thank all my colleagues in our lab, especially to Ji Peng who built the test bed. It's a happy and fruitful year we work together.

I would like to express my deepest gratitude to my parents and my sister. For what they have ever done, thank is never enough.

Table of Contents

LIST OF FIGURES IX

LIST OF TABLES XI

NOMENCLATURE XII

1 INTRODUCTION 1

1.1 MOTIVATION 1

1.2 BACKGROUND AND PREVIOUS WORK 3

1.2.1 Harmonic Drive 3

1.2.2 Friction Modeling 6

1.2.3 Fuzzy Logic System and Fuzzy Modeling 8

1.2.4 Optimization – Gradient and Evolutionary 8

1.2.5 LMI Based Optimization and Controller Design 11

1.3 OVERVIEW OF THE THESIS 12

2 MATHEMATIC MODEL OF FRICTION VARIATION WITH TEMPERATURE 13

2.1 THE EXPONENTIAL FRICTION MODEL 13

2.2 FRICTION MODEL WITH TEMPERATURE 15

2.3 THE MATHEMATIC MODEL OF THE HARMONIC DRIVE 24

2.4 SUMMARY 25

3 CASCADED FUZZY MODEL OF FRICTION VARIATION WITH TEMPERATURE 26

3.1 THE CASCADED FUZZY FRICTION MODEL 26
3.1.1 Friction model under certain temperature (the second layer model) 27
3.1.2 Fuzzy model with temperature (the first layer model) 30
3.1.3 The Cascaded Fuzzy Friction Model 31
3.1.4 Remarks 32
3.2 THE FUZZY MODEL OF THE HARMONIC DRIVE 33
3.2.1 State space equations of the system 33
3.2.2 State space equations of the system with integrator 37
3.3 SUMMARY 38
4 ESTIMATION OF PARAMETERS IN THE MODELS 40
4.1 THE EVOLUTIONARY PARALLEL GRADIENT SEARCH (EPGS) 40
4.2 PARAMETERS ESTIMATION OF THE MATHEMATIC MODEL 45
4.3 ESTIMATION OF THE PARAMETERS IN THE FUZZY MODEL 48
4.3.1 Estimation using EPGS 48
4.3.2 Estimation with least square method 52
4.3.3 Analysis 56
4.4 SUMMARY 56
5 FUZZY OPTIMAL CONTROLLER DESIGN-LMI APPROACH 57
5.1 PROBLEM STATEMENT 57
5.2 THE OPTIMAL CONTROLLERS 59
5.3 CONSTRAINTS ON THE INPUT AND OUTPUT OF THE CONTROLLERS 64
5.4 REMARKS 69
5.5 SUMMARY 71

6 CONTROL OF THE HARMONIC DRIVE 72

6.1 CONTROLLER DESIGN 72

6.1.1 Controller without temperature information 73

6.1.2 Controller design with temperature information 73

6.2 SIMULATION RESULTS AND ANALYSIS OF STEP INPUT TRACKING 74

6.2.1 LMI Controller without using temperature information 75

6.2.2 LMI Controller using the temperature information 77

6.2.3 LMI Controller with integrator and without using temperature information 80

6.2.4 LMI Controller with integrator and using the temperature information 82

6.2.5 PID Controller 84

6.2.6 Analysis of the Results 86

6.3 SIMULATION RESULTS AND ANALYSIS OF TEMPERATURE CHANGE 90

6.3.1 LMI Controller without Using Temperature Information 90

6.3.2 LMI Controller using Temperature Information 93

6.3.3 Analysis 95

6.4 SUMMARY 95

7 CONCLUSION AND FUTURE WORK 97

7.1 CONCLUSIONS 97

7.2 RECOMMENDATIONS FOR FUTURE WORK 99

REFERENCE: 101

APPENDIX A: SPECIFICATION OF THE HARMONIC DRIVE 112

APPENDIX B: OPTIMIZATION – GRADIENT SEARCH AND EA 115

B.1 GRADIENT BASED SEARCH 115

B.2 EVOLUTIONARY ALGORITHMS 116

APPENDIX C: LINEAR MATRIX INEQUALITIES (LMI) 118

List of Figures

FIGURE 1: THE HARMONIC DRIVE SYSTEM 3

FIGURE 2: THE HARMONIC DRIVE SYSTEM [80] 4

FIGURE 3: OPERATION PRINCIPLE [79] 5

FIGURE 4: FRICTION VS. VELOCITY 15

FIGURE 5: FRICTION CHANGED WITH TEMPERATURE 18

FIGURE 6: PARAMETERS VARYING WITH TEMPERATURE 23

FIGURE 7: STRUCTURE OF THE CASCADED FRICTION MODEL 32

FIGURE 8: ESTIMATION RESULTS OF THE MATHEMATIC MODEL 47

FIGURE 9: MEMBERSHIP FUNCTIONS WITH ESTIMATED PARAMETERS 50

FIGURE 10: ESTIMATION RESULTS OF PARAMETERS (FUZZY MODEL WITH EGPS) 51

FIGURE 11: MEMBERSHIP OF THE FIRST LAYER MODEL (LS) 53

FIGURE 12: ESTIMATION RESULTS OF PARAMETERS (FUZZY MODEL WITH LS) 55

FIGURE 13: CLOSED LOOP SYSTEM – CONTROLLER WITHOUT TEMPERATURE 73

FIGURE 14: CLOSED LOOP SYSTEM – CONTROLLER WITH TEMPERATURE 74

FIGURE 15: SIMULATION RESULTS – LMI CONTROLLER WITHOUT INTEGRATOR AND TEMPERATURE 77

FIGURE 16: SIMULATION RESULTS – LMI CONTROLLER WITHOUT INTEGRATOR BUT WITH TEMPERATURE 79

FIGURE 17: SIMULATION RESULTS – LMI CONTROLLER WITH INTEGRATOR BUT WITHOUT TEMPERATURE 81

FIGURE 18: SIMULATION RESULTS - LMI CONTROLLER WITH INTEGRATOR AND TEMPERATURE 83

FIGURE 19: SIMULATION RESULTS - PID CONTROLLER 86

FIGURE 20: SIMULATION RESULTS (WITH TEMPERATURE STEP CHANGING) – LMI CONTROLLER WITH INTEGRATOR BUT WITHOUT TEMPERATURE..... 92

FIGURE 21: SIMULATION RESULTS (WITH TEMPERATURE STEP CHANGING) – LMI CONTROLLER WITH INTEGRATOR AND TEMPERATURE..... 94

List of Tables

TABLE 1: FRICTION AT DIFFERENT VELOCITIES AND TEMPERATURES 19

TABLE 2: PARAMETERS VARYING WITH TEMPERATURE 21

TABLE 3: ESTIMATED PARAMETERS IN THE MATHEMATIC MODEL 45

TABLE 4: ESTIMATED PARAMETERS OF FUZZY MODEL 49

TABLE 5: ESTIMATED PARAMETERS – LOW SPEED END 52

TABLE 6: PARAMETERS OF THE MEMBERSHIP FUNCTION (LS) 52

TABLE 7: ESTIMATED PARAMETERS USING LS 54

TABLE 8: PERFORMANCE INDEX 1 – STEP REFERENCE 88

TABLE 9: PERFORMANCE INDEX 2 – STEP REFERENCE 88

TABLE 10: PERFORMANCE INDEX 1 – CONSTANT REFERENCE 95

TABLE 11: PERFORMANCE INDEX 2 – CONSTANT REFERENCE 95

Nomenclature

F_r	Friction
F_S	Static friction
F_E	Driving force (torque) to the system
v	Velocity
F_C	Coulombs friction
v_s	Stribeck velocity
ω	Velocity (rotary)
ω_s	Stribeck Velocity (rotary)
J	Inertial
B_m	Damping
T_m	Mechanical Torque
∇	Gradient operator
I	Identity Matrix
$\hat{}$	Estimation operator

1 Introduction

1.1 Motivation

Friction is the resistance force to the motion during sliding or rolling. It is directly opposite to the direction of motion and tangent to the contact surfaces [1][2]. Friction exists in all mechanical systems. Although sometime it is desirable to have high friction as in braking and coupling where friction is applied as driving force; in most cases, the existence of friction will deteriorate the performance of mechanical system. Friction may cause energy loss and lead to tracking errors, limit circle, stick-slip and dead band [3][4]. These undesirable effects of friction have to be compensated to meet the increasing requirement of high accuracy and high precision control in mechanical system, especially when the system has to be operated at low velocity near zero. In an application with such a requirement, the technique of model based friction compensation can be applied to counterbalance the effect of friction in a way that a counter force of same magnitude (but in opposite direction) is fed forward to the system. Since the counter force is calculated using the model of friction, the accuracy of the model is of key importance in the success of this technique.

In the research of control engineering, the models of friction are normally taken as function of only mechanical displacement and velocity. Although this kind of modeling has a lot of successful applications [6-20], the phenomenon of friction is much more complicated to be understood thoroughly. The magnitude of friction depends on a lot of other conditions such as the asperity of the contact surface, the normal force, the material, the lubricant condition [2]. Most importantly, when all other conditions are fixed after

manufactured, temperature becomes one of the significant conditions that may change the value of friction.

To the author's knowledge, the temperature effects have seldom been studied in the context of control engineering. In the modeling of friction, most researchers treat the temperature as a constant and ignore the friction change introduced by the temperature variation. This is a reasonable assumption when the machine operates in certain temperature. With the requirement of machine to operate in a larger range of temperature, this kind of assumption will lead to the loss of accuracy in the model of friction and also lead to the performance deterioration for the mechanical system.

In this thesis, we will study the effect of temperature in friction modeling for a harmonic drive system. The study will start from the nonlinear mathematic model of how friction changes with temperature and then continue with the fuzzy friction model that can be taken as the local linearization of the nonlinear model. The mathematic model will be integrated with the dynamic model of a harmonic drive to simulate the plant in the simulation. The fuzzy TS model of the harmonic drive will be established to describe the plant behavior varied with temperature. The parameters in both models are then estimated using the proposed optimization algorithm- Evolutionary Parallel Gradient Search (EPGS). In the controller design part, new constraints of LMI based optimal controller for fuzzy system are proposed to deal with the control problem in a harmonic drive with friction. In the thesis, we build a framework to deal with the control problem of a system with friction: modeling, parameter estimation and controller design.

1.2 Background and Previous Work

The related background knowledge and previous related works are introduced in this section including friction modeling, fuzzy logic system, gradient and evolutionary optimization and LMI based controller design.

1.2.1 Harmonic Drive

The harmonic drive gearing is invented by C. Walton Musser in the mid-1950s [81]. Because of their compact size and high reduction ratio, harmonic drives are often favored for electrometrical system with space and weight constraints such as robot system. With the advantages of zero backlash, high accuracy, fast response time and high vacuum compatibility, the harmonic drive is also widely used in medical equipment and high accuracy machine. The harmonic drive system in our research is an integral package consisting of an encoder, a DC servo motor and a precision harmonic drive gearhead as shown in following figure:

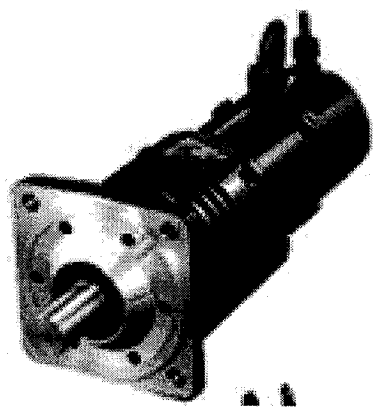

Figure 1: the Harmonic Drive System

Since the encoder and the DC motor are common to the mechatronic system, the special advantage of the harmonic drive system comes from the harmonic drive gearhead

(also called harmonic drive gearing box). The mechanism of the gearing box is comprised of three components: Wave Generator, Flexspline, and Circular Spline as shown in figure 2.

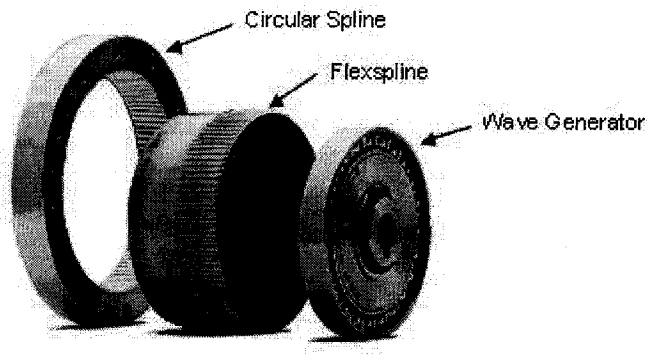

Figure 2: the Harmonic Drive System [80]

The Wave Generator is actually an assembly of a bearing and a steel disk which is called a Wave Generator plug. The outer surface of the Wave Generator plug has an elliptical shape that is carefully machined to a precise specification. A specially designed ball bearing is pressed around this bearing plug causing this bearing to conform to the same elliptical shape of the Wave Generator plug. The Wave Generator is typically used as the input which is attached to the servo motor in our sysetem.

The Flexspline is a thin-walled steel cup. This geometry allows the walls of the cup to be radially compliant, yet remain torsionally stiff since the cup has a large diameter. Gear teeth are machined into the outer surface near the open end of the cup. The cup has a rigid boss at one end to provide a rugged mounting surface. During assembly, the Wave Generator is inserted inside the Flexspline such that the bearing is at the same axial location as the Flexspline teeth. The Flexspline wall near the brim of the cup conforms to the same elliptical shape of the bearing. This causes the teeth on the outer surface of the Flexspline to also conform to this elliptical shape. Effectively, the

Flexspline now has an elliptical gear pitch diameter on its outer surface. The Flexspline is usually the output of the mechanism which is mounted with the output shaft in our system.

The Circular Spline is a rigid circular steel ring with teeth on the inside diameter. The Circular Spline is usually attached to the housing and does not rotate. The Circular Spline is located such that its teeth mesh with those of the Flexspline. The tooth pattern of the Flexspline (which is now elliptical -as a result of conforming to the Wave Generator's elliptical shape) engages the tooth profile of the Circular Spline (circular) along the major axis of the ellipse. This engagement is like an ellipse inscribed concentrically within a circle. Mathematically, an inscribed ellipse will contact a circle at two points. However, the gear teeth have a finite height. So there are actually two regions (instead of two points) of tooth engagement.

The principle of the gearing reduction is illustrated in figure 3 with the descriptions.

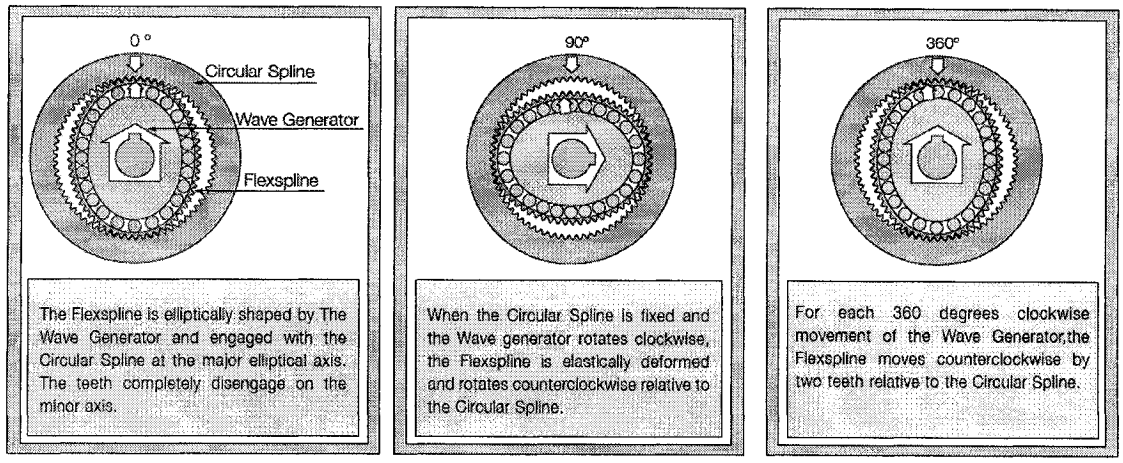

Figure 3: Operation principle [79]

With all the aforementioned advantages, the harmonic drive system is also known to suffer from friction problem. This thesis studies the effect of friction changing over temperature in a harmonic drive system and the results are used in the high precision control of the harmonic drive. The details on harmonic drive are found [17][19][82][83]. The specification of the harmonic drive in our research is in [79][80] (A simple specification is listed in Appendix A).

1.2.2 Friction Modeling

Friction is the tangential force between two contact surfaces. The value of this force depends on many conditions such as contact asperities, normal load, lubrication, sliding velocity, temperature and others. This complication makes it impossible to have an exact mathematical model of friction that covers all aspects. In control engineering, however, an approximation model can be built based on the measurable and observable kinetics variables, such as position and velocity. The reason for this kind of approximation is that the objective of friction modeling in control context is to predict and compensate friction with the knowledge of these variables.

In survey paper [3], the author enumerated the mathematic models available in the control engineering for friction compensation. In the class of static model, the author introduced constant model, linear model, exponential model, Karnopp model and Armstrong's model. In these models, friction is calculated as a function of displacement or velocity difference between the two contact surfaces. Different functions are applied to focus on different friction behaviors. A common form of friction in these models can be expressed as a combination of three components: static friction, Coulomb friction and viscous friction. Another class of friction model in [3] is dynamic model. As stated in the

name, a dynamic model takes friction as a dynamic function of velocity and displacement by introducing intermediate states and including the time derivative. The models addressed include the Dalh model, the Bristle model, the Reset Integrator Model, the LuGre model and others. Other models have also been presented recently based on or as modifies of the models above [8][9][10][11][12] in order to have a more accurate approximation presenting richer friction behaviors.

As an alternative to mathematic modeling, soft computing techniques have also been found in the friction compensation. Neural networks are applied as a black box for the friction model, where the mathematic function is replaced with layers of neurons and the friction is calculated adaptively without knowing the physical meaning of neurons and weights [13][14][16]. The applications of fuzzy modeling in friction compensation can be seen in [22][23][24][25]. In these papers, the piecewise characteristic of fuzzy logic system is utilized so that the friction can be compensated either directly by using the fuzzy model or indirectly by building fuzzy controller.

In all these research work, the effect of temperature in friction modeling is ignored even when friction does change with temperature in a lubricated system. Although this change of friction has been introduced in the studies of tribology [2] as the result of the lubricant character change, the mathematic model of friction changing over temperature that can be used in control engineering is still absent. In this thesis, we will first build the mathematic model of how the friction changes with temperature in a harmonic drive.

1.2.3 Fuzzy Logic System and Fuzzy Modeling

FLS (Fuzzy Logic System) is a knowledge expression and inference system based on Fuzzy Sets and Fuzzy Logic which simulates human reasoning process. Unlike the classical crisp bivalent sets and logic where things are either true or false, FLS helps model the ambiguous information by introducing the concept of membership and fuzzy inference [26][27][28]. In the cases where sharp boundaries are difficult or even impossible to get, as in the friction modeling where the exact temperature and velocity boundary of different friction behaviors is unreachable, FLS is a powerful tool that we can resort to.

Another advantage of modeling with fuzzy logic system is its universal approximation capability. Kosko [29] showed that a fuzzy system can approximate any continuous real function defined on a compact (closed and bounded in R) domain. It also shows in [30] that: "with an essentially arbitrary choice of (sufficiently differentiable) basis functions, the resulting fuzzy systems have the ability to approximate continuous functions and their derivatives uniformly on arbitrary compact sets of to the desired degree". With the approximation ability, FLS is a suitable tool modeling the complicated friction behavior.

In this thesis, FLS will be used to model friction with temperature variation in such a way that the nonlinear character of friction can be expressed in a fuzzy combination of linear fuzzy rules.

1.2.4 Optimization – Gradient and Evolutionary

In the research, optimization is used in parameters estimation to minimize the cost function of estimation errors. The proposed optimization method, Evolutionary Parallel

Gradient Search, interweaves gradient search and evolutionary algorithm to help the optimization process escaping from local minima.

In gradient based methods, the search directions are calculated using gradient information. The basic idea behind this kind of search is that, for a convex function to be optimized in a convex domain, the unique optimum value will always be located at the point where the gradient of the function equals to zeros unless it is on the boundary. For all gradient based optimization methods, therefore, the ultimate objective of their search is to find the point where the optimized function has its gradient as zeros. However, when the convexity of the function can't be guaranteed, these methods are blamed of being stuck at local optima since the points with zero gradients, or local minima, are no longer unique for non-convex optimization problems [32][33].

Parallel search is used in global optimization. In parallel search, the optimization starts from several points simultaneously which means we can find multiple local minima for one try. Although this method will definitely increase the opportunity reaching the global minimum, it still largely depends on the initialization of the start points [31].

Evolutionary algorithms (EA) are parallel stochastic optimization methods simulating the process of Natural Selection. In evolutionary algorithms, no matter what the direction of search is and how the direction is calculated, the implementation of "Fittest Survival" rule guarantees the optimization process improving over generations. Local optima, or premature in the term of evolutionary algorithms, also exist for the algorithms; however, with the parallel and stochastic characters inherent, EA is gifted with the ability of finding global optimum. The computation complexity and convergence time of EA are really large compared with the traditional optimization algorithms. The

reasons are its complicated calculations of search direction and large population of the parallel search [31][34].

Salomen [46] discussed the similarities and differences between the two optimization methods of gradient search and evolutionary algorithm. He also put forward in the same paper an Evolutionary Gradient Search (EGS) procedure, in which Evolutionary Strategy is used to calculate the approximation of gradient. Magoulas [47] in his paper proposed another possibility of the hybrid of gradient and EA (evolutionary strategy in his case), where Stochastic Gradient Descent is embedded as a sub step of EA. The algorithm was used in the training of Artificial Neural Network with good results.

The above mentioned algorithms combined the search methods of gradient search and evolutionary algorithm in the way that they took one as the main optimization method and the other as embedded sub step. EGS is basically a gradient search where the gradient is calculated using EA. This is inherently a method of local search although it will help us when the gradient information is not available. Magoulas, on the other hand, embedded gradient search into EA as a sub optimization for every generation. The combination of other local search methods, such as Simplex and Pattern Search, with EA can be seen in [35][36][37][40][45][48].

In Chapter 4, we will propose a new algorithm that interweaves the parallel gradient search and evolutionary algorithm so that both gradient search and evolutionary are carried out simultaneously to help the gradient search escaping from local minima. This algorithm is used in the parameters estimation of the research.

1.2.5 LMI Based Optimization and Controller Design

The stability of linear system can be determined by the existence of the Lyapunov matrix that satisfies the Lyapunov equality or inequality. The development of Linear Matrix Inequality based optimization, especially the appearance of its numerical solution based on interior point method, helps build a framework of finding such matrices that can guarantee stability of the linear system. In his book [54], Boyd showed that a wide variety of problems arising in system and control theory can be converted to standard convex and quasiconvex optimization problems that involve matrix inequalities. Recently, different strategies of using LMI in quadratic optimal control, robust control, H_2 and H_∞ based control and others have been explored [55][56][57][58][59]. All control algorithms based on LMI build their fundament on the Lyapunov inequality which will lead to a quadratic Lyapunov function: by satisfying the inequality, the stability of the system is guaranteed; by applying different additional constraints on the inequality and setting the optimization criterions, some certain performance requirement can be met.

LMI also found its application in the control of a certain type of Linear Parameter –varying systems where the systems can be described as a linear combination of LTI (Linear Time Invariant) systems at some vertexes.[60][61][62] The stability and performance criterion problems of LTI at each vertex can be formed into LMIs based on the system equation of each LTI system. The feedback controller can be built for each LTI by solving the LMIs. After finding controller for each vertex LTI using LMI, the overall controller can be calculated using the combination of these local controllers.

As to a nonlinear system, it is not so convenient to apply LMI in the controller design for the nonexistence of general form Lyapunov function. However, there are some

ways to convert the nonlinear system in to the combination of piecewise linear system [65][84]. One of these is to decompose a nonlinear system into Fuzzy TS system. Fuzzy TS system is a special type of LPV system that, instead of using linear combination, it applies fuzzy combination of different rules which represent local linear input-output relations of a nonlinear system. Nonlinear system, therefore, can be modeled as Fuzzy TS system by using local linearization. In [65], Tanaka addressed issues in control of TS Fuzzy model such as stability analysis, systematic design, performance analysis problem and how these issues can be reduced to the form of LMI optimization; on the top of that, a framework of control strategies named Parallel Distributed Compensation (PDC) based on LMI optimization are presented. Resent research of LMIs in Fuzzy TS system have been found on more relaxed constraints and better performance.[68][69][70]

1.3 Overview of the thesis

The thesis will be organized as follows. The mathematic model of friction with temperature consideration will be presented in chapter 2; the Cascaded Fuzzy Friction Model is proposed in chapter 3; in chapter 4, the Evolutionary Parallel Gradient Search algorithm is developed and applied to the parameters estimation problems for the model built in chapter 2 and 3; details of controller design for the Fuzzy TS system using LMI optimization technique are described in chapter 5; the controllers are built for the harmonic drive and the simulation results of the closed loop system are given in chapter 6; the thesis ends with conclusion and recommend future work in chapter 7.

2 Mathematic Model of Friction Variation with Temperature

In this chapter, we will study how the value of friction changes with temperature variation and build the mathematic model of the relations between friction and temperature. The model is built based on the exponential model in the assumption that the structure of the model does not change over temperature; what change are the parameters in the model.

2.1 The Exponential Friction Model

A common form of friction model in control context ([3]) is:

$$F_r = \begin{cases} F(v) & if \ v \neq 0 \\ F_S \cdot sign(F_E) & Otherwise \end{cases}, \tag{2-1}$$

where F_r is the magnitude of total friction experienced by the object; F_S is the static friction (Stiction); v is the relative velocity between the two contact surfaces; $F(v)$ is a function that matches the change of friction at non-zero velocity; F_E is the external force that drives the object to move.

The model takes the non-zero-velocity friction as a function of velocity; the friction at zero velocity is taken as equal to static friction.

In the widely used exponential model $F(v)$ is described as:

$$F(v) = [(F_S - F_C)e^{-(\frac{v}{v_s})^{\delta}} + F_C + F_v \mid v \mid] \cdot sign(v), \tag{2-2}$$

where, F_S is the static friction; F_C is the Coulomb friction; F_v is the viscous coefficient that results in the proportional viscous friction; v_s is the Stribeck velocity

which is a small velocity near zero (20 RPM in our research); δ is the constant mapping the shape for friction curve, normally an even number. In our research it is taken as 2.

In the case of a rotary system, the friction torque is:

$$F(\omega) = [(F_S - F_C)e^{-(\frac{\omega}{\omega_s})^{\delta}} + F_C + F_v \mid \omega \mid] \cdot sign(\omega) . \qquad (2\text{-}3)$$

ω is the velocity of rotation; the friction force in former equations is now changed to friction torque. In the rest of the thesis, we make no difference between friction and friction torque since all our research is carried on the rotary system.

Therefore, the overall friction model of both non-zero and zero velocity is:

$$F_r = \begin{cases} F(\omega) & if \ \ \omega \neq 0 \\ F_S \cdot sign(F_E) & Otherwise \end{cases}$$

$$F(\omega) = [(F_S - F_C)e^{-(\frac{\omega}{\omega_s})^{\delta}} + F_C + F_v \mid \omega \mid] \cdot sign(\omega) . \qquad (2\text{-}4)$$

The value of friction in above model will change as shown in the curve of following Figure 4. The nonlinear curve in the figure is Stribeck curve of friction due to the lubricating states changing from dry to mixed and then full lubricated [2]. From the curve, we can see that the friction experienced by the system starts from static friction then reduces nonlinearly at the velocity near zero, and finally increases proportional to the velocity.

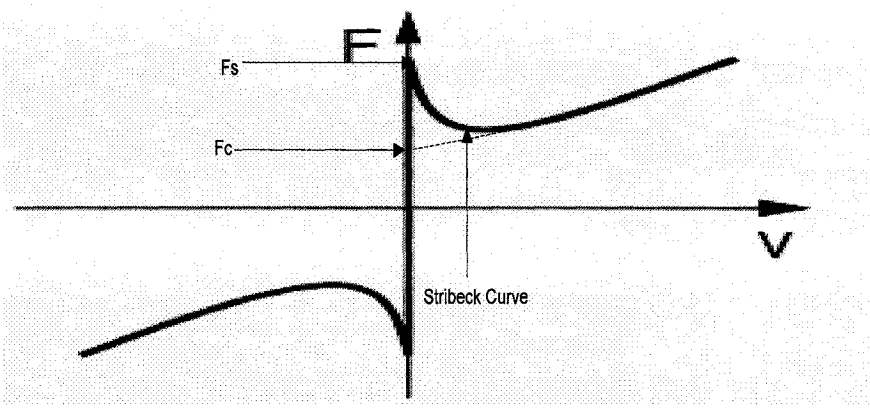

Figure 4: Friction vs. Velocity

In our research, we will use this model to approximate the friction inside the harmonic drive system at certain temperature; the variations of friction with temperature are modeled as the change of the parameters in the model.

2.2 Friction Model with Temperature

Temperature is an important variable in the value of friction force. In our research, we found that temperature play such an important role that model based friction compensation works only at a certain range of temperature. Different control efforts are required for different temperatures even when the system follows the same reference trajectory.

The dynamic of the harmonic drive without load in our research can be approximated by [78]:

$$J\dot{\omega} = T_m - F_r, \tag{2-5}$$

where, J is the inertia of the system; T_m is the applied torque to the drive.

Since the friction F_r changes with temperature, the dynamic of the system will also change with temperature. We can simply replace the friction F_r with the model in (2-3) to see the change in the dynamic of the system.

$$J\dot{\omega} = T_m - [(F_S - F_C)e^{-(\frac{\omega}{\omega_s})^{\delta}} + F_C + F_v \mid \omega \mid] \cdot sign(\omega) \tag{2-6}$$

In our research, we found that F_v changes with temperature. This is consistent with the character of lubricant that the viscosity of lubricant changes over temperature. Therefore, even without considering the change of F_S and F_C with temperature, the gain, damping and time constant are all changed when temperature changes. The change of such system with nonlinear friction is even more complicated.

To have a fully understanding of the friction change with temperature, we need to build the relations between the aforementioned exponential model and temperature.

Here, we have some assumptions:

1. The form of exponential model of friction does not change over temperature; that is, the friction model still has the same form as we described in (2-4) even at different temperature;

2. The Stribeck velocity does not change with temperature;

3. F_S, F_C and F_v are the parameters in the model that vary with temperature.

For the data showing such relations, we resort to the catalogue of the harmonic system [79]. In the catalogue, we obtain the following graphic of the torque required to drive the system at different velocities and different temperatures. When the system is running without load, the torque driving the system at steady state can be taken as equal to the friction experienced. The no load running torques varied with temperatures at

certain steady velocities of 500, 1000, 2000 and 3500 RPM are shown in Figure 5. The ambient temperature ranges from -10 to 40 °C. Among the different types of harmonic drive shown in the figure, the harmonic drive in our research is size 17 (Item Number: RHS-17-6006-TE100AL, for the details on the harmonic drive, please refers to the catalogue [79] and the Item Details on [80]; the simple specification is listed in Appendix A). The velocities are measured in the input (high speed) side; for the output (low speed) side velocities, a gear ratio of 50 is considered. The lubricant used is harmonic grease.

The data table of torque in different temperatures is built based on the figure below.

COMPONENT SET

Harmonic drive Grease SK-1A , SK-2

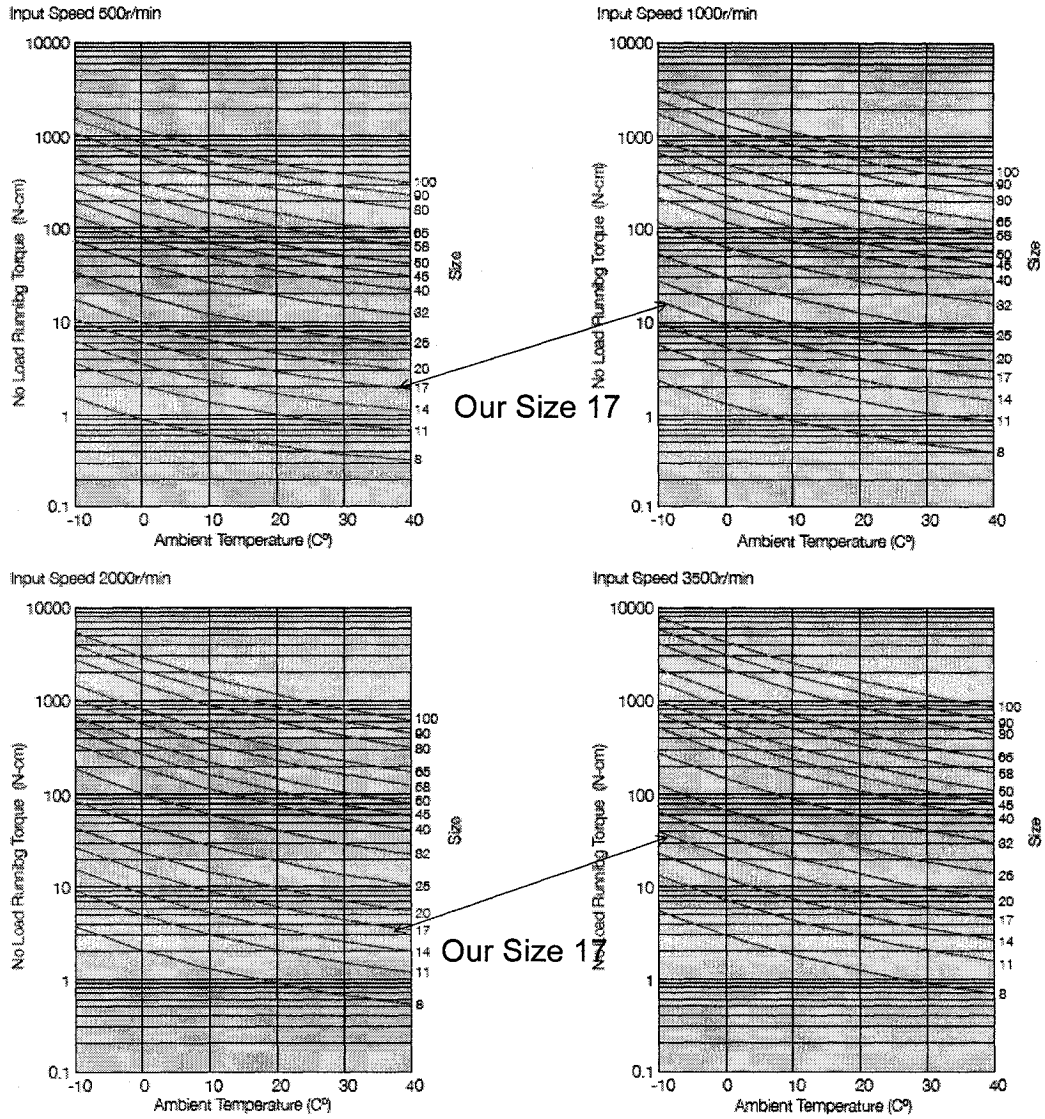

Figure 5: Friction changed with temperature

Table 1: Friction at different velocities and temperatures

Temperature (° C)	Torque at 500 RPM (NCm)	Torque at 1000 RPM (NCm)	Torque at 2000 RPM (NCm)	Torque at 3500 RPM (NCm)
-10	11.487	16.3	28	40.05
-7.5	9	14	24	35
-5	7.9	12	20	30
-2.5	6.9	10.5	16.5	25
0	5.9	9.1	13.3	21.6
2.5	5.25	8	12	19.8
5	4.7	7	11.2	17
7.5	4.2	6.3	10	14.2
10	3.8	5.7	8.9	12.4
12.5	3.5	5.1	8	11.6
15	3.2	4.7	7.2	10.1
17.5	3	4.3	6.5	9.2
20	2.8	4	6	8.4
22.5	2.6	3.5	5.5	7.6
25	2.4	3.3	5.1	7
27.5	2.2	3.05	4.7	6.4
30	2.1	2.9	4.3	5.9
32.5	2	2.7	4	5.4
35	1.9	2.5	3.8	5
37.5	1.9	2.3	3.5	4.7
40	1.8	2.2	3.2	4.4

Since the torques and velocities are all from steady state, the value of friction should be equal to the driving torque without load as in table 1. Following equation (2-4), the friction torques at these velocities can be calculated as:

$$F_r = F_C + F_v |\omega|. \tag{2-7}$$

The static friction and Stribeck curve in (2-4) are ignored since the data are measured at the relative high velocity, where:

$$|\frac{\omega}{\omega_s}| >> 1 \Rightarrow e^{-(\frac{\omega}{\omega_s})^2} \to 0.$$

Therefore, by fitting the data of driving torques in table 1 into the friction model, we have the values of F_v , F_C and F_S (calculated using the information in the catalogue with the start friction) at different temperatures in the following table; the curves of F_v, F_C and F_S with temperature are shown in Figure 6.

Table 2: Parameters varying with temperature

Temperature (° C)	F_v (NCm/RPM)	F_C (NCm)	F_S (NCm)
-10	0.0096198	7.1247	8.7247
-7.5	0.0086667	5.3333	6.9333
-5	0.0073571	4.6	6.2
-2.5	0.0059762	4.2667	5.8667
0	0.0051286	3.5	5.1
2.5	0.0047786	2.9	4.5
5	0.004081	2.8333	4.4333
7.5	0.0033095	2.8833	4.4833
10	0.0028381	2.7333	4.3333
12.5	0.0026857	2.35	3.95
15	0.0022762	2.3167	3.8167
17.5	0.0020476	2.1667	3.7167
20	0.0018476	2.0667	3.667
22.5	0.0016762	1.8667	3.4667
25	0.0015333	1.7667	3.3667
27.5	0.0013976	1.6417	3.2417
30	0.0012571	1.6	3.2
32.5	0.0011286	1.55	3.15
35	0.0010381	1.4833	3.0833
37.5	0.00095238	1.4333	3.0333
40	0.00087619	1.3667	2.9667

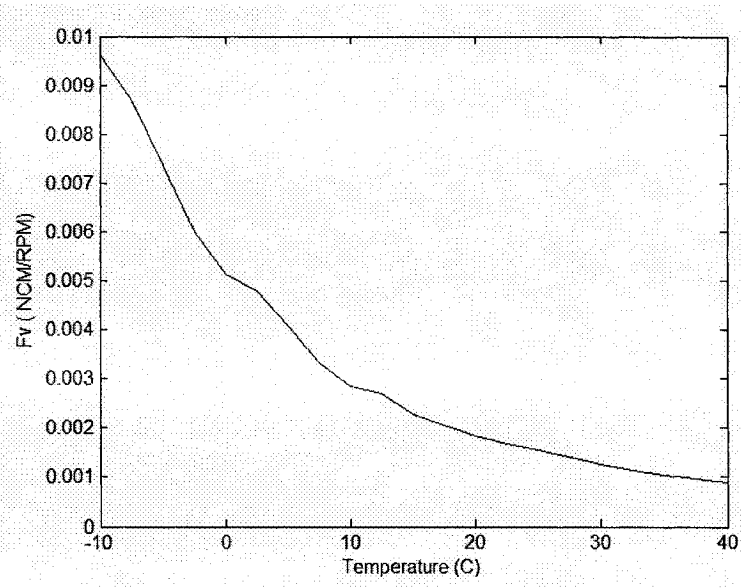

a. F_v vs. Temperature

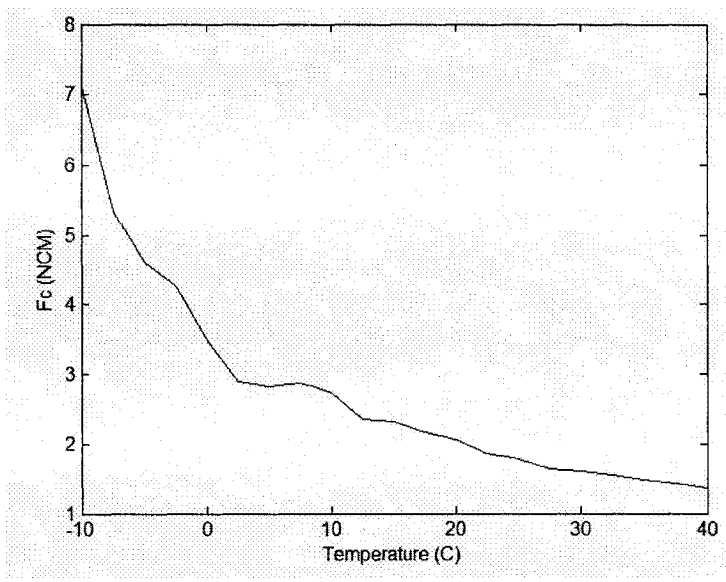

b. F_C vs. Temperature

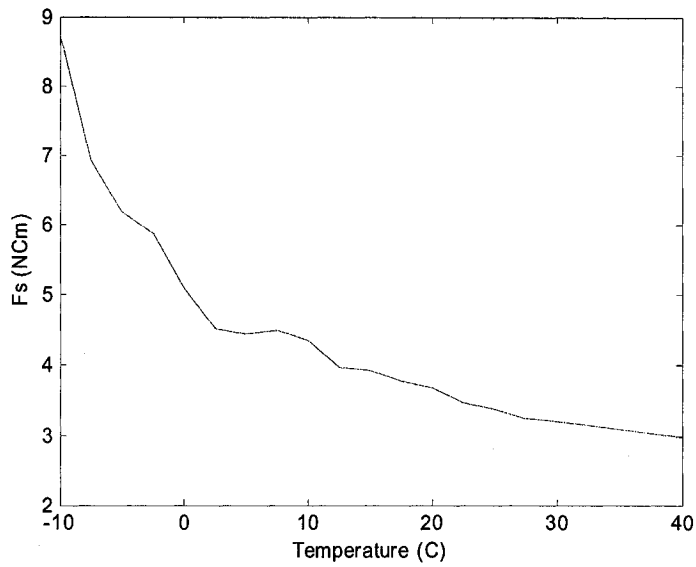

c. F_S vs. Temperature

Figure 6: Parameters varying with temperature

From the curves of F_v, F_C and F_S changing over temperature in Figure 6, we observed these parameters show some exponential characters. By choosing different functions and comparing, the exponential form expressions of the parameters are proposed as:

$$F_v = F_{v0} + F_{v1} e^{-\frac{T-T_0}{T_s}}$$

$$F_C = F_{C0} + F_{C1} e^{-\frac{T-T_0}{T_s}}$$

$$F_S = F_{S0} + F_{S1} e^{-\frac{T-T_0}{T_s}} \quad , \tag{2-8}$$

where, T is the ambient temperature; $F_{v0}, F_{v1}, F_{C0}, F_{C1}, F_{S0}, F_{S1}, T_0$ *and* T_s are parameters of the friction model and will be estimated in the chapter 4 using the data pairs in Table 2.

Based on the analysis above, the overall model of friction with the consideration of temperature variation is proposed as:

$$F_v = F_{v0} + F_{v1} e^{-\frac{T-T_0}{T_s}}$$

$$F_C = F_{C0} + F_{C1} e^{-\frac{T-T_0}{T_s}}$$

$$F_S = F_{S0} + F_{S1} e^{-\frac{T-T_0}{T_s}}$$

$$F(\omega) = [(F_S - F_C) e^{-(\frac{\omega}{\omega_s})^{\delta}} + F_C + F_v \mid \omega \mid] \cdot sign(\omega)$$

$$F_r = \begin{cases} F(\omega) & if \ \omega \neq 0 \\ F_S \cdot sign(F_E) & Otherwise \end{cases} . \qquad (2\text{-}9)$$

2.3 The Mathematic Model of the Harmonic Drive

In simple form, the harmonic drive actuator with friction can be modeled as [78]:

$$\ddot{\theta} = \frac{1}{J}(T_m - F_r), \qquad (2\text{-}10)$$

where, J stands for the inertia of the system which can be found in the data description of the harmonic drive; T_m is the mechanical torque fed into the system; F_r is the friction.

In our simulations in later chapters, the mathematic form of friction is used to build the system to be controlled. Therefore, the model of the whole harmonic drive can be described as:

$$\ddot{\theta} = \frac{1}{J}(T_m - F_r)$$

$$F_v = F_{v0} + F_{v1} e^{-\frac{T-T_0}{T_s}}$$

$$F_C = F_{C0} + F_{C1} e^{-\frac{T-T_0}{T_s}}$$

$$F_S = F_{S0} + F_{S1} e^{-\frac{T-T_0}{T_s}}$$

$$F(\omega) = [(F_S - F_C) e^{-(\frac{\omega}{\omega_s})^{\delta}} + F_C + F_v \mid \omega \mid] \cdot sign(\omega)$$

$$F_r = \begin{cases} F(\omega) & if \ \omega \neq 0 \\ F_S \cdot sign(F_E) & Otherwise \end{cases} . \qquad (2\text{-}11)$$

2.4 Summary

In this chapter, the general form of friction model is shown and the exponential model that the friction model with temperature is built on is introduced thereafter. The importance of temperature in friction modeling is discussed. By observing and analyzing the data of friction varying with temperature, the functions of how the parameters in exponential model change are built. Finally, the overall mathematic model of friction with the consideration of temperature is proposed and is applied to establish the dynamic model of the harmonic drive.

3 Cascaded Fuzzy Model of Friction Variation with Temperature

In the former chapter, we have built the mathematic model of friction which is difficult to be applied in the controller design due to its nonlinearity and complexity. In this chapter, a Cascaded fuzzy model of friction with temperature consideration is proposed so that friction and consequently the harmonic drive system with friction can be described as fuzzy TS model. Since the fuzzy model is the fuzzy combination of different fuzzy rules that can be taken as the local linearization of the nonlinear model at different operation states, the control algorithms of linear system can be applied to the local linearized model.

3.1 The Cascaded Fuzzy Friction Model

Fuzzy Logic System is gifted with the ability of processing incomplete and ambiguous information which makes it a perfect tool in the modeling of friction.

By observing the change of friction in Figure 4 of chapter 2, we know that the friction exhibits different behaviors at zero, low and high velocities. What makes it even more difficult to model this character of friction is that there is no sharp boundary where this kind of differences happens. With the consideration of temperature, the modeling can be more complicated since the temperatures of the contact surfaces and lubricant have complicated thermodynamics and can't be measured directly. The only information we can rely on is the environment temperature or the temperature from the skin of the system. Although it is difficult to model friction in classical mathematics because of the

incompleteness and ambiguity, it is easier to model it concisely with the linguistic knowledge of fuzzy logic system.

In this section, a cascaded fuzzy friction model is proposed. At first, the second layer fuzzy system with undetermined parameters is presented to estimate the friction at certain temperature; based on temperature information, the first layer model estimating the unknown parameters of the second layer model then follows. These two fuzzy systems are cascaded to form an integrated model of friction vs. temperature-velocity. Therefore, how friction changes over temperature and velocity can be deduced from the model.

3.1.1 Friction model under certain temperature (the second layer model)

When the temperature is treated as constant, the friction can be normally modeled as a function of the output of mechanical system - position or velocity - as shown in equation (2-4) in chapter 2, which is rewritten here:

$$F_r = \begin{cases} F(\omega) & if \ \ \omega \neq 0 \\ F_S \cdot sign(F_E) & Otherwise \end{cases}$$

$$F(\omega) = [(F_S - F_C)e^{-(\frac{\omega}{\omega_s})^{\delta}} + F_C + F_v \mid \omega \mid] \cdot sign(\omega). \qquad (3\text{-}1)$$

When the velocity of the system is zero, which means the system has not started, the friction is equal to the drive torque applied to the system. The maximum of friction is the static friction F_S when the system is just about to move. In friction compensation, the friction at zero can be always modeled as the constant F_S since it is the torque to

overcome. At high velocity, the friction consists of Coulombs friction and viscous friction which is totally linear with velocity since, when $\omega >> \omega_s$, $e^{-(\frac{\omega}{\omega_s})^{\delta}} \to 0$,

$$F(\omega) = [F_C + F_v \mid \omega \mid] \cdot sign(\omega) . \tag{3-2}$$

When the velocity is low, the friction of the system is a mix of that at zero and high velocity. The gradually changing of friction can be expressed as the nonlinear combination of friction at zero and higher velocity. This combination can be replaced with fuzzy inference.

To sum up, the two simple rules of the TS fuzzy friction model (where the velocity is divided into two levels) that takes the velocity as input and the value of friction as output can be expressed linguistically as:

If ω *(velocity) is zero, the value of friction* $F_r = F_S$;

If ω *is high, the value of friction* $F_r = (F_C + F_v \mid \omega \mid)$;

With the singleton fuzzification in the fuzzifier, the input velocity is classified into two fuzzy linguistic expressions: Zero and High; the memberships are $\mu_{v1}(\omega)$ and $\mu_{v2}(\omega)$ respectively. The defuzzification method used in the defuzzifier is the weighted center. Therefore, the output of the TS friction model can be calculated as:

$$F_r = \frac{\mu_{v1}(\omega) \cdot F_S + \mu_{v2}(\omega) \cdot (F_C + F_v \mid \omega \mid)}{\mu_{v1}(\omega) + \mu_{v2}(\omega)} \tag{3-3}$$

where, F_r is the friction experienced by the system; F_S is the static friction; F_C is the Coulomb friction; F_v is the viscous coefficient; F_E is the driving force.

These parameters of F_S, F_C and F_v are to be determined with the temperature information in the first layer fuzzy model. The sign of friction is the same as that of the

driving force (at zero velocity) or the velocity (non-zero) since the friction is considered as resistant force and will be subtracted from the dynamic equation of the harmonic drive system.

The membership functions are taken as the single side exponential function:

$$\mu_{v1}(\omega) = \begin{cases} e^{\frac{(\omega-\omega_z)^2}{\sigma_z^2}} & \omega \geq \omega_z \\ 1 & otherwise \end{cases} \tag{3-4}$$

$$\mu_{v2}(\omega) = \begin{cases} e^{\frac{(\omega-\omega_H)^2}{\sigma_H^2}} & \omega \leq \omega_H \\ 1 & otherwise \end{cases}, \tag{3-5}$$

where, ω_z and ω_H are the center of the membership functions that are defined as Zero and High respectively in the linguistic expression; σ_z and σ_H are the distribution width of the two membership functions. The values of ω_z and ω_H are set as 0 and 40 RPM (velocity at the high speed end) and the σ_z and σ_H are set as 40 and 80 RPM in this study.

Remarks: The TSK friction model in equation (3-3) can be further expressed in the form as:

$$F_r = \frac{\mu_{v1}(\omega)}{\mu_{v1}(\omega)+\mu_{v2}(\omega)}(F_S - F_C) + (F_C + (1 - \frac{\mu_{v1}(\omega)}{\mu_{v1}(\omega)+\mu_{v2}(\omega)})F_v|\omega|), \tag{3-6}$$

by substituting,

$$F_v' = (1 - \frac{\mu_{v1}(\omega)}{\mu_{v1}(\omega)+\mu_{v2}(\omega)})F_v,$$

we have:

$$F_r = \frac{\mu_{v1}(\omega)}{\mu_{v1}(\omega)+\mu_{v2}(\omega)}(F_S - F_C)+F_C+F_v'|\omega|. \quad (3\text{-}7)$$

Thus, the model has similar form as the exponential model in (3-1). The only difference is that the nonlinear part of exponential function is replaced with the normalized membership.

The fuzzy system becomes more accurate yet complicated when more fuzzy rules are applied. With the two simple fuzzy rules shown as above, however, we can establish a physically reasonable model.

3.1.2 Fuzzy model with temperature (the first layer model)

With fuzzy model under certain temperature, the friction can be determined if the parameters F_s, F_C and F_v in (3-3) are known. The values of these parameters depend on other conditions among which the most important one is temperature. However, the mathematic models of these parameters vs. temperature are not available for use in control engineering. Intuitively, the common sense such as "the higher the temperature, the lower the friction" does exist. Therefore, it's reasonable to use the following fuzzy rules to estimate these parameters:

If the temperature (T) is T_i, then F_s, F_C and F_v are F_{si}, F_{Ci} and F_{vi} respectively.

where, F_{Si}, F_{Ci} and F_{vi} $(i = 1,2\cdots N)$ are parameters in the ith temperature range which are supposed to decrease when the temperature T_i increases; N represents the number of fuzzy rules, which is five in our research.

By applying defuzzification, one obtains the values of these parameters in different temperatures:

$$F_S(T) = \frac{\sum_{i=1}^{N} \mu_{Ti}(T) \cdot F_{Si}}{\Sigma \mu_{Ti}(T)}$$

$$F_C(T) = \frac{\sum_{i=1}^{N} \mu_{Ti}(T) \cdot F_{Ci}}{\Sigma \mu_{Ti}(T)} \qquad (3\text{-}8)$$

$$F_v(T) = \frac{\sum_{i=1}^{N} \mu_{Ti}(T) \cdot F_{vi}}{\Sigma \mu_{Ti}(T)}$$

where, $\mu_{Ti}(T) = e^{-(\frac{T-T_i}{\sigma_i})^2}$ is the ith membership function of temperature.

3.1.3 The Cascaded Fuzzy Friction Model

With the two fuzzy models, second layer as in section 3.1.1 and first layer as in section 3.1.2, the cascaded fuzzy friction model for a large temperature range can be summarized as:

The first layer of the model supervises the change of temperature and determines the parameters and corresponding rules for the second layer. Based on the rules from the first layer, the second layer calculates the friction of the system. The structure of the cascaded fuzzy friction model is shown in Figure 7.

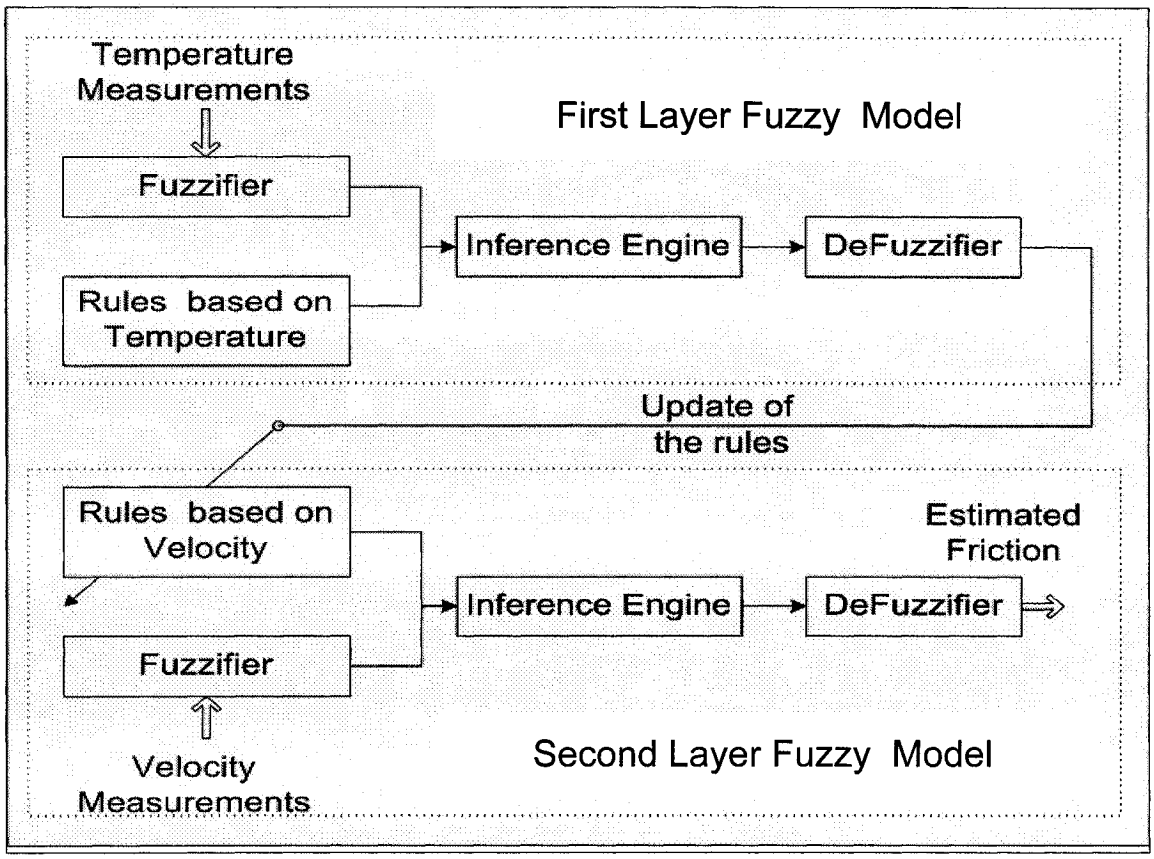

Figure 7: Structure of the Cascaded Friction Model

3.1.4 Remarks

The proposed model takes the measurements of temperature and velocity as inputs for different layers. With the two layers of fuzzy inference, the model estimates the friction experienced by the system.

An alternative method is to model the friction as a single fuzzy system with two inputs of T and ω. The fuzzy rules of such model are described as:

If T is low (T_i) *and* ω *is high* (ω_j), *the friction* $F_{rij} = F_{ij}(\omega, T)$,

where, i stands for the ith temperature range; j stands for jth velocity range.

There are several advantages of the proposed cascaded fuzzy friction model over the one above:

1. The proposed model decomposes the fuzzy system with two inputs into two fuzzy systems each of which has only one input. This reduction of dimensions leads to less parameters in the rules set.

2. The proposed model is more physically reasonable due to the decoupled effects of temperature and velocity.

3. The fuzzy inference processes of the two layers can be carried out in different time scales since the second layer of inference does not depend on that of the first layer as long as the parameters are known. This saves the computational efforts in the case where the change of temperature is slow since it is not necessary to calculate the parameters at every sampling instance.

3.2 The Fuzzy Model of the Harmonic Drive

The fuzzy TS model of the harmonic drive is built based on the Cascaded Fuzzy Model in this section. In our research, LMI technique is used to construct the controller which means the differential equation form of system dynamic need to be converted to state space expression. For the controller to be used in a digital control environment, the model of the harmonic drive is discritized. Besides the second order system of harmonic drive, a third order system with an integrator is also built for the controller design in the future.

3.2.1 State space equations of the system

The dynamic of the harmonic drive can be described as:

$$\ddot{\theta} = \frac{1}{J}(T_m - F_r). \tag{3-9}$$

Combined with the Cascaded Fuzzy Model, the dynamic of the system at certain temperature can be expressed in fuzzy rules:

If ω is zero, the system is:

$$\ddot{\theta} = \frac{1}{J}(T_m - F_S \cdot sign(F_E)); \tag{3-10}$$

If ω is high, the system is:

$$\ddot{\theta} = \frac{1}{J}(T_m - F_C \cdot sign(\dot{\theta}) - F_v |\dot{\theta}| \cdot sign(\dot{\theta})) = \frac{1}{J}(T_m - F_C \cdot sign(\dot{\theta}) - F_v \dot{\theta}). \tag{3-11}$$

Takes:

$$x_1 = \theta; \tag{3-12}$$

$$x_2 = \omega = \dot{\theta}, \tag{3-13}$$

in the state space form, the system now is converted to:

Rule for zero velocity is:

If ω is zero, the system is:

$$\dot{x}_1 = x_2 \tag{3-14}$$

$$\dot{x}_2 = \frac{1}{J}(T_m - F_S \cdot sign(F_E)). \tag{3-15}$$

Takes:

$$u = T_m - F_S \cdot sign(F_E) \tag{3-16}$$

$$x = [x_1 \quad x_2]^T, \tag{3-17}$$

the system can be expressed as:

$$\dot{x} = A_Z x + Bu \ , \tag{3-18}$$

where, $A_Z = \begin{vmatrix} 0 & 1 \\ 0 & 0 \end{vmatrix}$, $B = \begin{vmatrix} 0 \\ 1/J \end{vmatrix}$.

Rule for high velocity:

If ω is high, the system is:

$$\dot{x}_1 = x_2; \tag{3-19}$$

$$\dot{x}_2 = \frac{1}{J}(T_m - F_C \cdot sign(x_2) - F_v x_2) . \tag{3-20}$$

Takes:

$$u = T_m - F_C \cdot sign(x_2) \tag{3-21}$$

$$x = [x_1 \quad x_2]^T , \tag{3-22}$$

the system can be expressed as:

$$\dot{x} = A_H x + Bu \tag{3-23}$$

where, $A_H = \begin{vmatrix} 0 & 1 \\ 0 & -F_v / J \end{vmatrix}$, $B = \begin{vmatrix} 0 \\ 1/J \end{vmatrix}$.

Therefore, the fuzzy rules for certain temperature are summarized as:

If ω is zero, the system is:

$$\dot{x} = A_Z x + Bu ; \tag{3-24}$$

If ω is high, the system is:

$$\dot{x} = A_H x + Bu ;$$

(3-25)

The model needs to be converted to the discrete time domain for the control purpose. In our research, the model

$$\dot{x} = Ax + Bu \qquad (A = A_Z, \quad A_H) \tag{3-26}$$

is converted to difference equation as:

$$x(k+1) = (\tau_s A + I)x(k) + \tau_s Bu, \tag{3-27}$$

where, τ_s is the sampling time; I is the identity matrix.

This is an approximation of the state space expression in continuous time domain, since, when τ_s is small enough, we use the finite difference method to approximate the derivative:

$$\dot{x} \approx \frac{x(k+1) - x(k)}{\tau_s}. \tag{3-28}$$

By substituting the above equation into (3-26), one obtains:

$$\frac{x(k+1) - x(k)}{\tau_s} = Ax(k) + Bu \tag{3-29}$$

The above equation is rewritten as:

$$x(k+1) = (\tau_s A + I)x(k) + \tau_s Bu \tag{3-30}$$

The conversion may lose some accuracy; however, it is still a good approximation when the sampling time is small enough.

The fuzzy model of the harmonic drive with friction in discrete time domain is summarized as:

If ω is zero, the system is:

$$x(k+1) = (\tau_s A_Z + I)x(k) + \tau_s Bu$$

$$T_m = u + F_S \cdot sign(F_E)\ ; \tag{3-31}$$

If ω is high, the system is:

$$x(k+1) = (\tau_s A_H + I)x(k) + \tau_s Bu$$

$$T_m = u + F_C \cdot sign(x_2) \ , \tag{3-32}$$

where, $A_Z = \begin{vmatrix} 0 & 1 \\ 0 & 0 \end{vmatrix}$, $A_H = \begin{vmatrix} 0 & 1 \\ 0 & -F_v / J \end{vmatrix}$, $B = \begin{vmatrix} 0 \\ 1/J \end{vmatrix}$.

The control signal u will be calculated using the method introduced in chapter 5; T_m will be the final torque applied to drive the system.

Parameters of F_v, F_C and F_S are calculated from the first layer of the Cascaded Fuzzy Model using the information of temperature. For 5 rules in the first layer and two rules in the second layer, we will have totally one A_Z and five A_H. The system output equations are the same:

$$y(k) = Cx(k)$$

where, C is an identity matrix.

3.2.2 State space equations of the system with integrator

The states in the fuzzy model of last section are position and velocity. In a position control problem, the controller designed using state feedback of such a system is equivalent to a PD controller. Without integrator, the closed loop system may have steady state error if there exist modeling errors such as the inaccuracy of F_C and F_S. An augmented third order model is also built to include an integrator to the system.

Considering the system:

$$\dot{x} = Ax + Bu$$

$$y = Cx \ , \tag{3-33}$$

one extra state of x_0 is introduced to states vector x in the way:

$$\dot{x}_0 = x_1$$

$$x^* = [x_0 \quad x_1 \quad x_2]^T \tag{3-34}$$

Thus, the system changes to:

$$\dot{x}^* = A^* x^* + B^* u$$

$$y^* = C^* x^* \tag{3-35}$$

where, $A^* = \begin{vmatrix} 0 & a^* \\ 0 & A \end{vmatrix}$, $B^* = \begin{vmatrix} 0 \\ B \end{vmatrix}$, $C^* = \begin{vmatrix} 1 & 0 \\ 0 & C \end{vmatrix}$; and a^* denotes vector [1 0].

In the simulation, the third order model is built based on the system in the former section. A^* B^* and C^* are constructed using the A_Z, A_H, B and C for each fuzzy rules and thus become A_Z^*, A_H^*, B^* and C^* for the new fuzzy model of the harmonic drive with integrator. The system is converted to the discrete time domain using the same method.

3.3 Summary

In this chapter, a Cascaded Fuzzy Model that describes the variation of friction with environment temperature is proposed. The model simplified a two-dimensional problem into two one- dimension fuzzy models so that the number of model parameters is reduced. The model is then used in constructing the fuzzy TS model of the harmonic drive in state space equations form for the control purpose. In order to use the model in discrete time domain, the state space equations are discritized. An augmented third order

system with integrator is also built to eliminate the steady state errors. The estimation of parameters in the models will be addressed in the next chapter.

4 Estimation of Parameters in the models

The parameters are still to be estimated for the models developed in the former chapters. The parameters estimation is usually formulated as an optimization problem that a cost function measuring the estimation errors is formed and minimized. For nonlinear system, gradient based optimization methods are often used in searching the minimum of estimation errors.[52][53] Local minima, however, exist in the nonlinear optimization problem. In parameters estimation of the models, the existence of local minima will lead to inaccurate estimation.

In this chapter, we will propose a new algorithm of optimization – Evolutionary Parallel Gradient Search (EPGS) and use it to estimate the parameters of the models built. The objective of the algorithm is to find the global minimum in the optimization problem with multiple local minima. The Parallel Gradient Search enables the optimization process to start multi-thread searching at different points simultaneously therefore the opportunity of finding the global minimum is increased. The incorporation of evolutionary concepts in the search helps the search process keep looking for better solutions and ignore the unsatisfied ones. (A simple introduction of gradient search and Evolutionary Algorithm can be seen in the Appendix. [31][32][33][34].)

4.1 The Evolutionary Parallel Gradient Search (EPGS)

In the gradient search, the updating direction is calculated using the gradient information of the cost function without using the value of the cost function [33]. Evolutionary Algorithm, on the other hand, only uses the value of the cost function to keep the best track of searching survive while the gradient information is ignored even

when the gradient is available in the real number optimization problem of continuous cost function [31]. While the value of the cost function tells us how good the current search is, the norm of gradient tells us the expectation of the improvement in the next search at current step. In this study, the Evolutionary Parallel Gradient Search algorithm is proposed to update its search using both the value of the cost function and the gradient so that the optimization will keep the searches with best value of the cost function and the best trend.

The basic idea of Evolutionary Parallel Gradient Search illustrated as follows: The gradient searches start simultaneously from several points; selection, clone, crossover and mutation are applied at each step thereafter to keep the optimization escape from local optima.

The optimization problem discussed is defined as:

Minimize $f(X)$, (4-1)

Subject to: $x_1 \le X \le x_2$.

where, $X \in R^n$ is the optimization variable vector of the problem; $f(X): R^n \to R$ is a real-valued function of vector X that is continuous in R.

The gradient vector of the cost function is defined as:

$$\nabla f(X) = \frac{\partial f(X)}{\partial X}, \tag{4-2}$$

and the norm of the gradient is denoted by $\| \nabla f(X) \|$.

The optimization starts from multiple random points of parallel searches. In each step, the value of the cost function and the gradient are calculated. For the searches with best $f(X)$, they will be updated using gradient search method and then copied directly to

the next generation (Clone). In this way, we keep the best values to the next generation as in EA and at the meantime we can guarantee the improvement with proper chosen step size as in gradient search.

The searches with best trends of the optimization are also kept. A function that estimates the trend of the optimization is defined as:

$$g(X) = f(X) - \| \nabla f(X) \|. \tag{4-3}$$

Since the larger the $\| \nabla f(X) \|$ is, the larger improvement we can expect after the update using gradient search, we can keep the searches with best optimization trend by selecting those with smallest $g(X)$. The reason of including $f(X)$ in this function is that we want to ignore these searches with too large $f(X)$ but with a large $\| \nabla f(X) \|$ since they are too far away from the local minima. The selected ones should have good trend and reasonable value of cost function. Different weights of $f(X)$ and $\| \nabla f(X) \|$ can be applied in the building of $g(X)$ in defining different importance of these two values in the trend. The ones selected by $g(X)$ follow the same procedure: updated with gradient and then copied to the next generation (Clone).

The searches already chosen from above two steps will be passed to the mating pool as fathers of the next generation. Mothers will be chosen from the rest of the search population. Mating of crossover will be applied to those parents to generate their offspring. The reason of separating parents in this way is to prevent premature of the population. Since the searches in the fathers group may be very close to each other after generations, the optimization will be stuck at local minima if we only choose the parents from the ones with best fitness (fathers group). Mutation happens to these offspring at certain rate. These offspring will be filled into the population of next generation.

The rest will be generated randomly if there are still vacancies in the population of next generation.

The procedure of the algorithm can be summarized as following:

1. Initialization. Choose parameters for the optimization process including: learning rate of gradient search λ_l, population of the searches N, clone rate λ_f by fitness function, clone rate λ_g by combination of gradient and fitness function, crossover rate λ_c, mutation threshold μ. A function of $g(X) = f(X) - \| \nabla f(X) \|$ is defined as second criterion of selection so that $\lambda_g N$ individuals with large gradient (better trend of the minimization) are also kept.
2. Start of the optimization: Randomly choose N points in the universe of optimization variable X_1^0, X_2^0, ... X_N^0 for step $k = 0$.
3. In each step k: Calculate the values of fitness function of $f(X_i^k)$, gradient $\nabla f(X_i^k)$ and $g(X_i^k)$ with X_i^k $(i = 0 \ldots N)$.
4. Check if the end condition is met. If yes end; otherwise continue to 5.
5. Update the $\lambda_f N$ individuals with best $f(X_i^k)$ using gradient search and then clone them directly to the next generation
$$X_j^{k+1} = X_j^k - \lambda_l \nabla f(X_j^k), \qquad j = 1 \ldots \lambda_f N$$
6. Update the $\lambda_g N$ individuals with best $g(X_i^k)$ using gradient search and then clone them directly to the next generation
$$X_j^{k+1} = X_j^k - \lambda_l \nabla f(X_j^k), \qquad j = 1 \ldots \lambda_g N$$

7. Choose $\lambda_c N$ individuals randomly from the formerly selected $\lambda_f N + \lambda_g N$ as $X1$, and another $\lambda_c N$ individuals randomly from the rest as $X2$; Mate the two groups with crossover at a random position of r_j^k, where r_j^k is a random value from 0 to 1:

$$X'_j{}^{k+1} = r_j^k X1_j^k + (1 - r_j^k) X2_j^k \qquad j = 1 \ldots \lambda_c N$$

8. Apply mutation to the X'^{k+1} above in the rate of μ: the mutation happens when $abs(m_j^k) < \mu$ where m_j^k is a random number form -1 to 1. The mutation is in the form: $X_j^{k+1} = X'_j{}^{k+1} + m_j^k (x_2 - x_1)$ where, x_1, x_2 are upper and lower bound of X. For the ones without mutation, $X'_j{}^{k+1}$ is directly passed to the next generation as: $X_j^{k+1} = X'_j{}^{k+1}$.

9. Generate the rest individuals randomly to make the total population as N.

10. If X_j^{k+1} is beyond the bound x_1 or x_2, set X_j^{k+1} equal to x_1 or x_2.

11. Goto 3.

The end condition of the optimization process is normally taken as the non-improvement of the fitness or the reach of maximum step. When the optimal value of the fitness function is known, the error between the best value of fitness function of current step and the optimal one can also be used as end condition.

4.2 Parameters Estimation of the Mathematic Model

In this section, we will use the EPGS algorithm to estimate the parameters of the mathematic model in chapter 2. The mathematic model of friction with temperature is rewritten here:

$$F_v = F_{v0} + F_{v1} e^{-\frac{T-T_0}{T_s}}$$

$$F_C = F_{C0} + F_{C1} e^{-\frac{T-T_0}{T_s}}$$

$$F_S = F_{S0} + F_{S1} e^{-\frac{T-T_0}{T_s}} . \qquad (4\text{-}4)$$

Define:

$$X = [F_{v0} \quad F_{v1} \quad F_{C0} \quad F_{C1} \quad F_{S0} \quad F_{S1} \quad T_0 \quad T_s]' .$$

as the parameters to be estimated. The estimation criterion is to minimize the sum of the overall error square as:

$$\min J = \frac{1}{2} \sum_{k=1}^{n} \{[F_{v,T_k} - \hat{F}_{v,T_k}(\hat{X})]^2 + [F_{C,T_k} - \hat{F}_{C,T_k}(\hat{X})]^2 + [F_{S,T_k} - \hat{F}_{S,T_k}(\hat{X})]^2\} \quad (4\text{-}5)$$

where n is the length of the data pairs; the subscript T_k stands for the value is taken at the temperature of T_k.

Treating J as the function $f(X)$ in (4-1) and following the procedure of EPGS optimization in section 1, we have the estimated parameters listed in the following tables (the optimized value of the cost function J equals to 0.93):

Table 3: Estimated parameters in the mathematic model

F_{v0} (NCm/RPM)	F_{v1} (NCm/RPM)	F_{C0} (NCm)	F_{C1} (NCm)	F_{S0} (NCm)	F_{S1} (NCm)	T_0 (°C)	T_S (°C)
0.0011702	0.01181	1.5204	6.6525	3.1204	8.2525	-12.803	11.28

The estimated values of F_v, F_C and F_S based on above parameters and their real values are compared in Figure 8, where the solid curves are the estimated values and the dashed curve are the real values. Since the values are estimated using the data from high speed end, the friction calculated using the model will be multiplied with the reduction ratio of 50 when added to the lower speed end.

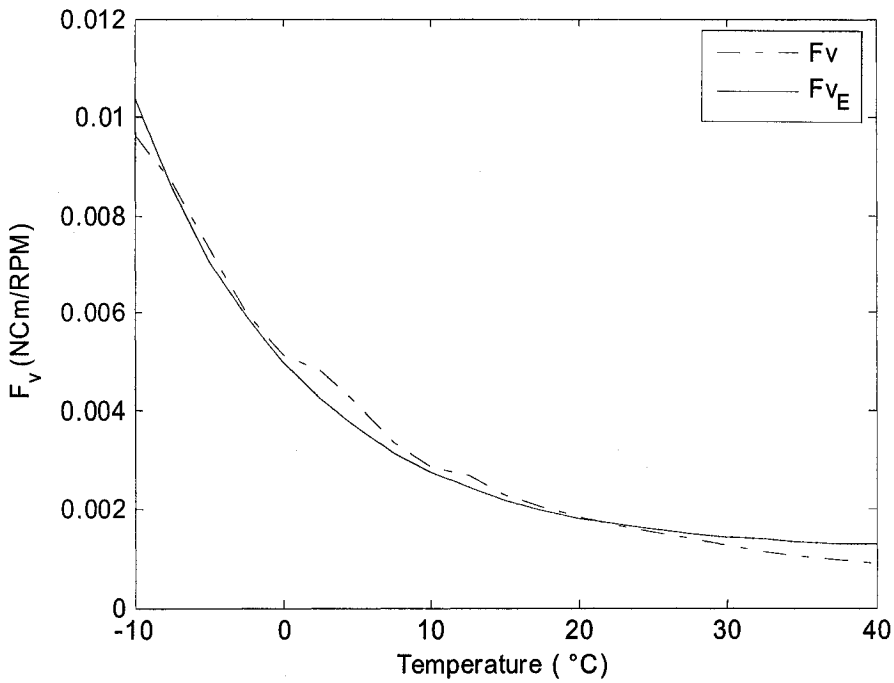

a. F_v and Estimated $\hat{F}_v$ (Fv_E)

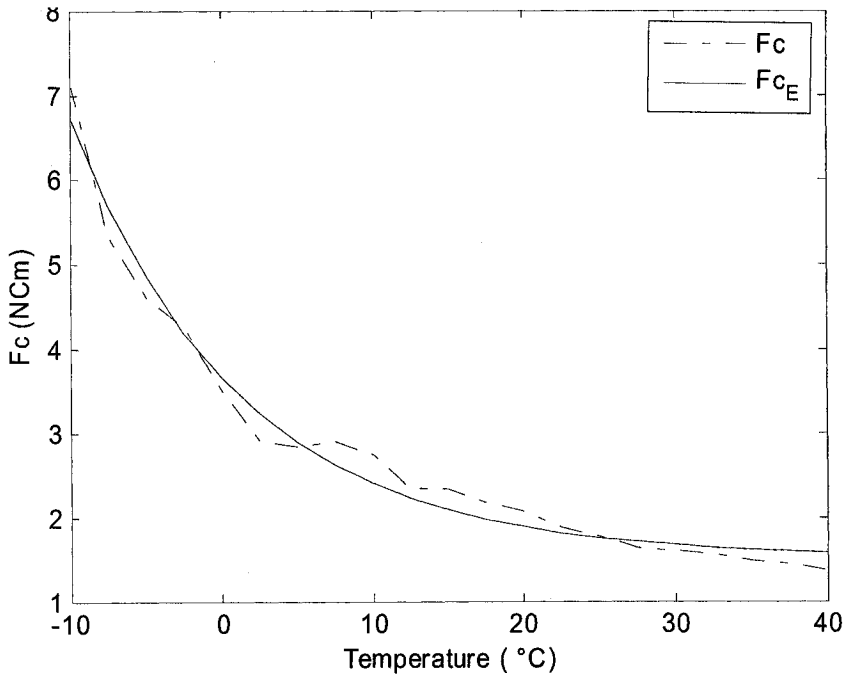

b. F_C and Estimated $\hat{F}_C(Fc_E)$

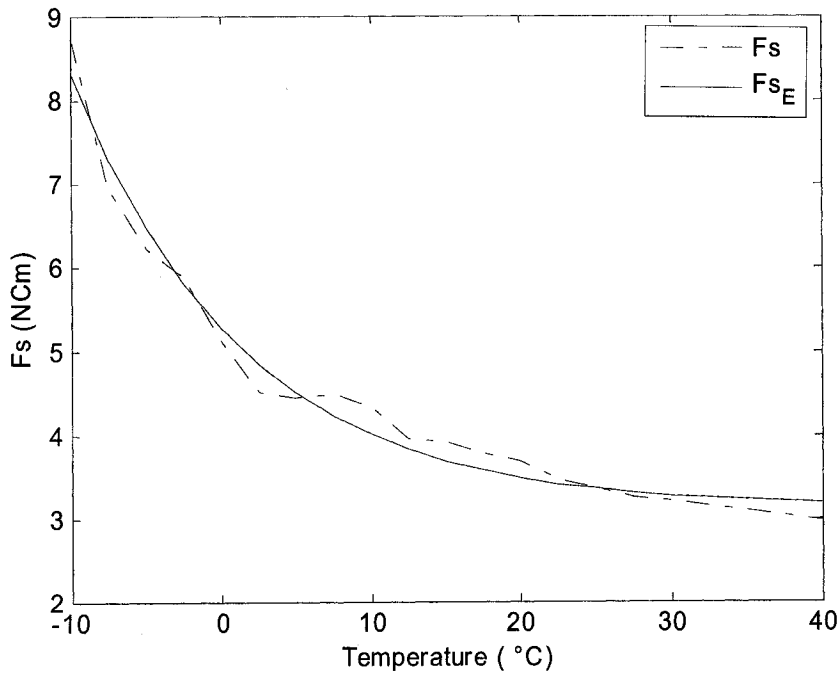

c. F_S and Estimated $\hat{F}_S(Fs_E)$

Figure 8: Estimation results of the mathematic model

4.3 Estimation of the parameters in the Fuzzy model

The EPGS is also applied to the parameters estimation of the Cascaded Fuzzy Model we present in chapter 3. Since the rules in the second layer model (friction vs. velocity) are the output of the first layer model, the parameters to be estimated are T_i and σ_i in the membership function and F_{Si}, F_{Ci} and F_{vi}, $i = 1, 2 \cdots N$ (N=5 in this thesis) in the rules of the first layer. In this section, we will estimate the parameters in the first layer model using EPGS; as a comparison, the results of linear least square method are also present.

4.3.1 Estimation using EPGS

The output of the first layer can be calculated after defuzzification:

$$F_S(T) = \frac{\sum_{i=1}^{N} \mu_{Ti}(T) \cdot F_{Si}}{\Sigma \mu_{Ti}(T)}$$

$$F_C(T) = \frac{\sum_{i=1}^{N} \mu_{Ti}(T) \cdot F_{Ci}}{\Sigma \mu_{Ti}(T)} \qquad (4\text{-}6)$$

$$F_v(T) = \frac{\sum_{i=1}^{N} \mu_{Ti}(T) \cdot F_{vi}}{\Sigma \mu_{Ti}(T)}$$

$$\mu_{Ti}(T) = e^{\frac{(T-T_i)^2}{\sigma_i^2}} \qquad (4\text{-}7)$$

where, $i = 1 \ldots N$ (N is the number of the rules, which is 5 in our research); μ is the exponential membership function; T_i is the center of the exponential function; σ_i is the distribution width for the center T_i.

In the estimation process, the above equation will be used to calculate the estimated values of F_S, F_C and F_v; the real values are shown in Table 2. The parameters to be estimated include the parameters in the membership functions (T_i, σ_i) and the parameters in the fuzzy rules (F_{Si}, F_{Ci} and F_{vi}). Let

$$X = [T_i \quad \sigma_i \quad F_{Si} \quad F_{Ci} \quad F_{vi}], \qquad i = 1 \ldots N$$

be the parameters to be optimized.

The cost function or the function to be optimized is defined as:

$$\min J = \frac{1}{2}\sum_{k=1}^{n}\{[F_{v,T_k} - \hat{F}_{v,T_k}(\hat{X})]^2 + [F_{C,T_k} - \hat{F}_{C,T_k}(\hat{X})]^2 + [F_{S,T_k} - \hat{F}_{S,T_k}(\hat{X})]^2\} \quad (4\text{-}8)$$

where n is the length of the data pairs; the subscript T_k stands for the value taken at the temperature of T_k.

Treating J as the function $f(X)$ in (4-1) and following the procedure of EPGS optimization in section 1, we have the estimated parameters listed in the following tables (the optimized value of the cost function J is 0.13):

Table 4: Estimated parameters of fuzzy model

i	T_i (° C)	σ_i (° C)	F_{Si} (NCm)	F_{Ci} (NCm)	F_{vi} (NCm/RPM)
1	-12.266	1.106	8.8059	7.2059	0.0097752
2	-6.3269	1.0367	6.9638	5.3638	0.008942
3	-3.0956	2.1594	5.9136	4.3136	0.0063127
4	11.033	7.4413	4.560	2.960	0.004052
5	21.224	9.8052	3.1927	1.5927	0.0011374

The membership functions are illustrated in the following figure:

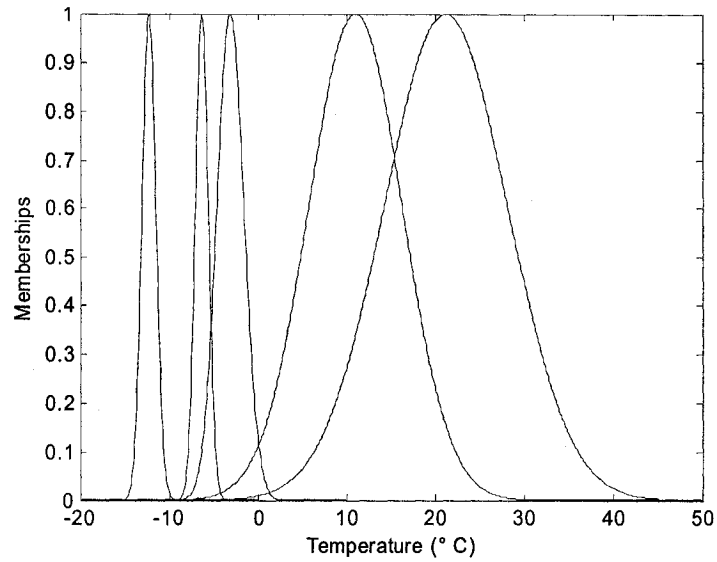

Figure 9: Membership functions with estimated parameters

The comparisons between the real values of F_v, F_C F_S and their estimated values are shown in the next figure.

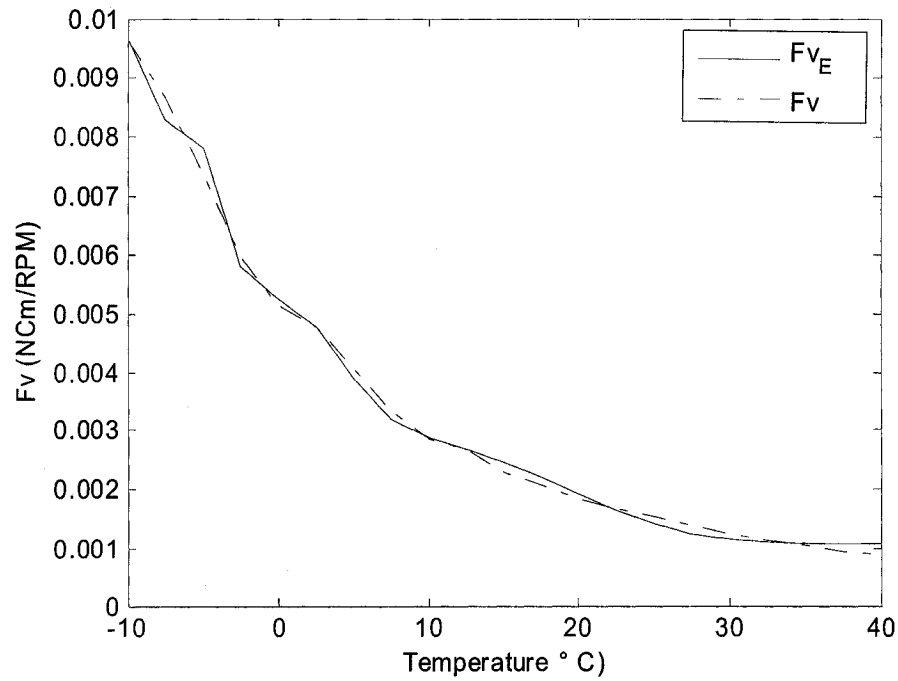

a. F_v and Estimated $\hat{F}_v (Fv_E)$

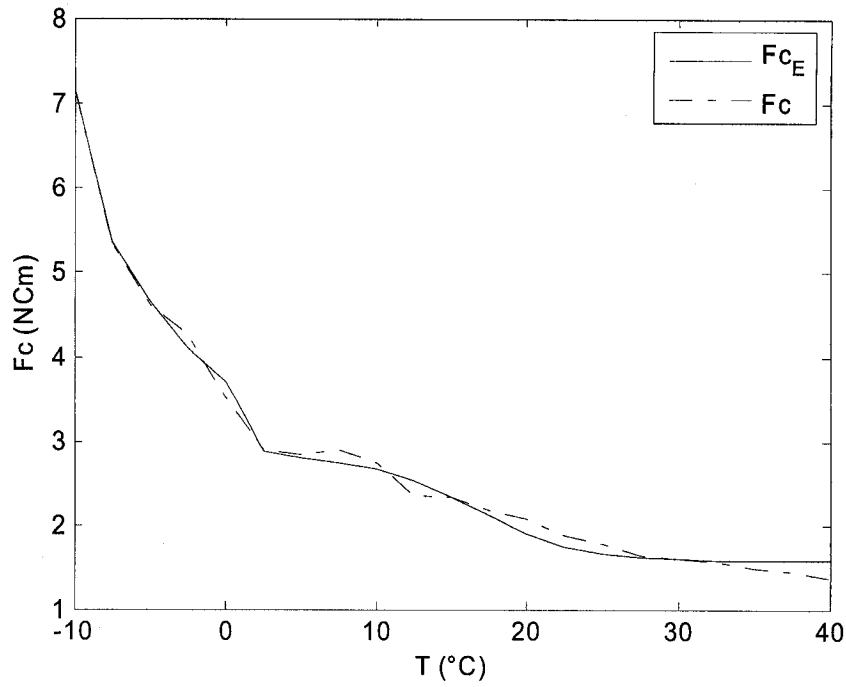

b. F_C and Estimated $\hat{F}_C(Fc_E)$

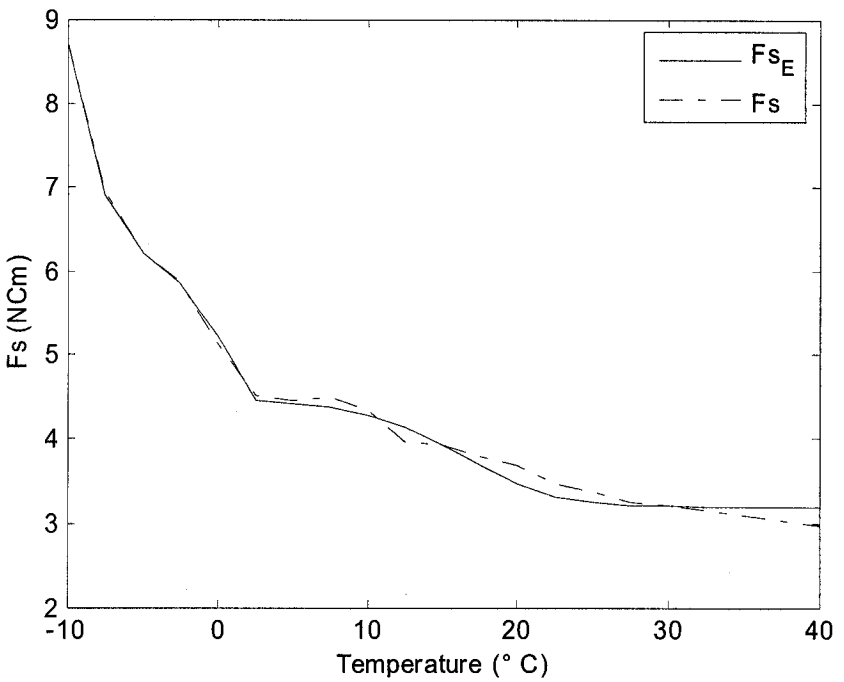

c. F_S and Estimated $\hat{F}_S(Fs_E)$

Figure 10: Estimation results of parameters (fuzzy model with EGPS)

Since the data for estimation are taken from the high speed end, the parameters at the low speed end are listed in Table 5:

Table 5: Estimated parameters – low speed end

i	T_i (° C)	σ_i (° C)	F_{Si} (NCm)	F_{Ci} (NCm)	F_{vi} (NCm/RPM)
1	-12.266	1.106	440.295	360.295	24.44
2	-6.3269	1.0367	348.19	268.19	22.355
3	-3.0956	2.1594	295.68	215.68	15.78
4	11.033	7.4413	228	148	10.13
5	21.224	9.8052	159.635	76.635	2.845

These parameters at the low speed end will be used in establishing the fuzzy model for controller design purpose since the dynamic of the harmonic drive is obtained based on the output shaft.

4.3.2 Estimation with least square method

For the purpose of comparison, we also estimated the parameters in the fuzzy model with least square method. In order to use this method, parameters in the nonlinear parts of the model have to be fixed. By observing the curves of F_S, F_C and F_v over environment temperature T as in Figure 6, the parameters in the membership function are set as in the following table:

Table 6: Parameters of the membership function (LS)

T_i (°C)	T_1 = -10	T_2 = -7.5	T_3 = 0	T_4 = 10	T_5 = 20
σ_i (°C)	σ_1 =1	σ_2 =1.75	σ_3 =3.5	σ_4 =7.5	σ_5 =10

The following figure shows the shape of the membership functions:

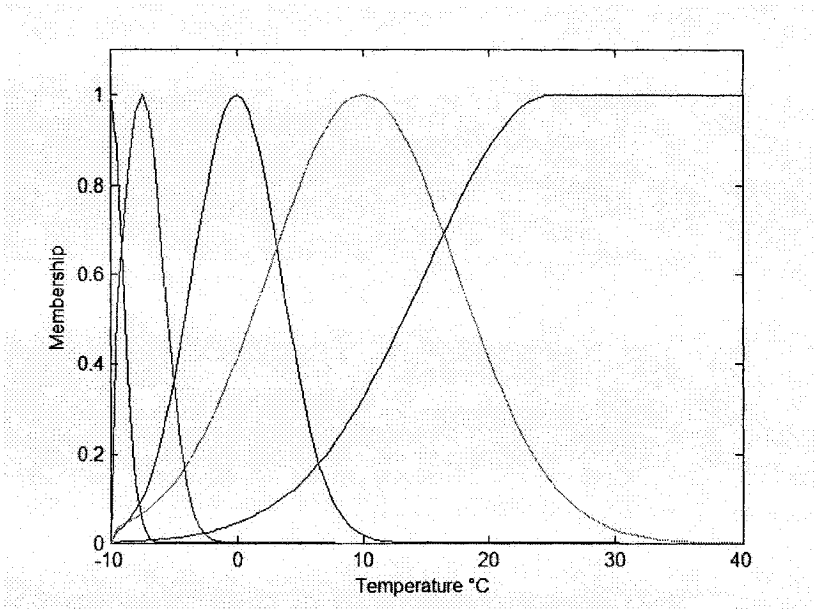

Figure 11: Membership of the first layer model (LS)

Thus the memberships function can be calculated with the value of temperature. The estimation process uses the data in Table 2 where the data pairs of F_S, F_C, F_v and T are available. The estimated values $\hat{F}_S$, $\hat{F}_C$ and $\hat{F}_v$ are calculated using the fuzzy model (4-6).

Let $X = [F_{Si} \quad F_{Ci} \quad F_{v_i}] \qquad (i = 1 \ldots N)$

The cost function are chosen as the Least Square of Error of estimation of F_s, F_C and F_v:

$$\min J = \frac{1}{2}\sum_{k=1}^{n}\{[F_{v,T_k} - \hat{F}_{v,T_k}(\hat{X})]^2 + [F_{C,T_k} - \hat{F}_{C,T_k}(\hat{X})]^2 + [F_{S,T_k} - \hat{F}_{S,T_k}(\hat{X})]^2\} \quad (4\text{-}9)$$

where, F_{S,T_k} stands for the value of F_S at temperature T_k; and same for all other expressions. n denotes the total available data pairs in Table 2. The parameters to be estimated are different F_{Si}, F_{Ci} and F_{vi} that can minimize these cost functions. The estimation problem is indeed a linear least square of error estimation of linear parameters.

The values of the parameters from the estimation are shown in the Table 7 (the optimized value of the cost function J is 0.79):

Table 7: Estimated parameters using LS

T (°C)	-10	-7.5	0	10	25
F_{si} (Ncm)	8.7122	7.4077	5.6062	4.5832	3.0639
F_{ci} (Ncm)	7.1223	5.8077	4.1062	2.9832	1.4639
F_{vi} (Ncm/rpm)	0.0086	0.0085	0.0060	0.0030	0.0009

The results are shown in the following figure.

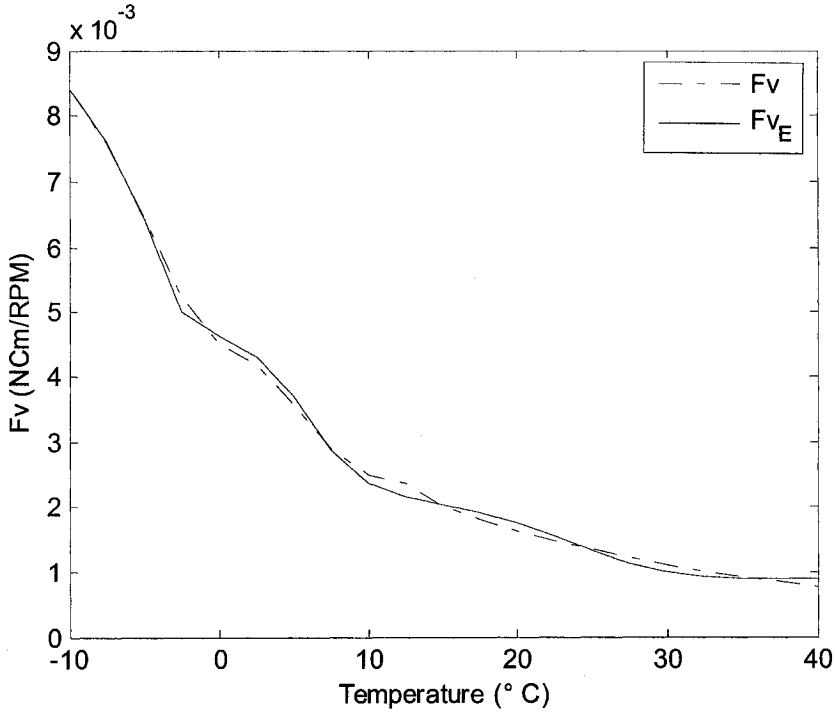

a. F_v and Estimated $\hat{F}_v (Fv_E)$

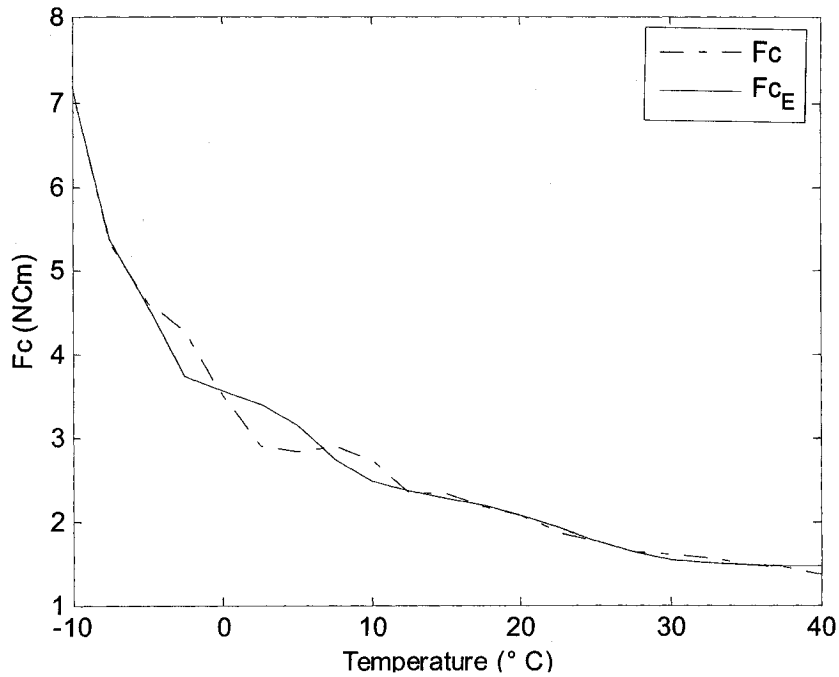

b. F_C and Estimated $\hat{F}_C(Fc_E)$

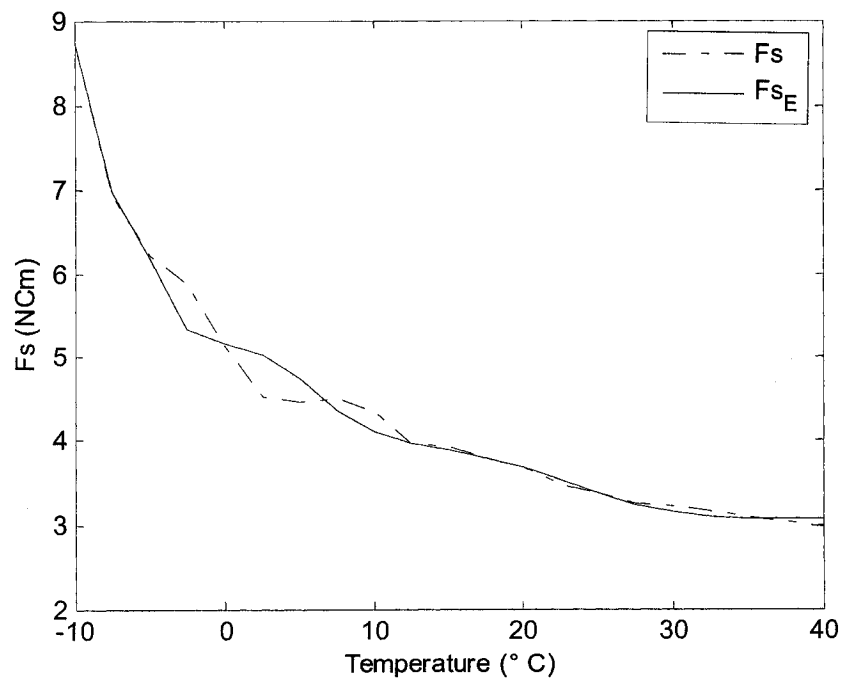

c. F_S and Estimated $\hat{F}_S(Fs_E)$

Figure 12: Estimation results of parameters (fuzzy model with LS)

4.3.3 Analysis

The results of EPGS in Figure 10 are similar to the estimated results using least square method. Both methods can model the friction changing with temperature accurately. From the values of the cost function, the result from EPGS (0.13) is better than that from least square method (0.79). The performance of optimization is improved. Besides, the parameters in membership functions of least square are chosen after several times of trial and error tests. In the method of EPGS, these parameters are chosen by the program automatically. The only thing we need to do is to set the range of each parameter to make the parameters physically reasonable.

4.4 Summary

In this chapter, Evolutionary Parallel Gradient Search has been proposed to estimate the parameters in the models of former chapters. The objective of the algorithm is to help the gradient search method finding global minimum. The estimations have been done for both the mathematic model and the fuzzy model. As a comparison, the result of estimation of the fuzzy model using LS method is also presented. The estimation results show that the algorithm is capable of finding solution in the complicated nonlinear parameters estimation problem of friction modeling. The estimated parameters are used in establishing the model of the harmonic drive and designing the controller.

5 Fuzzy Optimal Controller Design-LMI Approach

After building the fuzzy model in chapter 3 and estimating parameters in chapter 4, this chapter will discuss the controller design problem for such system. With the fuzzy model of friction, the harmonic drive system can be modeled as a fuzzy TS system as we discussed in chapter 3. The stability of the fuzzy TS system can be guaranteed if a Lyapunov function can be found for the system. Since a fuzzy TS system can be modeled as a fuzzy combination of linear system at different operation condition, the techniques of Linear Matrix Inequalities (LMI) can be applied. In this chapter, we will study the LMI based optimal controller of fuzzy TS system. In our study, new constraints are applied to the design procedure in seeking better performance. The constraints are imposed in the LMI form and will be shown in the proposed optimal controller. The proof of stability and optimal criterion are given.

5.1 Problem Statement

The Fuzzy TS model of harmonic drive system to be controlled can be generalized in the following form:

Model Rule i:

If $\phi = \phi_i$ (i=1..N for all N rules of the system), then:

$$\begin{aligned} x(k+1) &= A_i x(k) + Bu(k) \\ y(k) &= Cx(k) \end{aligned}, \tag{5-1}$$

where, A_i, B and C are the matrices in the fuzzy rules as we described in chapter 3: for the system without integrator, they are A_Z, A_H, B and C respectively; for the

system with integrator, they are A_Z^*, A_H^*, B^* and C^*. Therefore, the system dynamic model can be obtained after applying fuzzy inference and defuzzification operation as:

$$x(k+1) = \sum_{i=1}^{N} \alpha_i x(k+1) = \sum_{i=1}^{N} \alpha_i (A_i x(k) + Bu(k)) = \sum_{i=1}^{N} \alpha_i A_i x(k) + Bu(k)$$

$$y(k) = Cx(k), \tag{5-2}$$

where, α_i is the membership of the ith rule and is the function of ϕ that satisfies:

$$\sum_{i}^{N} \alpha_i(\phi) = 1$$

$$\alpha_i(\phi) \geq 0; \tag{5-3}$$

and, ϕ is the vector of variables as the input to the fuzzy inference system.

For the system as (5-2), the controller design problem is defined as: Find a feedback gain F at every sampling time thus the control signal can be calculated as:

$$u(k) = F(k)x(k). \tag{5-4}$$

With this control signal, the stability of the closed loop system:

$$x(k+1) = \sum_{i=1}^{N} \alpha_i A_i x(k) + BF(k)x(k)$$

$$y(k) = Cx(k) \tag{5-5}$$

can be guaranteed; meanwhile, certain performance criterion will also be optimized.

In this study, the upper bound of following quadratic cost function is applied as the optimal criterion:

$$J = \sum_{k=0}^{\infty} \{y^T(k)Wy(k) + u^T(k)Ru(k)\}, \tag{5-6}$$

where, $W = W^T > 0$ and $R = R^T > 0$ are constant weights matrix.

The reason of choosing such criterion is that, with proper chosen weight matrices, both input and output of the system can be tuned and optimized.

5.2 The Optimal Controllers

In this section, a new LMI optimization constraint is proposed to solve the feedback controller design problem of fuzzy TS system as described in section 5.1. The constraint is then applied to design the optimal controller. (The simple description of LMI and its implement in control are given in Appendix C. For more detail of LMI and it's application in control, please refer to [31][65]).

Theorem 1: For the fuzzy system (5-2) with initial states of $x(0)$, the state feedback controller designed as following will stabilize the system and minimize the performance requirement stated in (5-6):

If there exist λ, F_j, G_j, Q_j and Q_l ($j,l = 1..\ N, N$ is the number of the fuzzy rules) that satisfy the following LMIs optimization problem:

$$\min \lambda \tag{5-7}$$

with the constraints of:

$$Q_j = Q_j^T \tag{5-8}$$

$$Q_j > 0 \tag{5-9}$$

$$\begin{bmatrix} \lambda & x^T(0) \\ x(0) & Q_j \end{bmatrix} > 0 \tag{5-10}$$

$$\begin{bmatrix} G_j + G_j^T - Q_j & (A_j G_j + B F_j G_j)^T & G_j^T C^T & G_j^T F_j^T \\ A_j G_j + B F_j G_j & Q_l & 0 & 0 \\ C G_j & 0 & W^{-1} & 0 \\ F_j G_j & 0 & 0 & R^{-1} \end{bmatrix} > 0 \tag{5-11}$$

or equivalently for LMIs, takes $F_j = M_j G_j^{-1}$

$$\begin{bmatrix} G_j + G_j^T - Q_j & (A_j G_j + B M_j)^T & G_j^T C^T & M_j^T \\ A_j G_j + B M_j & Q_l & 0 & 0 \\ C G_j & 0 & W^{-1} & 0 \\ M_j & 0 & 0 & R^{-1} \end{bmatrix} > 0, \tag{5-12}$$

then, the controller designed using the solution of the LMIs in the way:

$$u = \sum_{j=1}^{N} \alpha_j F_j x(k) \tag{5-13}$$

will guarantee the stability of the fuzzy TS system as stated in (5-2) and set the upper bound of the cost function as:

$$J = \sum_{k=0}^{\infty} \{y(k)^T W y(k) + u(k)^T R u(k)\} < x(0)^T P x(0) < \lambda \tag{5-14}$$

$$P = \sum_{j=1}^{N} \alpha_j P_j = \sum_{j=1}^{N} \alpha_j Q_j^{-1} \tag{5-15}$$

where: A_j, B C are the system, input and output matrix in the fuzzy rule as stated in (5-1); W and R are the weights matrix in (5-6); a_j is the membership of each rule.

Proof:

With $Q_j > 0$ ($Q_j = Q_j^T$), we have:

$$(Q_j - G_j)^T Q_j^{-1} (Q_j - G_j) \geq 0 \tag{5-16}$$

which means:

$$G_j + G_j^T - Q_j \leq G_j^T Q_j^{-1} G_j . \tag{5-17}$$

Thus the LMIs above will guarantee:

$$\begin{bmatrix} G_j^T Q_j^{-1} G_j & (A_j G_j + BF_j G_j)^T & G_j^T C^T & G_j^T F_j^T \\ A_j G_j + BF_j G_j & Q_l & 0 & 0 \\ CG_j & 0 & W^{-1} & 0 \\ F_j G_j & 0 & 0 & R^{-1} \end{bmatrix} > 0. \tag{5-18}$$

With Schur Complement, the polynomial form of the LMI is:

$$G_j^T Q_j^{-1} G_j - (A_j G_j + BF_j G_j)^T Q_l^{-1} (A_j G_j + BF_j G_j) - G_j^T (C^T WC + F_j^T RF_j) G_j > 0. \tag{5-19}$$

Takes:

$$\begin{aligned} P_j &= Q_j^{-1} \\ P_l &= Q_l^{-1} \end{aligned}, \tag{5-20}$$

the polynomial is changed to:

$$G_j^T P_j G_j - (A_j G_j + BF_j G_j)^T P_l (A_j G_j + BF_j G_j) - G_j^T (C^T WC + F_j^T RF_j) G_j > 0. \tag{5-21}$$

By multiplying G_j^{-T} and G_j^{-1} on left and right sides respectively, we obtain:

$$P_j - (A_j + BF_j)^T P_l (A_j + BF_j)^T - (C^T WC + F_j^T RF_j) > 0 \tag{5-22}$$

and,

$$P_j - (A_j + BF_j)^T P_l P_l^{-1} P_l (A_j + BF_j)^T - (C^T WC + F_j^T RF_j) > 0. \tag{5-23}$$

In matrix form, the above two inequalities are equivalent to:

$$\begin{bmatrix} P_j & (P_l(A_j + BF_j))^T & C^T & F_j^T \\ P_l(A_j + BF_j) & P_l & 0 & 0 \\ C & 0 & W^{-1} & 0 \\ F_j & 0 & 0 & R^{-1} \end{bmatrix} > 0. \tag{5-24}$$

By multiplying the matrix with α_j then summing up for $j = 1 \ldots N$; and taking:

$$P = \sum_{j=1}^{N} \alpha_j P_j \,, \tag{5-25}$$

we have:

$$\begin{bmatrix} P & \sum_{j=1}^{N} \alpha_j (A_j + BF_j)^T P_l^T & C^T & \sum_{j=1}^{N} \alpha_j F_j{}^T \\ P_l \sum_{j=1}^{N} \alpha_j (A_j + BF_j) & P_l & 0 & 0 \\ C & 0 & W^{-1} & 0 \\ \sum_{j=1}^{N} \alpha_j F_j & 0 & 0 & R^{-1} \end{bmatrix} > 0 \,. \tag{5-26}$$

We define :

$$A = \sum_{j=1}^{N} \alpha_j (A_j + BF_j) \tag{5-27}$$

as the system matrix of the whole closed loop system and

$$F = \sum_{j=1}^{N} \alpha_j F_j \tag{5-28}$$

as the state feedback gain. Thus the following inequality holds:

$$\begin{bmatrix} P & A^T P_l^T & C^T & F^T \\ P_l A & P_l & 0 & 0 \\ C & 0 & W^{-1} & 0 \\ F & 0 & 0 & R^{-1} \end{bmatrix} > 0 \tag{5-29}$$

Again, by multiplying the matrix with α_l and summing up by $l = 1 \ldots N$, one obtains:

$$\begin{bmatrix} P & A^T P & C^T & F^T \\ PA & P & 0 & 0 \\ C & 0 & W^{-1} & 0 \\ F & 0 & 0 & R^{-1} \end{bmatrix} > 0 \,. \tag{5-30}$$

The above inequality can be written in polynomial form as:

$$P - A^T PP^{-1}PA - C^T WC - F^T RF > 0. \tag{5-31}$$

The stability of the system can be guaranteed from (Appendix C):

$$A^T PA - P < -C^T WC - F^T RF < 0. \tag{5-32}$$

By multiplying $x(k)^T$ and $x(k)$ on the left and right sides of (5-31) respectively, we have:

$$x^T(k)Px(k) - x^T(k)A^T PAx(k) - x^T(k)C^T WCx(k) - x^T(k)F^T RFx(k) > 0. \tag{5-33}$$

Since the control signal:

$$u(k) = Fx(k) \tag{5-34}$$

and the output signal:

$$y(k) = Cx(k) \ , \tag{5-35}$$

we have:

$$x(k)^T Px(k) - x(k)^T A^T PAx(k) - y(k)^T W(k)y - u(k)^T Ru(k) > 0 \tag{5-36}$$

which means:

$$y(k)^T W(k)y + u(k)^T Ru(k) < x(k)^T Px(k) - x(k)^T A^T PAx(k). \tag{5-37}$$

For the closed loop system, where:

$$\begin{matrix} x(k+1) = Ax(k) \\ y(k) = Cx(k) \end{matrix} \ , \tag{5-38}$$

the inequality (5-37) can be reformulated as:

$$y(k)^T W(k)y + u(k)^T Ru(k) < x(k)^T Px(k) - x(k+1)^T Px(k+1). \tag{5-39}$$

By summing up by k from 0 to ∞ for the stable system, we have:

$$\sum_{k=0}^{\infty} \{y(k)^T W(k)y + u(k)^T Ru(k)\} < x(0)^T Px(0). \tag{5-40}$$

Since the following inequality is enforced:

$$\begin{bmatrix} \lambda & x^T(0) \\ x(0) & Q_j \end{bmatrix} > 0, \tag{5-41}$$

we have:

$$\lambda - x^T(0) Q_j^{-1} x(0) > 0, \tag{5-42}$$

and, by replacing Q_j^{-1} with P_j:

$$\lambda - x^T(0) P_j x(0) > 0. \tag{5-43}$$

By multiplying the inequality with α_j and summing up by $j = 1 \ldots N$, we have:

$$\lambda - x^T(0) P x(0) > 0. \tag{5-44}$$

Therefore, the cost function is bounded as:

$$\sum_{k=0}^{\infty} \{y(k)^T W(k) y + u(k)^T R u(k)\} < x(0)^T P x(0) < \lambda \tag{5-45}$$

By minimizing λ, we can minimize the upper bound of the cost function.

5.3 Constraints on the Input and Output of the Controllers

The constraints can be applied to the input and output signal with LMI conditions.

1. Constraints on the input signal:

Theorem 2: Considering the state feedback controller design problem of the fuzzy system (5-2), the constraint can be enforced on the control signal by adding the extra LMI in the following form to the controller designed in the section 5.2:

$$\begin{vmatrix} G_j + G_j^T - Q_j & G_j^T F^T{}_j \\ F_j G_j & \mu^2 I \end{vmatrix} \geq 0 \quad . \tag{5-46}$$

With the LMI, the following constraint for the input (control signal) can be guaranteed:

$$\|u\|_2^2 < \mu^2 \lambda \tag{5-47}$$

where, $\|u\|_2$ is the norm of the input (control) signal; μ is the constant of the maximum norm of the control signal which depends on the design of the system.

Proof:

Since, the following inequality holds:

$$G_j + G_j^T - Q_j \le G_j^T Q_j^{-1} G_j, \tag{5-48}$$

the inequality:

$$\begin{vmatrix} G_j + G_j^T - Q_j & G_j^T F^T{}_j \\ F_j G_j & \mu^2 I \end{vmatrix} \ge 0$$

can be transformed to:

$$\begin{vmatrix} G_j^T Q_j^{-1} G_j & G_j^T F^T{}_j \\ F_j G_j & \mu^2 I \end{vmatrix} \ge 0. \tag{5-49}$$

By Multiplying the inequality with $\begin{vmatrix} G_j^{-T} & 0 \\ 0 & I \end{vmatrix}$ on the left side, and $\begin{vmatrix} G_j^{-1} & 0 \\ 0 & I \end{vmatrix}$ on the right side, the inequality is now changed to:

$$\begin{vmatrix} Q_j^{-1} & F_j^T \\ F_j & \mu^2 I \end{vmatrix} \ge 0; \tag{5-50}$$

or,

$$\begin{vmatrix} P_j & F_j^T \\ F_j & \mu^2 I \end{vmatrix} \ge 0 \tag{5-51}$$

by replacing Q_j^{-1} with P_j.

By multiplying the inequality with a_j and summing for $j = 1 \ldots N$, we have:

$$\begin{vmatrix} P & F^T \\ F & \mu^2 I \end{vmatrix} \geq 0 . \tag{5-52}$$

Using Schur Complement, the inequality can be expressed in polynomial form:

$$\mu^2 I > 0, \tag{5-53}$$

and,

$$P - \frac{1}{\mu^2} F^T F \geq 0 \tag{5-54}$$

Thus the following inequality holds:

$$\mu^2 P \geq F^T F . \tag{5-55}$$

By multiplying the inequality with $x(k)^T$ on left side and $x(k)$ on right side, we have:

$$\mu^2 x(k)^T P\, x(k) \geq x(k)^T F^T F x(k) = u(k)^T u(k) = \|u\|_2^{\,2} . \tag{5-56}$$

Since the Lyapunov function is decreasing with k as we discussed in former section about the stability of the system (see (5-32)), we have:

$$x(k)^T P\, x(k) < x(k-1)^T P\, x(k-1) < x(0)^T P\, x(0), \tag{5-57}$$

which means the norm of control signal is bounded.

From (5-44):

$$x(0)^T P\, x(0) < \lambda, \tag{5-58}$$

we have:

$$\|u\|_2^{\,2} < \mu^2 \lambda \tag{5-59}$$

2. Constraint on the output signal

Theorem 3: Considering the state feedback controller design problem of the fuzzy system (5-2), the constraint can be enforced on the output signal by adding the extra LMI in the following form to the controller designed in the section 5.2:

$$\begin{vmatrix} G_j + G_j^T - Q_j & G_j^T C^T \\ CG_j & \gamma^2 I \end{vmatrix} \geq 0.$$

With the LMI, the following constraint for the output can be guaranteed:

$$\|y\|_2^2 < \gamma^2 \lambda \tag{5-60}$$

where,

$\|y\|_2$ is the norm of the output signal; γ is the constant of the maximum norm of the output signal which depends on the design of the system.

Proof:

Since, the following inequality holds:

$$G_j + G_j^T - Q_j < G_j^T Q_j^{-1} G_j, \tag{5-61}$$

the inequality:

$$\begin{vmatrix} G_j + G_j^T - Q_j & G_j^T C^T \\ CG_j & \gamma^2 I \end{vmatrix} \geq 0$$

can be transformed to:

$$\begin{vmatrix} G_j^T Q_j^{-1} G_j & G_j^T C^T \\ CG_j & \gamma^2 I \end{vmatrix} \geq 0. \tag{5-62}$$

By multiplying the inequality with $\begin{vmatrix} G_j^{-T} & 0 \\ 0 & I \end{vmatrix}$ on the left side, and $\begin{vmatrix} G_j^{-1} & 0 \\ 0 & I \end{vmatrix}$ on the right side, the inequality is now changed to:

$$\begin{vmatrix} Q_j^{-1} & C^T \\ C & \gamma^2 I \end{vmatrix} \geq 0, \tag{5-63}$$

or,

$$\begin{vmatrix} P_j & C^T \\ C & \gamma^2 I \end{vmatrix} \geq 0 \tag{5-64}$$

by replacing of Q_j^{-1} with P_j.

By multiplying the inequality with a_j and sum by j, then we have:

$$\begin{vmatrix} P & C^T \\ C & \gamma^2 I \end{vmatrix} \geq 0. \tag{5-65}$$

Using Schur Complement, the inequality can be expressed in polynomial form:

$\gamma^2 I > 0$

$$P - \frac{1}{\gamma^2} C^T C \geq 0. \tag{5-66}$$

Therefore, we obtain the inequality:

$$\gamma^2 P \geq C^T C. \tag{5-67}$$

By multiply the inequality with $x(k)^T$ on left side and $x(k)$ on right side, we have:

$$\gamma^2 x(k)^T P\, x(k) \geq x(k)^T C^T C x(k) = y(k)^T y(k) = \|y\|_2^2. \tag{5-68}$$

Since the Lyapunov function is decreasing with k (see (5-32)), we have:

$$x(k)^T P\, x(k) < x(k-1)^T P\, x(k-1) < x(0)^T P\, x(0) \tag{5-69}$$

which means he norm of control signal is then bounded.

From (5-44):

$$x(0)^T P\, x(0) < \lambda, \tag{5-70}$$

we have:

$$\|y\|_2^2 < \mu^2 \lambda . \tag{5-71}$$

5.4 Remarks

The procedure of design controllers using the theorems above can be summarized as following:

1. With the fuzzy TS model of the system and chosen cost function, the LMI based optimization as stated in the theorem is solved offline. Since the solution of the LMI does not depend on the online information, F_j of each rule is available;
2. The membership a_j of each rule in the fuzzy TS system is calculated at each sampling time with the online information of the input variable of the fuzzy TS system. This input variable or variables are what we use to calculate the membership function, for example, temperature T and the velocity ω;
3. The overall feedback gain is then calculated as $F(k) = \alpha_j F_j$;
4. The control signal of current is calculated and applied to the system as $u(k) = F(k)x(k)$.

One assumption of this procedure is that the information of the input to the fuzzy TS system is available at each sampling time. There are some occasions when this information can not be obtained online. In such case, it is useless to calculate the feedback gain F_j of each rule since the fuzzy combination is unknown without knowing the memberships. Instead, a single feedback gain without using online information is

need. The design of the controller $u(k) = Fx(k)$, where F is the constant state feedback gain calculated offline, then can be formulated as following.

For the fuzzy system (5-2), the state feedback controller designed as following will minimize the performance requirement stated in (5-6).

If there exist λ, F, G and Q as the feasible solutions for following LMIs optimization:

$$\min \lambda \tag{5-72}$$

with the constraints of:

$$Q = Q^T \tag{5-73}$$

$$Q > 0 \tag{5-74}$$

$$\begin{bmatrix} \lambda & x^T(0) \\ x(0) & Q \end{bmatrix} > 0 \tag{5-75}$$

$$\begin{bmatrix} G + G^T - Q & (A_j G + BFG)^T & G^T C^T & G^T F^T \\ A_j G + BFG & Q & 0 & 0 \\ CG & 0 & W^{-1} & 0 \\ FG & 0 & 0 & R^{-1} \end{bmatrix} > 0, \tag{5-76}$$

then the controller:

$$u(k) = Fx(k) \tag{5-77}$$

can guaranteed the stability of the system and minimize the performance requirement stated in (5-6); however, the upper bound of the cost function (λ) in this case might be different from that of the controller designed in section 5.2.

Anther consideration is the use of $x(0)$ in the LMI. It is unrealistic to recalculate the feedback gain offline whenever the initial states changes; therefore, a reasonable upper bound of the states of the system can be used instead.

5.5 Summary

In this chapter, the optimal controller on Fuzzy TS System is proposed by solving LMI based optimization problem. The proof of stability and optimal criterion are given. The procedure of constructing controller with the LMI solution is also presented. In next chapter, the controller will be applied to control the harmonic drive.

6 Control of the Harmonic Drive

In this chapter, we will integrate the results of former chapters to the control of the harmonic drive system with friction changing over temperatures: the mathematic model of the harmonic drive in chapter 2 will be applied as the plant to be controlled; the Fuzzy TS Model of the harmonic drive in chapter 3 will be used to design the controller. The objective of the control is to tracking reference position signal in a temperature varying environment. The controller is constructed using the LMI method proposed in chapter 5 to meet the optimal criterion. Simulation and the results will be given to verify the proposed controller.

6.1 Controller Design

The objective of the controller design is to find a feedback gain so that the control signal at each sampling time can be calculated as $u(k) = F(k) \cdot x(k)$. The control signal at every sampling time should guarantee the stability of the harmonic drive system and tracking the reference position signal.

The reference signal in our simulation has two forms:

1. Step signals range from 0.001 rad to 10 rad with temperature varying from -10 to 40 °C in a sine form of frequency 1 Hz. This is to simulate the machine tracking a large range of different signal in an environment with temperature variation.
2. Constant signals range from 0.001 rads to 1 rad with temperature increasing from -10 to 45 °C in a step of 5 °C every second

Both types of state space expressions of the fuzzy TS model in chapter 3 are used in the controller design: the model with the integrator and the one without. With the consideration of the availability of the temperature information, two controllers are designed for each model. Therefore, totally four controllers are designed in the study.

6.1.1 Controller without temperature information

We will develop a controller without using the information of temperature first because the temperature information may not be available all the time yet the controller has to be working in the whole temperature range. In the case where the measurement of temperature can not be used in the controller, the memberships in the Cascaded Fuzzy Model of friction can not be built online. Thus, a single feedback gain for all rules is needed. This gain is calculated offline with the solution of LMI optimization and used as the feedback gain of the controller. The controller is designed using the method (5-77) discussed in section 5.4. The block diagram of the closed loop system is shown in following figure, where r is the reference signal; y is the output of the system.

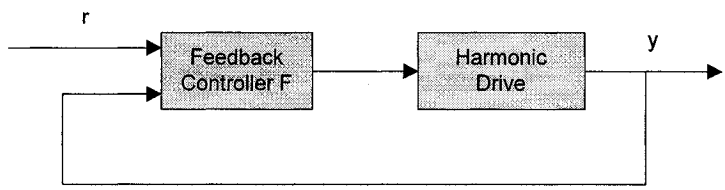

Figure 13: Closed loop system – Controller without temperature

6.1.2 Controller design with temperature information

When the temperature information is available, the memberships in the fuzzy system can be calculated online; therefore, the feedback gain of the controller can be calculated as a fuzzy combination of the feedback gains of all rules, which are obtained

by solving the LMIs offline. The block diagram of the closed loop system is shown in following figure, where r is the reference signal; y is the output of the system; T is the temperature.

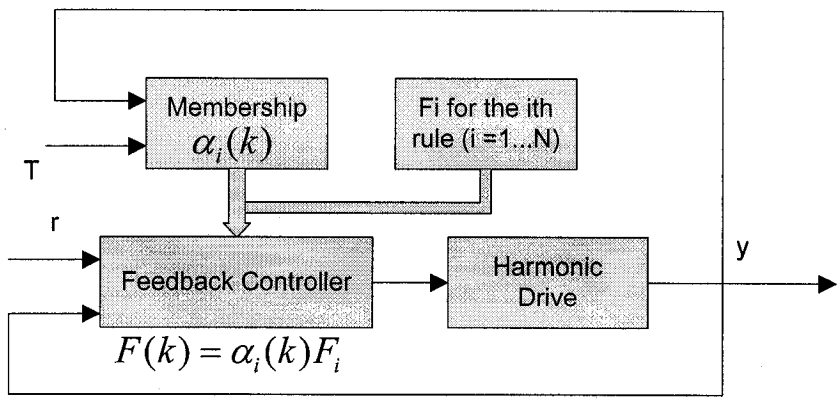

Figure 14: Closed loop system – Controller with temperature

The design of controller follows the technique introduced in theorem 1 of chapter 5. In the controller design of the harmonic drive, A_j is the system matrix of discrete state space expression in each fuzzy rule (A_Z A_H at different temperature of the rules); B is the input matrix; C is identity matrix since all the states are measurable and become outputs.

6.2 Simulation Results and Analysis of Step Input Tracking

In this section, the simulation results for the controllers are presented. The position output of the harmonic drive will track the steps signals in the range of 0.001 rad to 10 rad. Different step sizes are applied at different position range: 0.002 rad for range 0.001 rad to 0.01 rad, 0.02 rad for range 0.01 rad to 0.1 rad, 0.2 rad for range 0.1 rad to 1 rad and 2 rad for range 1 rad to 10 rad. The temperature of the system will change from -10 to 40 °C as a sine signal at frequency of 1 rad/s ($T = \sin(t)$, where T stands for

temperature, t stands for time in second). Four controllers are designed using LMI technique: two without integrator (one with temperature information and the other without) and two with integrator (one with temperature information and the other without). To compare the performance of the closed loop, the results from PID controller are also present.

6.2.1 LMI Controller without using temperature information

The results are shown in Figure 15, where r stands for reference signal; and the theta is the position of the harmonic drive.

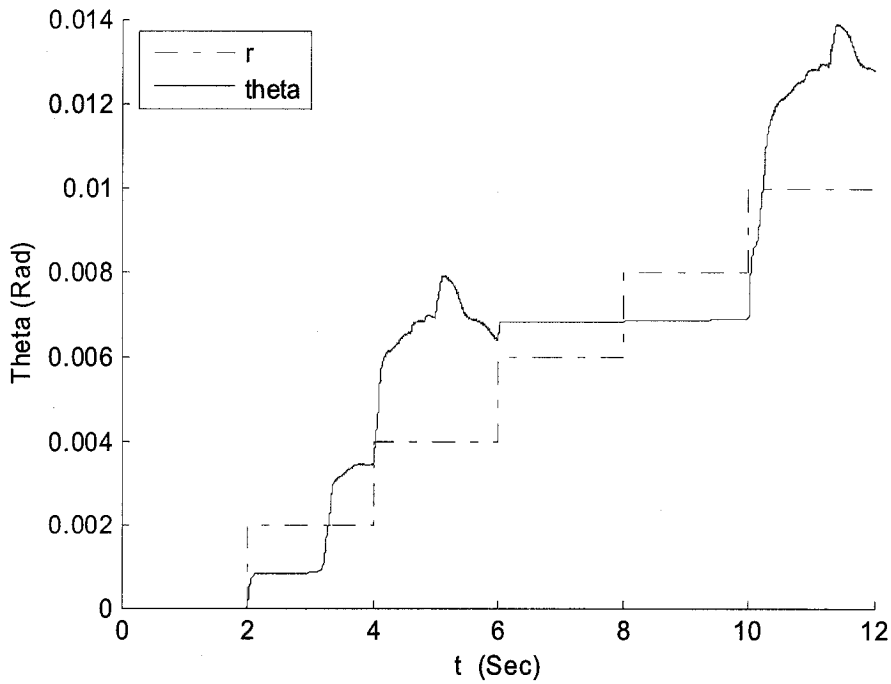

a. Steps from 0.001 to 0.01 rad

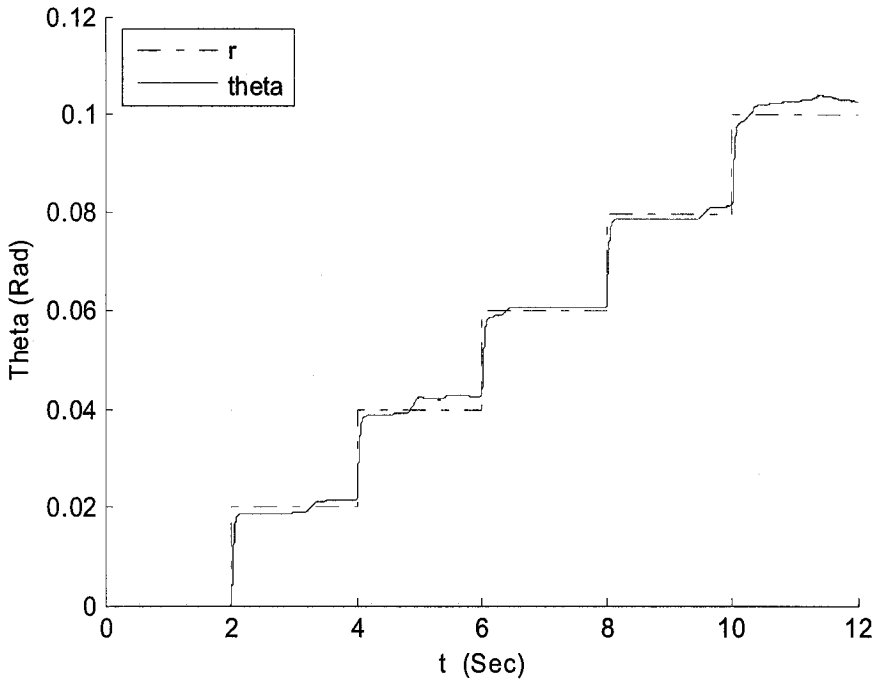

b. Steps from 0.01 to 0.1 rad

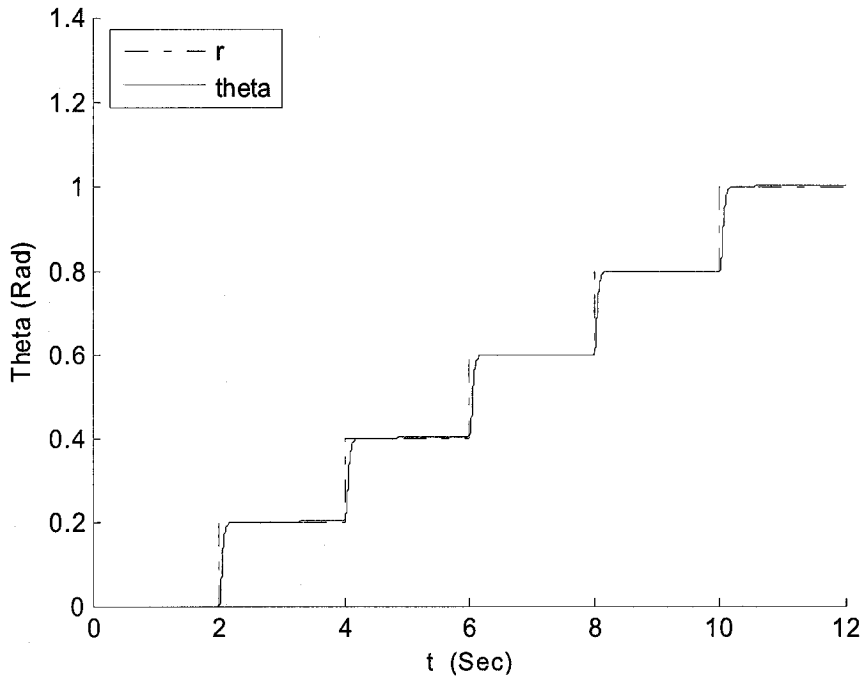

c. Steps from 0.1 to 1 rad

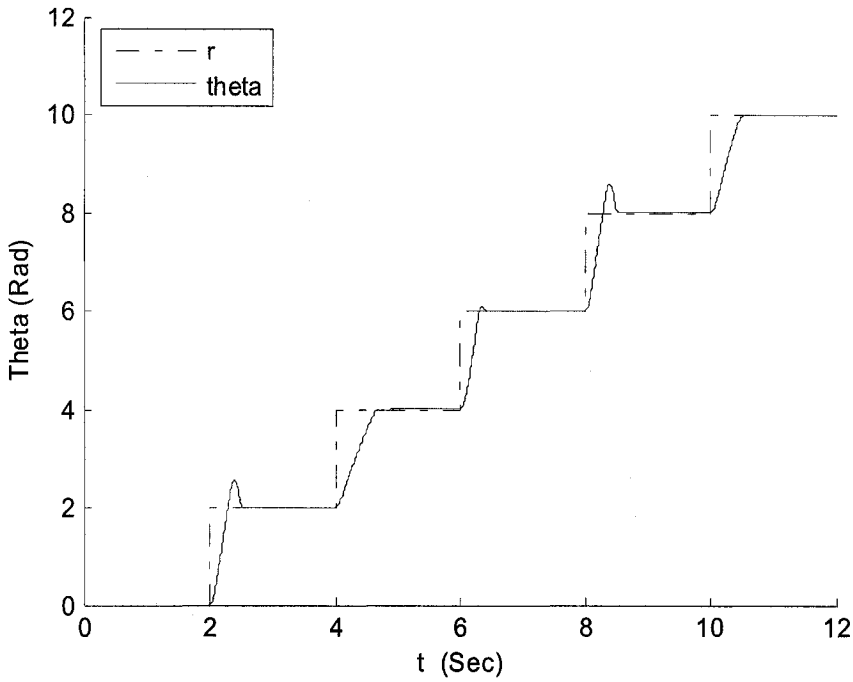

d. Steps from 1 to 10 rad

Figure 15: Simulation results – LMI Controller without integrator and temperature

6.2.2 LMI Controller using the temperature information

The results are shown in Figure 16.

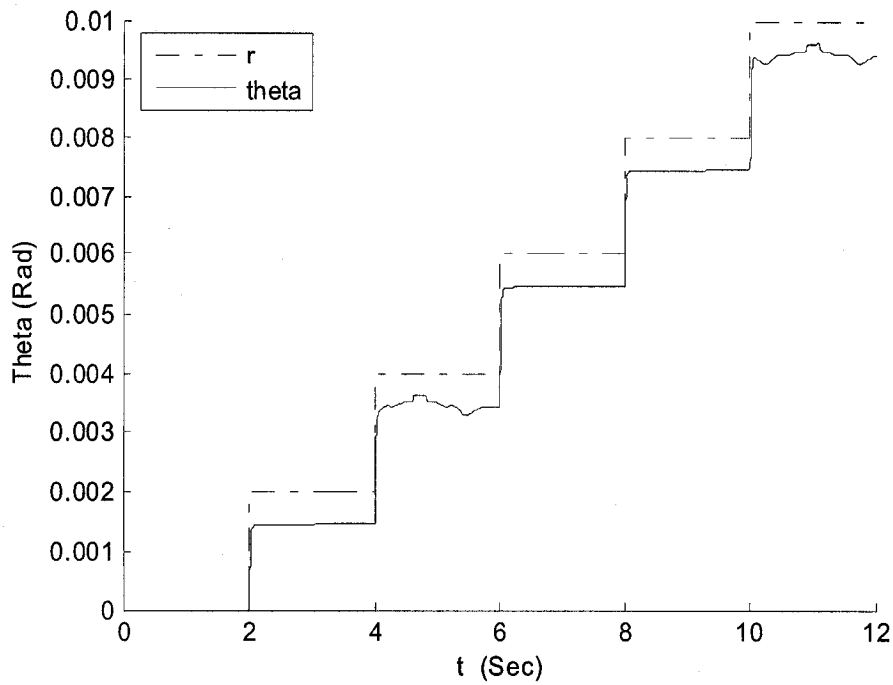

a. Steps from 0.001 to 0.01 rad

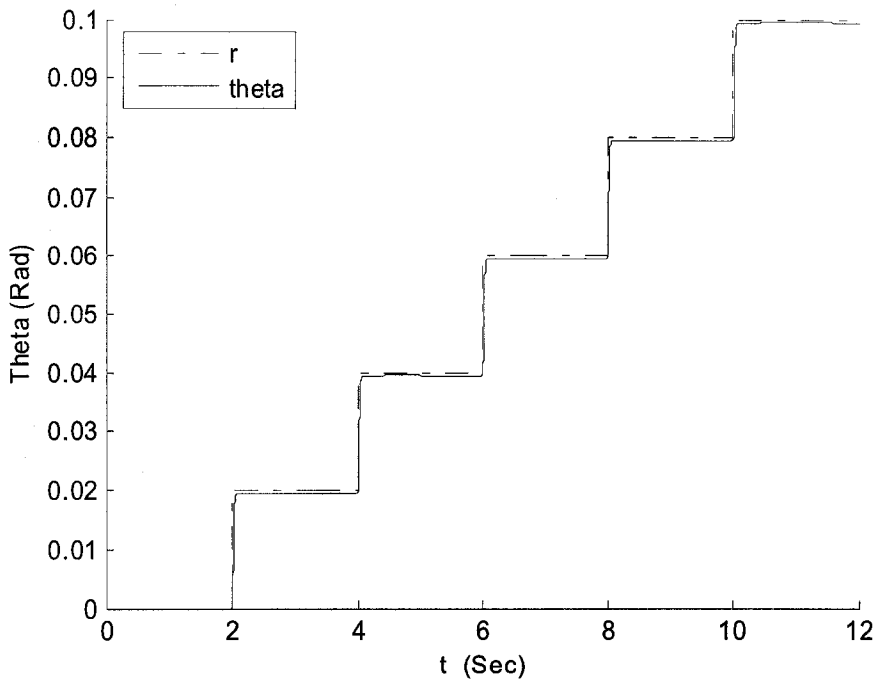

b. Steps from 0.01 to 0.1 rad

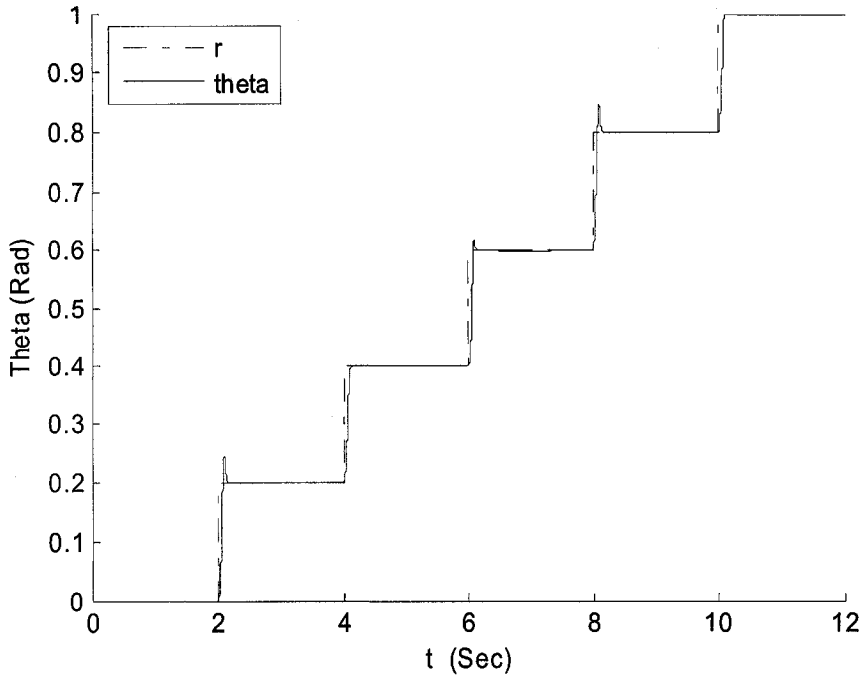

c. Steps from 0.1 to 1 rad

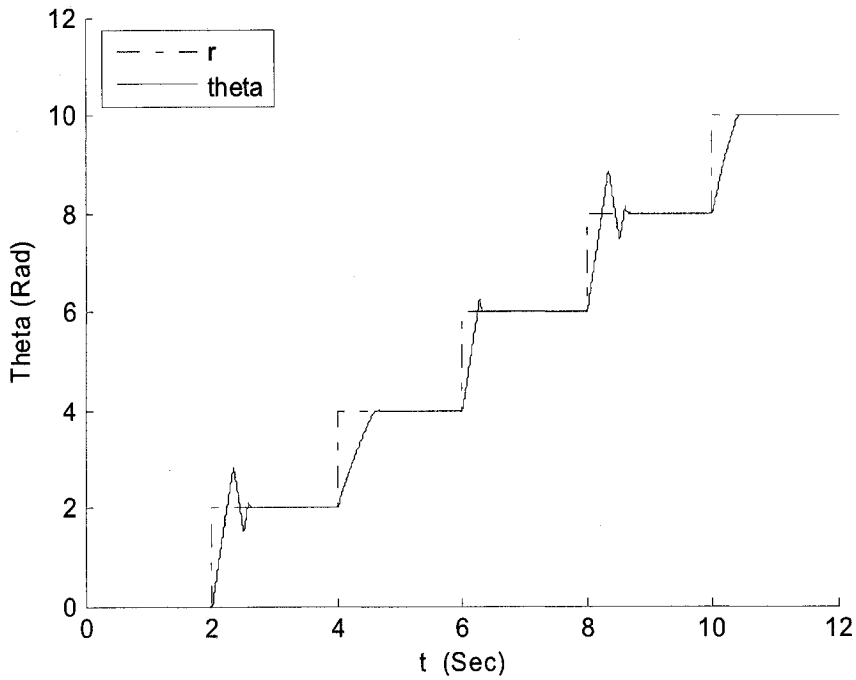

d. Steps from 1 to 10 rad

Figure 16: Simulation results – LMI Controller without integrator but with temperature

6.2.3 LMI Controller with integrator and without using temperature information

The results are shown in Figure 17.

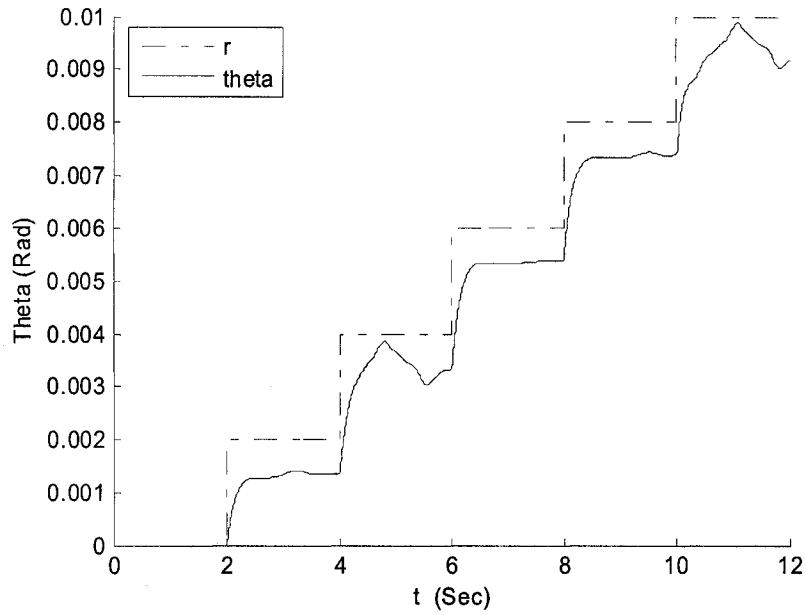

a. Steps from 0.001 to 0.01 rad

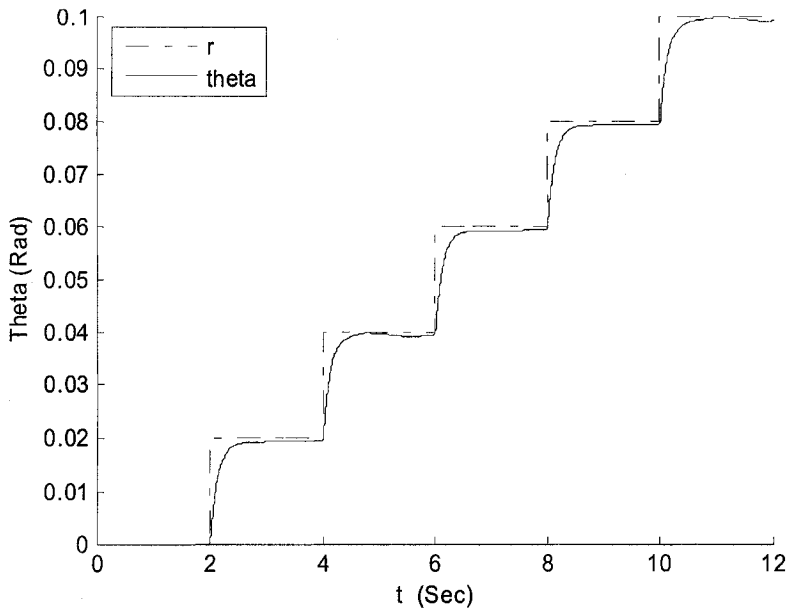

b. Steps from 0.01 to 0.1 rad

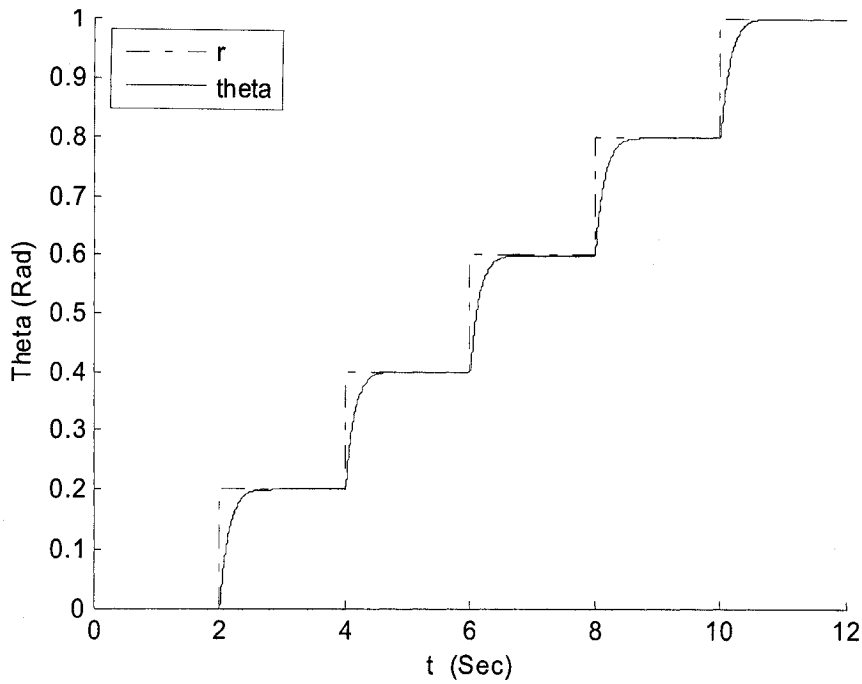

c. Steps from 0.1 to 1 rad

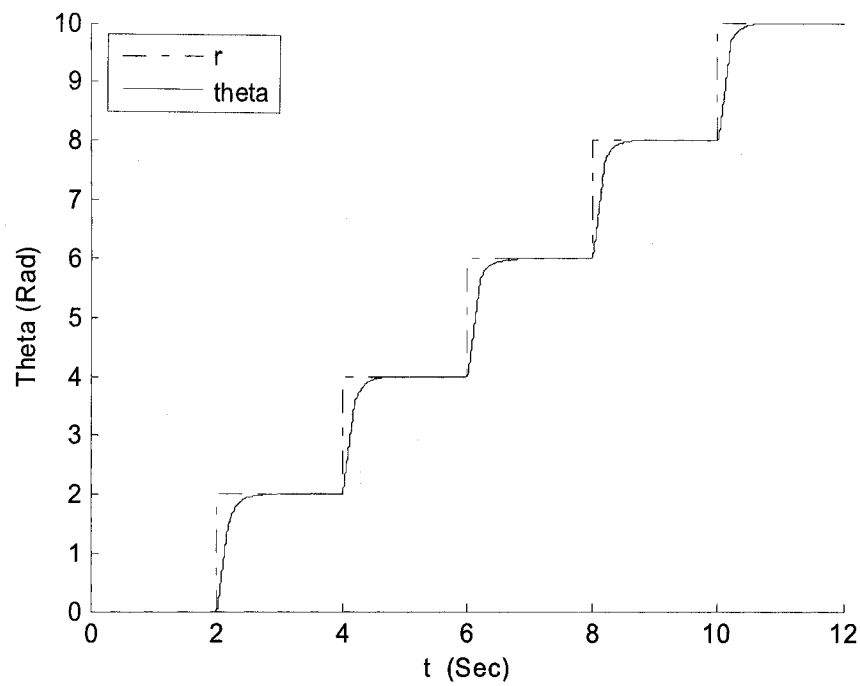

d. Steps from 1 to 10 rad

Figure 17: Simulation results – LMI Controller with integrator but without temperature

6.2.4 LMI Controller with integrator and using the temperature information

The results are shown in Figure 18.

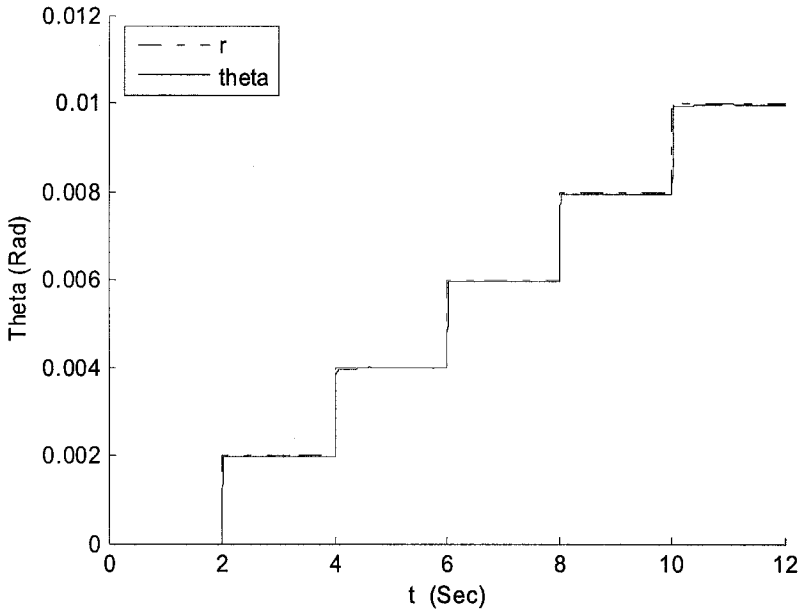

a. Steps from 0.001 to 0.01 rad

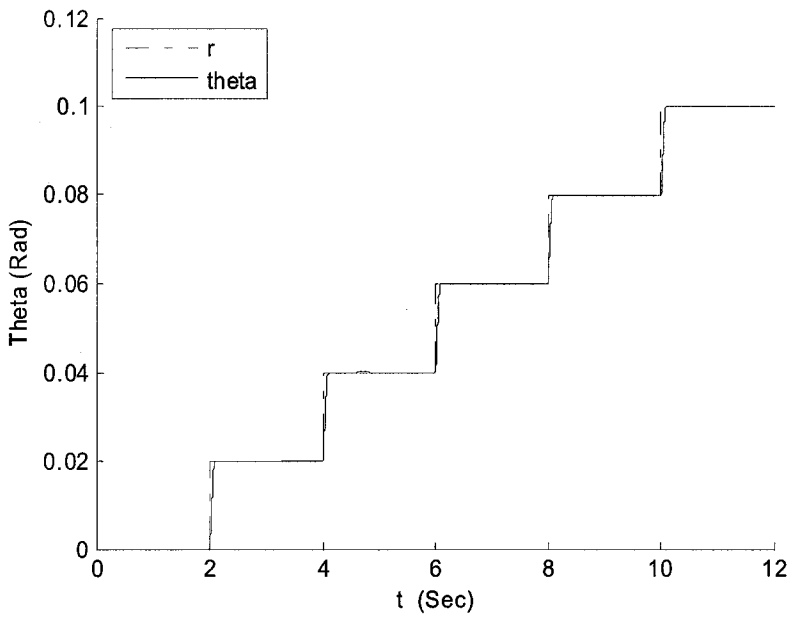

b. Steps from 0.01 to 0.1 rad

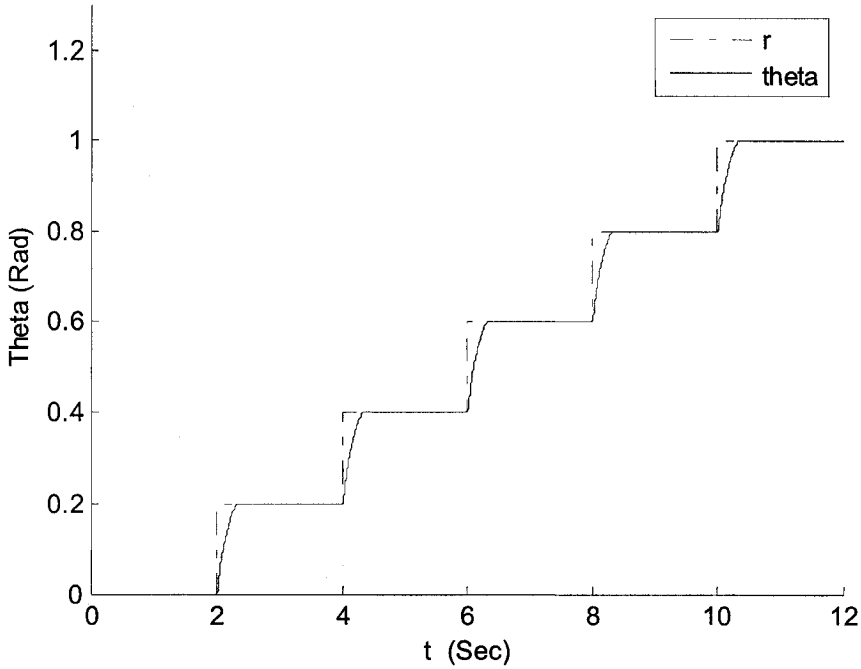

c. Steps from 0.1 to 1 rad

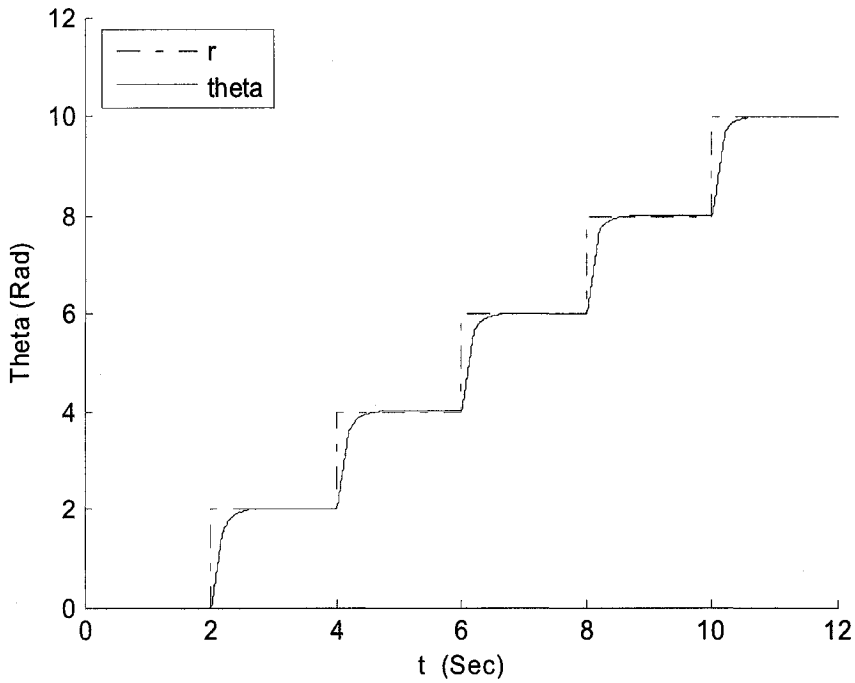

d. Steps from 1 to 10 rad

Figure 18: Simulation results - LMI Controller with integrator and temperature

6.2.5 PID Controller

The parameters of PID controller are optimized using Simulink toolbox of System Response Optimization (the values of these parameters are: 430.1 for P, 1430.1 for I, and 7.95 for D). The reference signal is chosen as a step input of 0.1 rad for the optimization. Other reference signals at different magnitude such as 0.01 and 1 rad are used as well. Since the system is nonlinear, the parameters optimized for one signal in our research is not suitable for others. The results show here are with the parameters having best results when following the step signal form 0.01 rad to 10 rad.

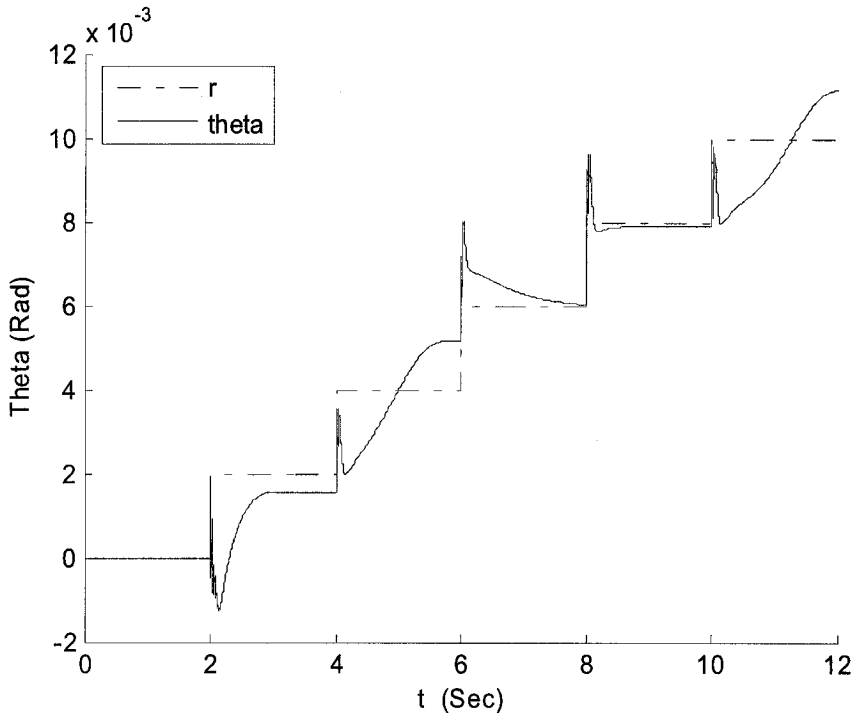

a. Steps from 0.001 rad to 0.01 rad

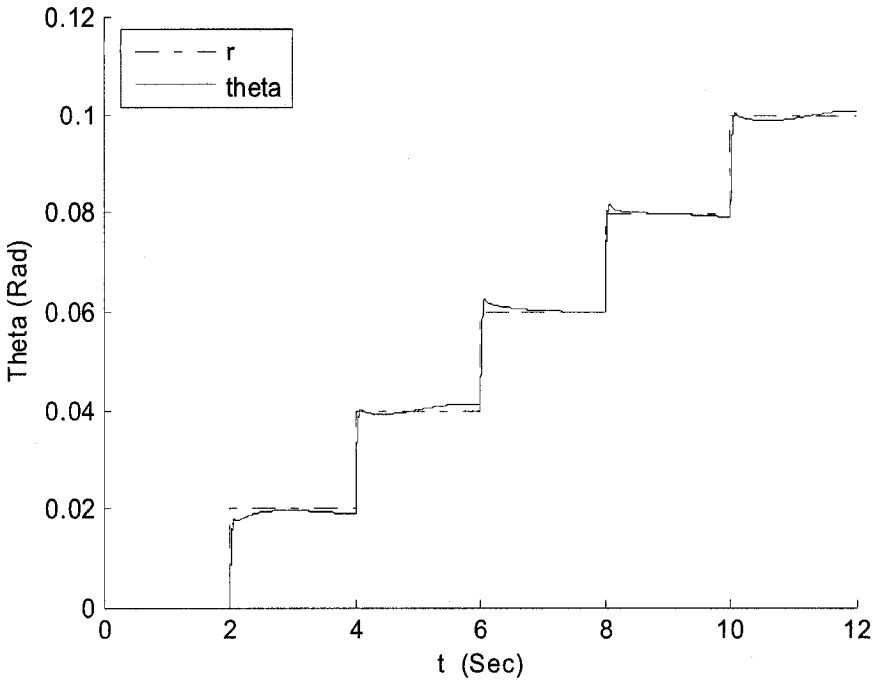

b. Steps from 0.01 to 0.1 rad

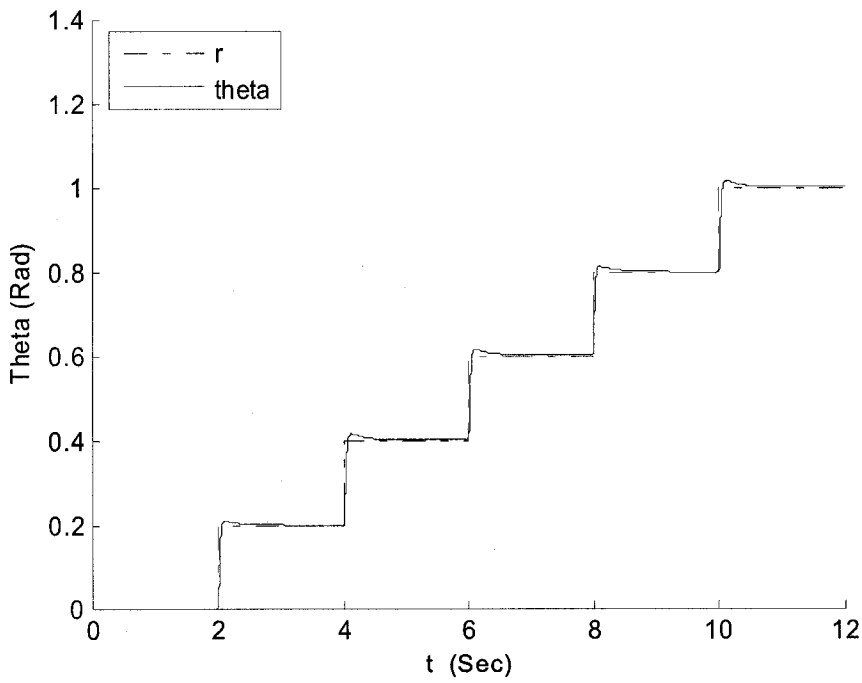

c. Steps from 0.1 to 1 rad

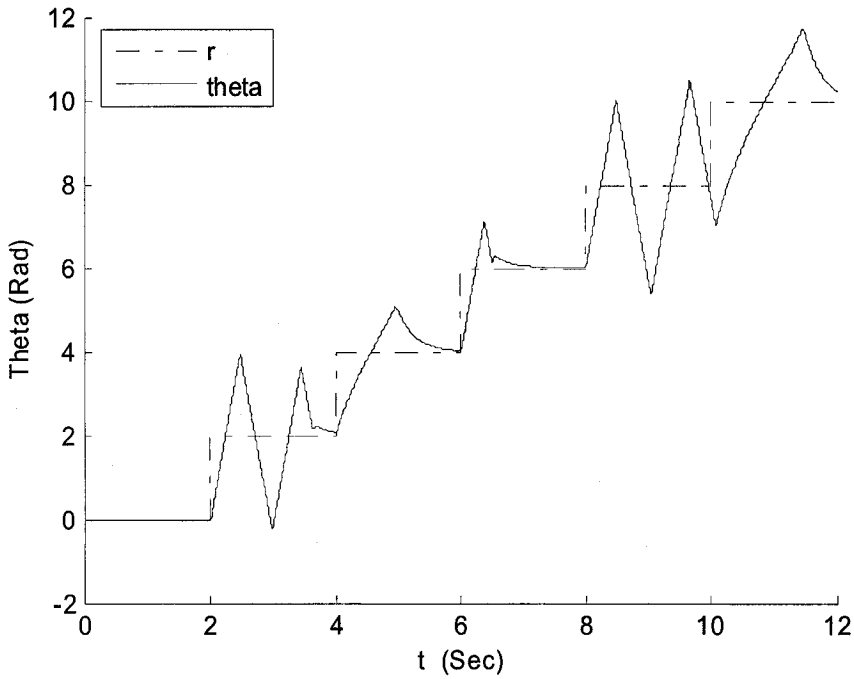

d. Steps from 1 to 10 rad

Figure 19: Simulation results - PID controller

6.2.6 Analysis of the Results

The reason for designing 4 controllers is that we have two conditions to consider: with or without temperature information and with or without integrator. The fuzzy model of the harmonic drive is used to find the feedback gain of each fuzzy rule offline. With the information of temperature, the feedback gain of the system at current temperature and current velocity can be calculated online. However, when the measurement of temperature is not available, the proposed Cascaded Fuzzy Model can still help us to find the feedback gain without using the online information of temperature. The present of integrator is to reduce the steady state errors. When the nonlinear system is modeled as fuzzy TS model, inaccuracy of the modeling will lead to errors. For position control, the

introducing of integrator to the system dynamic equation will reduce the steady state error.

The graphic of the simulation results are shown in section 6.2.1 to 6.2.5. To have a deeper understanding of the simulation results, two Performance Indexes are defined.

Performance Index 1:

$$PI1 = \sum_{k=1}^{n} {e_k}^2 ,$$

where, k is the step of simulation; n is total steps of simulation; e_k is the error in each step.

Performance Index 2:

$$PI2 = \sum_{k=1}^{n} \left| \frac{e_k}{r_k} \right| ,$$

where, k is the step of simulation; n is total steps of simulation; e_k is the error in each step; r_k is the reference signal in each step.

The first PI is the accumulated square of error in the whole simulation process. Since the reference signal to follow is from 0.001 rad to 10 rad in our simulation, the value of this PI may not represent the performance accurately because of the magnitude change in reference signals. The second PI is introduced so that the relative errors can be shown. The PIs of both four controllers are shown in the tables below. Following the sequence of graphic results in this section, the controllers listed as 1, 2, 3, and 4 in the tables stand for the LMI controllers without integrator and temperature, with temperature without integrator, with integrator but without temperature and with integrator and temperature.

Table 8: Performance Index 1 – Step reference

Range (Rad)	0.001 - 0.01	0.01 -0.1	0.1 - 1.0	1.0 - 10
Controller 1	0.0372	0.0666	8.2523	3.18E+03
Controller 2	0.0436	0.0536	7.9018	2.36E+03
Controller 3	0.0071	0.1498	15.8546	1.82E+03
Controller 4	1.56E-04	0.0457	14.9184	1.81E+03
PID Controller	0.0088	0.0267	3.528	1.09E+04

Table 9: Performance Index 2 – Step reference

Range (Rad)	0.001 - 0.01	0.01 -0.1	0.1 - 1.0	1.0 - 10
Controller 1	3.61E+03	382.3288	267.1309	530.5198
Controller 2	1.28E+03	368.393	83.118	455.7531
Controller 3	7.02E+02	434.3771	347.6903	356.1562
Controller 4	109.7897	86.9482	282.2239	347.2837
PID Controller	1.78E+03	201.346	106.626	1.70E+03

From the graphic results and the Performance Index results of the simulation, it is noticed that the controller with integrator and temperature (controller 4) has the best performance in all four LMI controllers and the PID controller when tracking the signal in range 0.001 rad to 10 rad. For both PI 1 and PI 2, controller 4 has minimum values in three ranges. It should be note that when following large position signals such as from 1.0 rad to 10 rad, the results for all controllers are similar. The main difference is in small position following.

The analysis in this section will show how and why the performances of these four controllers are different from each other.

1. The use of temperature information:

The feedback gain of controller without using temperature information is calculated offline based on the solution to the LMI problem. As we can see from Figure 15 and Figure 17, the performance of such controllers varying with the operation points since their feedback gains are totally calculated offline and cannot adapt with the change of operation condition. The other two controllers are also calculated based on the offline solutions to the LMIs; however, they use the information of temperature to calculate the membership and feedback gain online adaptively. From the results of Figure 16 and Figure 18, we can see the performances of the controllers using temperature information are better than those of the controllers without using the temperature information as in Figure 15 and Figure 17.

2. The integrator

The present of integrator to the system will help reduce the steady state error. For the position control problem, a state feedback controller of the second order system of the harmonic drive is equivalent to a PD controller. As we can see from Figure 15 and Figure 16, the tracking errors, especially for a small position, can not be compensated properly. With the integrators, the results are improved greatly especially in the tracking of small signals.

3. Compared to PID controller

When introducing integrator to the harmonic drive system, the controllers designed using LMI are equivalent to PID controllers since the states used in the

controller are velocity, position and integrator of position. However, the gains in the controllers are adaptively changing with the information of the system temperature and velocity. Since the nonlinear character of friction is mainly in the low velocity area, the loss of performance will happen in the low velocity (when tracking small position change) for improper gain. In the PID controller, the parameters are optimized for following the step signal of 0.1 rad. From the results of Figure 19, we can see that the PID controller performs best when tracking the signals range from 0.1 rad to 1 rad and 0.01 rad to 0.1 rad; for range 1 rad to 10 rad, the system has large overshot and even unstable for some signals; for range 0.001 rad to 0.01 rad, the system cannot follow the reference. For a nonlinear system, especially in the case of friction modeling where a constant resistant exists, different gains of the controller will be needed for different conditions. The feedback gain in the LMI controller with temperature is calculated online using the information of the operating condition thus a better performance can be guaranteed.

6.3 Simulation Results and Analysis of Temperature Change

To further verify the proposed controller, we have done simulation for sudden temperature change when the system following a constant signal. The results of the two LMI controllers with integrator are presented. The reference input of the system is constant position signal from 0.001 rad to 1 rad. The temperature increases 5 ° C per second from -10 ° C in a step form.

6.3.1 LMI Controller without Using Temperature Information

The results are shown in Figure 20.

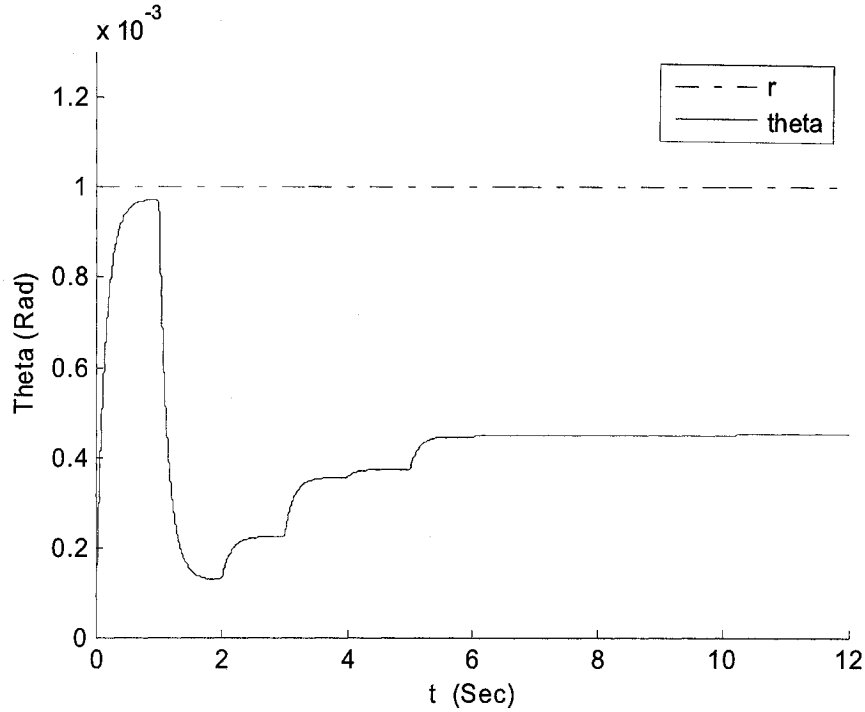

a. Tracking signal: 0.001 rad

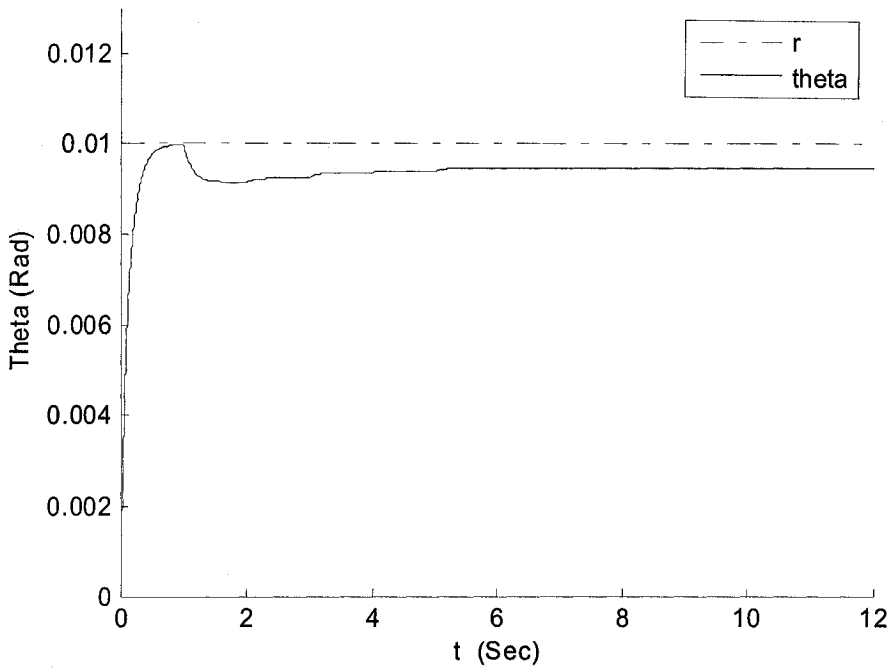

b. Tracking signal: 0.01 rad

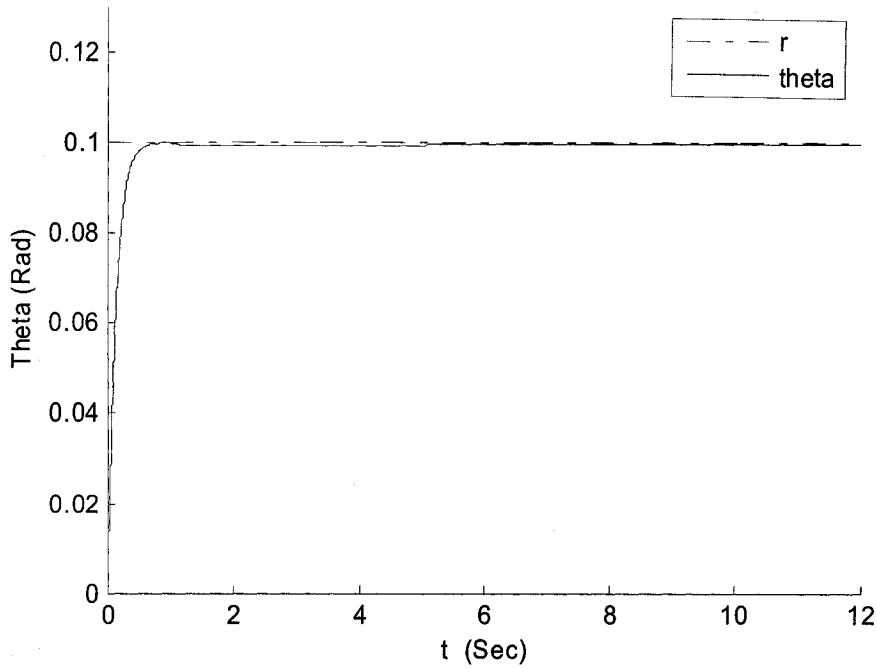

c. Tracking signal: 0.1 rad

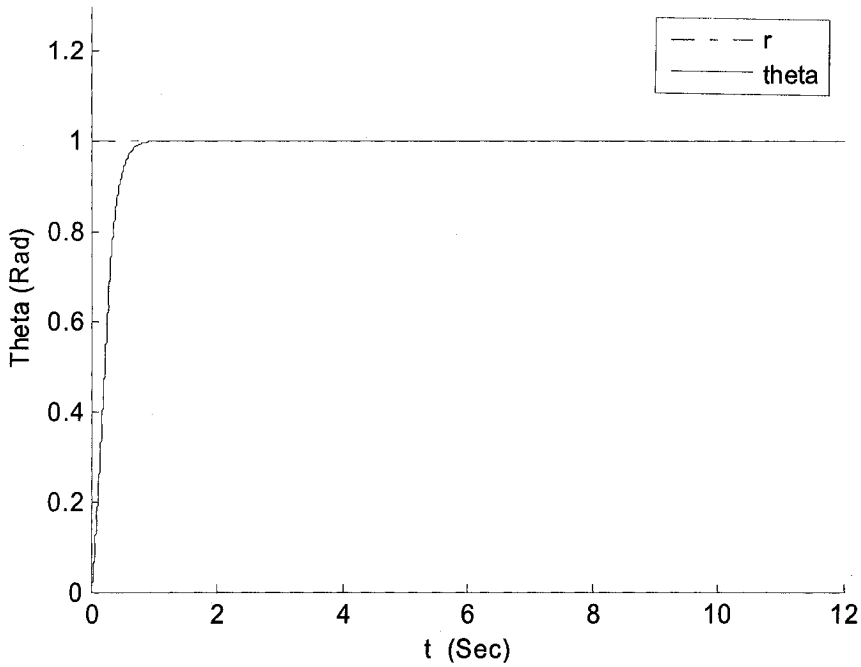

d. Tracking signal: 1 rad

Figure 20: Simulation results (with temperature step changing) – LMI Controller with integrator but without temperature

6.3.2 LMI Controller using Temperature Information

The results are shown in Figure 20.

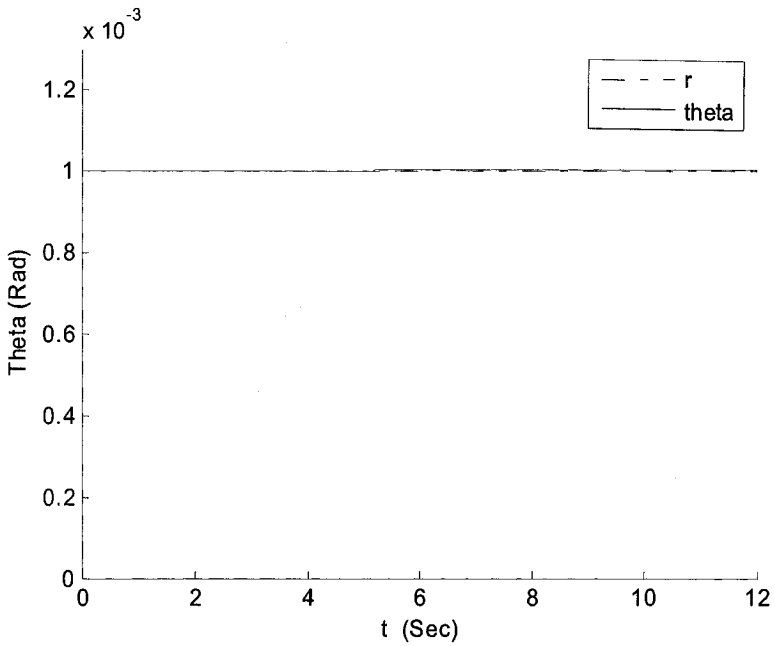

a. Tracking signal: 0.001 rad

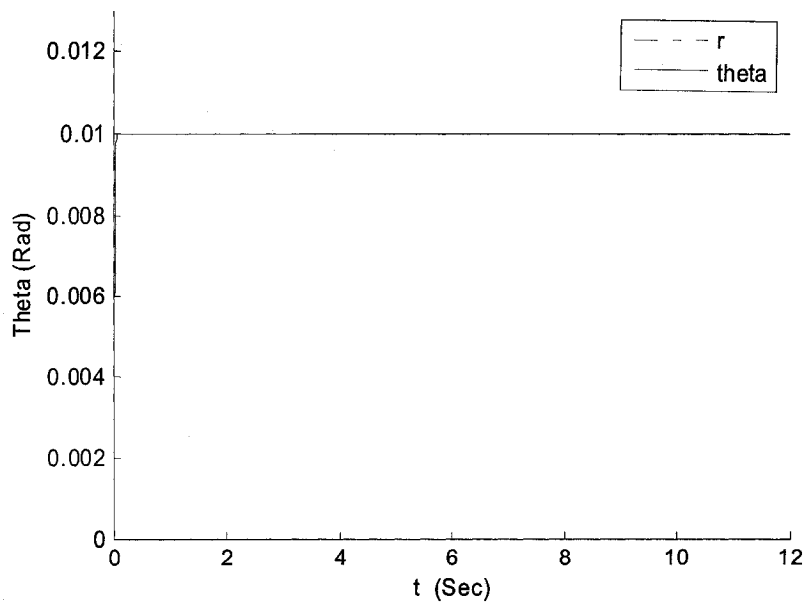

b. Tracking signal: 0.01 rad

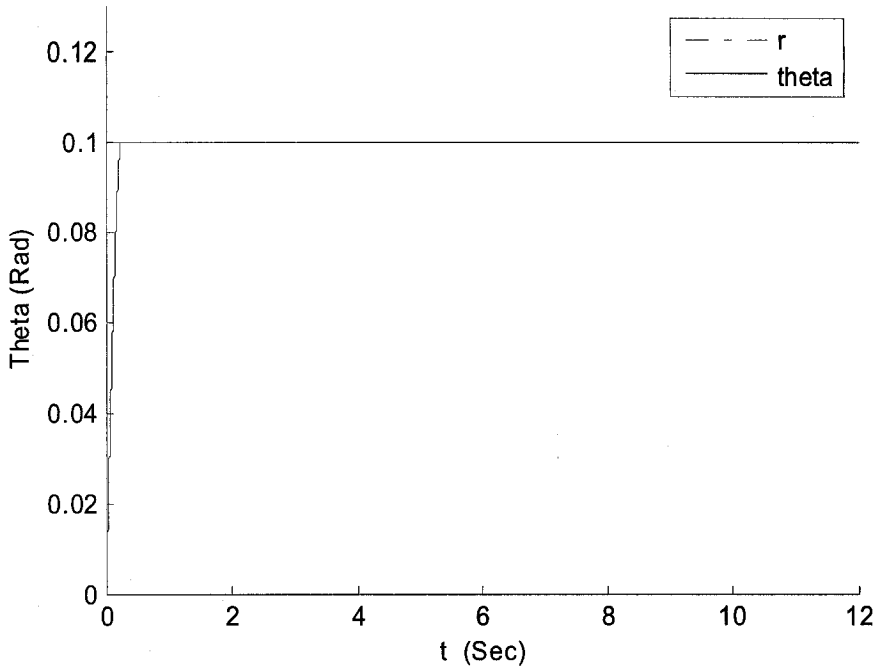

c. Tracking signal: 0.1 rad

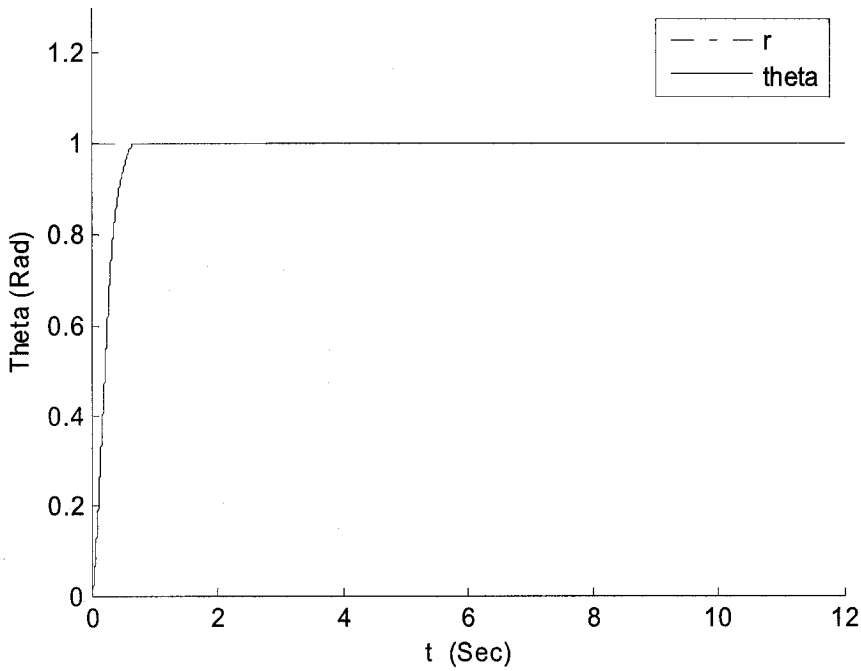

d. Tracking signal: 1 rad

Figure 21: Simulation results (with temperature step changing) – LMI Controller with integrator and temperature

6.3.3 Analysis

The Performance Indexes as defined in 6.2.6 are listed in the following tables.

Table 10: Performance Index 1 – Constant reference

Signal (Rad)	0.001	0.01	0.1	1.0
Controller 3	4.30E-03	0.0104	0.7448	160.3481
Controller 4	5.36E-06	1.60E-03	0.6245	160.1289

Table 11: Performance Index 2 – Constant reference

Signal (Rad)	0.001	0.01	0.1	1.0
Controller 3	6.86E+03	798.3793	205.0648	250.8786
Controller 4	32.8214	27.2289	100.151	245.718

Simulation results show that the performance of the controller with both integrator and temperature (controller 4) is almost unchanged when the environment temperature changes; the other controller with integrator and without temperature (controller 3) has been effected largely by the temperature especially when tracking small reference. This is reasonable since controller 4 calculate the feedback gain online with the information of both temperature and velocity. As a result, the controller using temperature information will be our first choice in control of such a nonlinear system; the other one will work only in the occasion when the temperature information is difficult to get.

6.4 Summary

In this chapter, the LMI based fuzzy controllers have been designed for a harmonic drive system based on the fuzzy models proposed before. Extensive simulations have been carried out to test the performance of the proposed controllers on the model of

the harmonic drive with friction. The simulations include tracking step signals of different magnitudes with environment temperature changing in sine form and tracking step signals under step changing temperatures. The results of simulation shows that LMI based controller with both integrator and temperature information performs the best compared with other controllers.

7 Conclusion and Future Work

7.1 Conclusions

In this thesis, we have studied the phenomenon of how friction changes with temperature in a lubricated system of harmonic drive. The mathematic model of such phenomenon is built and the dynamic of the harmonic drive is expressed with the consideration of temperature. Fuzzy model of friction is developed to convert the nonlinear system as a fuzzy combination of linear system. EPGS algorithm has been proposed to estimate the parameters in the fuzzy model. Optimal Controllers of the fuzzy model are built using LMI optimization technique. The main contributions of the research are as follows:

1. The mathematic model of friction with temperature is established:

   Temperature plays an important role in the accuracy of friction modeling. In most case, however, temperature is taken as constant and its effects are ignored. The proposed model considers the information of temperature and takes the parameters in the model as functions of temperature. The friction at different temperature, therefore, can be estimated with the information of temperature and velocity. The estimation result of the model is consistent with the real values of friction.

2. The Cascaded Fuzzy model of friction is proposed:

   The Cascaded Fuzzy model of friction is proposed to convert the nonlinear model of friction to a fuzzy combination of linear functions. The model utilized two

layers of structure so that the parameters in the rules of the second layer can be determined by the first layer with the information of temperature. The value of friction is then calculated by the second layer with these parameters and the information of velocity. With this model, not only we can estimate the value of friction accurately but also we can apply the linear controller design technique to the system with such nonlinear friction.

3. The EPGS algorithm is proposed for the parameters estimation.

Evolutionary Parallel Gradient Search algorithm is proposed to help the gradient method to escape from local minima in optimization problem. The algorithm starts multi-thread gradient search at random points and applies the concepts in Evolutionary Algorithm such as Selection, Clone, Crossover and Mutation to each search. With parallel search, the algorithm increases the opportunity of hitting the global minimum; with the evolutionary technique, the algorithm guarantees the improving of the searching over steps. The algorithm is applied in our problem of parameters estimation. For both mathematic model and the fuzzy model, the algorithm succeeds in finding the proper values of the parameters.

4. An LMI based Fuzzy controller is designed.

A new constraint is applied to the LMI optimization based controller design procedure. By applying this constraint, an optimal controller design method of the Fuzzy TS system is proposed with the proof of stability. The proposed controller calculates the feedback gain of each fuzzy rule offline; by utilizing the online

information of temperature and velocity, the feedback gain of the whole system is calculated online in each sampling time as a fuzzy combination of the offline feedback gains.

5. Application to the harmonic drive

The controller is applied to the control problem of the harmonic drive with friction. From the simulation results, the proposed controller shows excellent performance in tracking a large range of position signal from 0.001 to 10 rad with temperature variation in both sine form and step form.

7.2 Recommendations for Future Work

1. Experiment setup for the harmonic drive system

To test the previous results in the real system, the experiment hardware for the harmonic drive system should be prepared including: the mechanical setup for the harmonic drive; the chamber simulating the temperature changing environment; data acquisition system; sensor system; temperature regulation system and others.

2. Experiments on the test bed of harmonic drive system

Data collection for the real system is needed in order to have the accurate parameters of the friction models. The controller is also to be tested in the test bed that simulates the real environment with temperature change.

3. Experiments in larger temperature range

The models in the thesis are built for the system operating in a large temperature range. The temperature range is from -10 to 40 ° C for the data collected from the catalog of the manufacture. With experiment setup, this range should be enlarged with the data collected in the experiment environment.

4. Test on other systems

The friction models built in this thesis are supposed to work for all lubricated mechanical system with friction. Therefore, the test and justification for the models in other systems are needed.

Reference:

[1] B. Bhushan., " Introduction to Tribology". John Wiley & Sons, 2003.

[2] B. Bhushan., "Modern Tribology Handbook." CRC Press, 2001.

[3] H. Olsson, K. J. Astrom, C. C. de Wit, M. Gafvert and P. Lischinsky. "Friction models and friction compensation," *European Journal of Control,* Vol 4, no. 3, pp. 176-195, 1998.

[4] C. C. de Wit, C., Olsson, H., Astrom, K.J. and Lischinsky, P. "A new model for control of systems with friction." IEEE Transactions on Automatic Control, Volume 40, Issue 3, Page(s):419 – 425, , Mar. 1995.

[5] V. Lampaert, J. Swevers and F. A. Bender. "Comparison of model and non-model based friction compensation techniques in the neighborhood of pre-sliding friction." Proceeding of the American Control Conference, 2004.

[6] F. Al-Bender, V. Lampaert and J. Swevers. "The Generalized Maxwell-Slip Model: A novel Model for Friction Simulation and Compensation." IEEE Transactions on Automatic Control, Vol. 50, No. 11, Page(s): 1883 -1887, Nov. 2005.

[7] D. Stajić, N. Perić and J. Deur. "Friction Compensation Methods in Position and Speed Control Systems." IEEE International Symposium on Industrial Electronics, Bled, Slovenia, pp. 1261-1266, 1999.

[8] V. J. Majd and M. A. Simaan. "A continuous friction model for servo systems with stiction." Proceedings of the 4th IEEE Conference on Control Applications, Page(s):296 – 301, Sep. 1995.

[9] G. Ferretti, G. Magnani and P. Rocco. "Single and multistate integral friction models." IEEE Transactions on Automatic Control, Vol. 49, Issue 12, Page(s):2292 – 2297, Dec. 2004.

[10] G. Ferretti, G. Magnani and P. Rocco. "An integral friction model." P. IEEE International Conference on Robotics and Automation, Vol 2, Page(s):1809 – 1813, 2004.

[11] C. Makkar, W. E. Dixon, W. G. Sawyer and G.Hu. "A New Continuously Differentiable Friction Model for Control Systems Design." IEEE International Conference on Advanced Intelligent Mechatronics, Page(s): 600-605, 2005.

[12] L. Marton. "Friction model for low velocities: proprieties and applications." Proceedings of the Fourth International Workshop on Robot Motion and Control, Page(s):333 – 338, 17-20 June, 2004.

[13] M. Fun and M.T. Hagan "Modular neural networks for friction modeling and compensation." IEEE International Conference on Control Applications, Page(s):814 – 819, 1996.

[14] D.W. Vos, L. Valavani and A.H. von Flotow. "Intelligent model reference nonlinear friction compensation using neural networks and Lyapunov based adaptive control." IEEE International Symposium on Intelligent Control, Page(s):417 – 422, 1991.

[15] P. S. Gandhi, F. H. Ghorbel and J. Dabney. "Modeling, Identification, and Compensation of Friction in Harmonic Drives." IEEE Conference on Decision and Control, Page(s): 160 -166, Dec. 2002.

[16] J. Juang and J.i Chen, "On combining adaptive estimation and robust control for friction compensation", Fifth World Congress on Intelligent Control and Automation, Vol. 5, Pages: 4396 - 4400, Jun. 2004.

[17] R. Dhaouadi, F. H. Ghorbel and P. S. Gandhi. "A New Dynamic Model of Hysteresis in Harmonic Drives." IEEE Transactions on Industrial Electonics, Vol. 50 No. 6, Page(s): 1165 – 1171, Dec. 2003.

[18] H. Du and S. S. Nair. "Modeling and Compensation of Low-Velocity Friction with Bounds." IEEE Transactions on Control System Technology, Vol. 7, No. 1, Page(s): 110 – 121, Jan 1999.

[19] R. Dhaouadi. "A Nonlinear Observer for Friction Estimation and Compensation in Harmonic Drives." The Fifth International Conference on Power Electronics and Drive Systems, 2003. Vol. 1, Page(s):259 - 263, 17-20 Nov. 2003.

[20] J. Swevers, F. Al-Bender, C. G. Ganseman and T. Prajogo. "An Integrated Friction Model Structure with Improved Presliding Behavior for Accurate Friction Compensation." IEEE Transactions on Automatic Control, Vol. 45, No. 4, 675 – 686, Apr. 2000.

[21] Anthony Tzes, Pei-Yuan Peng and John Guthy. "Genetic-Based Fuzzy Clustering for DC-Motor Friction Identification and Compensation." IEEE Transaction on Control Systems Technology, Vol 6, No. 4, Page(s): 462-472, Jul. 1998.

[22] J. T. Teeter, M. Y. Chow and J. J. Jr. Brickley. "A novel fuzzy friction compensation approach to improve the performance of a DC motor control

system." IEEE Transactions on Industrial Electronics, Volume 43, Issue 1, Page(s):113 – 120, Feb. 1996.

[23] Y. Wang, X. Huang, L. Zhao and T. Chai. "Friction compensating modeling and control based on adaptive fuzzy system." Control, Automation, Robotics and Vision Conference, Page(s):2041 - 2045 Vol. 3, 2004.

[24] S. Jee and Y. Koren. "A self-organizing fuzzy logic control for friction compensation in feed drives." American Control Conference, Page(s):205 - 209 vol. 1, 1995.

[25] K. Y. Byung and W. C. Ham. "Adaptive Control of Robot Manipulator Using Fuzzy Compensator." IEEE Transactions on Fuzzy System, Vol. 8, NO. 2, Page(s): 186-199, Apr. 2000.

[26] L. Zadeh, "Fuzzy Sets." Information and Control, Vol. 8 pp. 338-353, 1965.

[27] H. T. Nguyen, N. R. Prasad, C. L. Walker and E. A. Walker. "A first course in Fuzzy and Neural control." CRC Press, 2002.

[28] J. M. Mendel. "Fuzzy logic systems for engineering: a tutorial." Proceedings of the IEEE Volume 83, Issue 3, Page(s):345 – 377, Mar. 1995.

[29] Kosko, "Fuzzy systems as universal approximators," IEEE Trans. Comput., vol. 43, pp. 1329–1333, Nov. 1994.

[30] M. Landajo, M. J. Río, and R. Pérez. "A Note on Smooth Approximation Capabilities of Fuzzy Systems," IEEE Transactions on Fuzzy System, Vol. 9, No. 2, pp. 229-237, Apr. 2001.

[31] K. M. Passino. "Biomimicry for optimization, control, and automation." London; New York : Springer, 2005.

[32] L. D. Berkovitz. "Convexity and optimization in R^n." John Wiley & Sons, Inc., New York, 2002.

[33] C. T. Kelley. "Iterative Methods for Optimization." SIAM, 1999.

[34] T. Back, U. Hammel and H. P. Schwefel. "Evolutionary computation: comments on the history and current state." IEEE Transactions on Evolutionary Computation Volume 1, Issue 1, Page(s):3 - 17, Apr. 1997.

[35] N. K. Bambha, S. S. Bhattacharyya, J. Teich and E. Zitzler. "Systematic Integration of Parameterized Local Search into Evolutionary Algorithms." IEEE Transactions on Evolutionary Computation, Vol. 8, No. 2, Page(s): 137 – 155, Apr. 2004.

[36] E. Zitzler, J. Teich and S. S. Bhattacharyya. "Optimizing the Efficiency of Parameterized Local Search within Global Search." Congress on Evolutionary Computation, Vol. 1, Page(s):365 – 372, Jul. 2000.

[37] G. Folino, C. Pizzuti and G. Spezzano. "Parallel Hybrid Method for SAT That Couples Genetic Algorithms and Local Search." IEEE Transactions on Evolutionary Computation, Vol. 5, No. 4, Page(s): 323 -334, Aug. 2001.

[38] P. N. Suganthan, N. Hansen, J. J. Liang, K. Deb, Y. -P. Chen, A. Auger and S. Tiwari. "Problem Definitions and Evaluation Criteria for the CEC 2005 Special Session on Real-Parameter Optimization."

[39] J. J. Liang, T. P. Runarsson, E. Mezura-Montes, M. Clerc, P. N. Suganthan, Carlos A. C. Cello and K. Deb. "Problem Definitions and Evaluation Criteria for the CEC 2006 Special Session on Real-Parameter Optimization."

[40] A. Auger and N. Hansen. "Performance Evaluation of an Advanced Local Search Evolutionary Algorithm." Proceedings of the IEEE Congress on Evolutionary Computation, CEC 2005.

[41] D. Del Vecchio and R. M. Murray. "Observability and Local Observer Construction for Unknown Parameters in Linearly and Nonlinearly Parameterized Systems." Proceeding of the American Control Conference, Page(s): 4748 – 4752, 2003.

[42] J. Hurtig and S. Yurkovich. "Parameter Set Estimation for Nonlinear System." Proceedings of the 33rd Southeastern Symposium on System Theory, Page(s):275 – 280, Mar. 2001.

[43] P. Coirault. J. C. Trigeassou, D. Kerignard and J. P. Gaubert. "Recursive Parameter Identification of an Induction Machine Using a Non Linear Programming Method." IEEE Proceeding of International Conference on Control Applications. Page(s): 644 – 649, Sep. 15-18, 1996.

[44] C. Bohn and H. Unbehauen. "Sensitivity Models for Nonlinear Filters with Application to Recursive Parameter Estimation for Nonlinear State-Space Methods." IEE Proceeding of Control Theory Application, Vol. 148, No. 2, Page(s): 137 – 145, 2001.

[45] D. V. Arnold. "An Analysis of Evolutionary Gradient Search." IEEE Congress on Evolutionary Computation, pp. 47-54, 2004.

[46] R. Salomon. "Evolutionary Algorithms and Gradient Search: Similarities and Differences." IEEE Transaction on Evolutionary Computation, Vol. 2, No. 2, Page(s): 45 – 55, Jul. 1998.

[47] G. D. Magoulas, V. P. Plagianakos and M. N. Vrahatis. "Hybrid Methods Using Evolutionary Algorithms for On-line Training." Proc. IEEE Int. Joint Conf. Neural Networks, Washington, DC, pp. 2218--2223, 2001.

[48] H. K. Birru, K. Chellapilla and S. S. Rao. "Local Search Operator in Fast Evolutionary Programming." IEEE Congress on Evolutionary Computation, Vol. 2 6-9, Page(s): 1506 – 1513, 1999.

[49] J. M. Leski. "TSK-Fuzzy Modeling Based on ε-Insensitive Learning." IEEE Transaction on Fuzzy Systems, Vol. 13, No. 2, Page(s): 181 – 193, 2005.

[50] P. C. Panchariya, A. K. Palit D. Popovic and A. L. Sharma. "Nonlinear System Identification using Takagi-Sugeno Type Neuro-Fuzzy Model." IEEE Second International Conference on Intelligent Systems, Page(s): 76 – 81, Jun. 2004.

[51] P. Bortolet. and R. Palm. "Identification, Modeling and Control by Means of Takagi-Sugeno Fuzzy Systems." Proceedings of the Sixth IEEE International Conference on Fuzzy Systems, Vol 1, Page(s):515 – 520, 1997.

[52] J. R. Raol, G. Girija and J. Singh. "Modeling and Parameter Estimation of Dynamic Systems." The Institution of Electrical Engineers, London, 2004.

[53] A. Gelb. "Applied Optimal Estimation." The MIT Press, 1974.

[54] S. Boyd, L. El Ghaoui, E. Feron and V. Balakrishnan. "Linear Matrix Inequalities in Systems and Control Theory." SIAM Studies in Applied Mathematics, Vol. 15, SIAM, Philadelphia, 1994.

[55] I. E. K¨ose, F. Jabbari and W. E. Schmitendorf. "A Direct Characterization of L2-Gain Controllers for LPV Systems." IEEE Transactions on Automatic Control, Vol. 43, No. 9, Sep. 1998.

[56] P. Gahinet and P. Apkarian. "A linear matrix inequality approach to H_2 control." Int. J. Robust and Nonlinear Control, 4421-448, 1994.

[57] P. Apkarian, P. Gahinet and G. Beck. "Self-scheduled H_∞ control of linear parameter varying systems: a design example." automatica, 31, (9), pp. 1251–1261, 1995.

[58] P. Apkarian, and H. D. Tuan. "Parameterized LMIs in control theory." SIAM J. Control Optim. 38, (4), pp. 1241–1264, 2000,.

[59] M. Ait-Rami and L. El Ghaoui "Solving non-standard Riccati equations using LMI optimization." Proceedings of the 34th IEEE Conference on Decision and Control, Vol 4, 13-15, Page(s):3855 – 3856, Dec. 1995.

[60] M.V. Kothare, V. Balakrishnan and M. Morari, "Robust Constrained Model Predictive Control using Linear Matrix Inequalities." Automarica, Vol.32, No. IO, pp. 1361- 1379, 1996.

[61] N. Wada, K. Saito and M. Saeki. "Model predictive control for linear parameter varying systems using parameter dependent Lyapunov function." The 2004 47th Midwest Symposium on Circuits and Systems, Vol. 3, Page(s):111 – 133, 2004.

[62] G. Scorletti and V. Fromion "A new LMI approach to performance control of linear parameter-varying systems." American Control Conference, 1998. Vol. 1, 24-26, Page(s):542 – 546, Jun. 1998.

[63] R. R. Coulibaly. "A Matrix Inequalities Approach to H_∞ Control In A Behavioral Framework." PhD Dissertation. UMI 2003.

[64] I. Tetsuya. "A unified matrix inequality approach to linear control design." PhD Dissertation. UMI 1993.

[65] K. Tanaka and H. O. Wang, "Fuzzy Control Systems Design and Analysis." New York: Wiley, 2001.

[66] M. C. M. Teixeira, E. Assuncao and R. G. Avellar. "On relaxed LMI-Based design for fuzzy controllers." IEEE International Fuzzy Systems Conference, Page(s): 704-707, 2001.

[67] T. Takagi and M. Sugeno. "Fuzzy Identification of Systems and Its Applications to Modeling and Control." IEEE Transactions on System, Man, and Cybernetics, 15(1): 116-132, 1985.

[68] H. Wu. "Reliable LQ Fuzzy Control for Nonlinear Discrete-Time Systems via LMIs." IEEE Transactions on System, Man, and Cybernetics —Part B: Cybernetics, Vol. 34, No. 2, Apr. 2004.

[69] H. D. Tuan, P. Apkarian, T. Narikiyo and Y. Yamamoto, "Parameterized linear matrix inequality techniques in fuzzy control systems design." IEEE Trans. Fuzzy Syst., vol. 9, no. 2, pp. 324–332, Apr. 2001.

[70] M. C. M. Teixeira, E. Assuncao, and R. G. Avellar. "On relaxed LMI-based designs for fuzzy regulators and fuzzy observers." IEEE Transactions on Fuzzy Systems, Vol 11, Issue 5, Page(s):613 – 623, Oct. 2003.

[71] B. Castillo-Toledo and J. A. Meda-Campana. "The Fuzzy Discrete-Time Robust Regulation Problem: An LMI Approach." IEEE Transactions on Fuzzy Systems, Vol 12, No. 3, Page(s): 360-367, Jun 2004.

[72] E. Kim and D. Kim. "Stability Analysis and Synthesis for an Affine Fuzzy System via LMI and ILMI: Discrete Case." IEEE Transactions on System, Man, and Cybernetics –Part B: Cybernetics, Vol. 31, No.1, Page(s): 132-140, Feb. 2001.

[73] M. Margaliot and G. Langholz. "New Approaches to Fuzzy Modeling and Control: Design and Analysis." World Scientific, 2000.

[74] A. Graham. "Matrix theory and applications for engineers and mathematicians." Ellis Horwood Ltd., 1979.

[75] X. Zhan. "Matrix inequalities." Springer, 2002.

[76] R. A. Horn and C. R. Johnson. "Matrix Analysis." Cambridge, U.K.: Cambridge Univ. Press, 1985.

[77] R. C. Dorf and R. H. Bishop. "Modern control system." Prentice Hall, 2005.

[78] J. P. Hauschild, G. Heppler and J. McPhee, *Friction Compensation of Harmonic Drive Actuators*, 6th International Conference on Dynamics and Control of Systems and Structures in Space, pp.683-692, Jul. 2004.

[79] http://www.hdsi.net/downloads/pdf/CSF_CSG_052605.pdf.

[80] http://www.catalognavigator.com/hdsystems/cfm/index.cfm?page=3&vid=1&ProductID=1558&catid=7&companyid=182377.

[81] http://www.waltmusser.org/

[82] http://www.harmonicdrive.net

[83] http://www.hdsi.net/

[84] H. K. Khalil. "Nonlinear System." Prentice –Hall Inc. 2002.

[85] Z.Y. ZHAO, W.F. XIE and A. B. RAD. "A Cascaded Fuzzy Model of Friction over Large Temperature Variation", NAFIPS 2006, Montreal, June 3-6, 2006.

Appendix A: Specification of the Harmonic Drive

Specifications	
Rated Output Power (W)	62
Rated Torque (Nm)	9.8
Rated Output Speed (rpm)	60
Reduction Ratio (R:1)	50
Size	17
Output Configuration	Shaft
Maximum Output Speed (rpm)	80
Encoder Resolution (ppr)	1000
Encoder Output Circuit Type	Line Driver 5V
Tach-Generator Option	Yes
Tach-Generator Output (V/ 1000 rpm)	7 +/- 10%
Special Options	No Special Options
Rated Current (A)	1.7
Max. Cont. Stall Torque (Nm)	11
Maximum Output Torque (Nm)	34
Maximum Current (A)	4.3
Rated Voltage (V)	75
Torque Constant (Nm/A)	9.6
BEMF (V/rpm)	1.0
Motor Resistance (Ohms)	4.8
Motor Inductance (mH)	2.3
Electrical Time Constant (ms)	0.5

Mechanical Time Constant (ms)	4.7
Power Rate (kW/sec)	1.1
Moment of Inertia at Output (kgm^2)	0.089
Thermal Resistance (deg C/W)	1.2
Thermal Time Constant (min)	16
Actuator Accuracy (arc-min)	1.5
Actuator Repeatability (arc-sec)	+/-5
Insulation Class	F
Insulation Resistance	100 MOhms at 500 VDC
Insulation Voltage	1000 VAC (1 min)
Lubrication Type	Grease (SK-2)
Minimum Ambient Operating Temperature (C)	-10
Maximum Ambient Operating Temperature (C)	40
Minimum Ambient Storage Temperature (C)	-20
Maximum Ambient Storage Temperature (C)	60
Minimum Ambient Operating Humidity (%)	20
Maximum Ambient Operating Humidity (%)	80
Vibration	5 - 400 Hz, max. 2.5 G
Shock Resistance	30g, 11ms
Torque-Speed Gradient (in-lb/rpm)	18
Torque-Speed Gradient (Nm/rpm)	2.1
Viscous Damping Constant (in-lb/rpm)	0.48
Viscous Damping Constant (Nm/rpm)	0.054

Maximum Radial Load (N)	784
Maximum Radial Load (lb)	176
Maximum Axial Load (N)	784
Maximum Axial Load (lb)	176

Appendix B: Optimization – Gradient Search and EA

The optimization problem discussed in this thesis has the following form of searching X^* that:

$$X^* = \arg\min f(X)$$

where $f(X): R^n \to R$: is a real-valued function of vector $X \in R^n$.

B.1 Gradient Based Search

Optimization methods based on gradient information include methods such as Gradient Descent, Newton, Conjugate and many others. These methods differ in the way how the gradient and gradient related information are used in the calculation of the searching direction and step size. In our research, we choose the Gradient Descent method over others because of its simplicity so that we can focus on the interaction between local search (gradient) and global search (EA) instead of the gradient methods themselves.

Simply, the Gradient Descent methods for the optimization problem above can be described as:

With an initial X^0, iteratively at current step of k, the update of X^k can be calculated as:

$$X^{k+1} = X^k - \eta \nabla f(X^k)$$

This update $k \to \infty$ will lead to the local minimum X^* of $f(X)$ that $\nabla f(X^*) = 0$.

Where, η is the step size of update; $\nabla f(X^k)$ is the gradient vector of $f(X)$ over X at current step k.

$$\nabla f(X^k) = \frac{\partial f(X^k)}{\partial X^k}$$

The end condition of the iterative process is normally taken as non-improvement of the function value of $f(X)$ or the (near) zero value of $\nabla f(X^k)$.

B.2 Evolutionary Algorithms

Evolutionary algorithms mimic the process of natural evolution, the driving process for the emergence of complex and well-adapted organic structures. Depending on the methods of encoding, mating and reproducing, EA can be further subcategorized into Genetic Algorithm, Evolutionary Programming and Evolutionary Strategy[31]. Nevertheless, the same concept is "Survival of the fittest" which means the candidates (parameter values in the domain of optimization) with better fitness (value of the cost function to be optimized) have better chance to be chosen in the reproduction.

The basic concepts used in our algorithms of Evolutionary Algorithms include Selection, Clone, Crossover and Mutation.

1. Selection: Evolutionary Algorithms is a parallel optimization process where a large number or populations of search are carried out simultaneously. In each iterative step, those search or individuals in the term of EA will be justified by the fitness values (value of the cost function) and only the ones with better results will be allowed in the next generation (step) of the search, either directly or through some kind of reproducing. Therefore, at each generation, the fitness value of all searches must be evaluated and sorted to make the best through. This is the process of selection.

2. Clone: There are ways of how the selected individuals represent themselves and pass on their information in the search process of next generation. One of them is Clone. In clone, all the information contained in the current search will be simply passed to the next generation as the start point of further searching.
3. Crossover: Another way of passing information to the next generation is mating. In mating, different individuals exchange their information through the technique of Crossover to generate their offspring. These offspring will be the start points of the further searching.
4. Mutation: In the process of optimization, the individuals may contain similar information so that the further searching is stuck in the local minimum (Premature in terms of EA). The introducing of Mutation keeps the individuals different from each other by randomly changing parts of the information in some individuals when necessary.

Appendix C: Linear Matrix Inequalities (LMI)

A standard linear matrix inequality has the form [31], to find x to satisfy:

$$F(x) = F_0 + \sum_{i=1}^{m} x_i F_i > 0, \tag{0-1}$$

where $x \in R^m$ is the variable to be solved and the symmetric matrixes $F_i = F_i^T \in R^{nxn}$, $i = 0,...,m$, are given function of x in matrix form. The inequality symbol in the above equation means that $F(x)$ is positive definite, i.e., $u^T F(x)u > 0$ for all nonzero $u \in R^n$. The problem of negative definite, $F(x) < 0$, can be transformed to standard LMI in $-F(x) > 0$.

Multiple LMIs, where $F_1(x) > 0,..., F_n > 0$, can be expressed as a single diagonal LMI,

$$F(x) = \begin{vmatrix} F_1(x) & & & & \\ & F_2(x) & & & \\ & & \bullet & & \\ & & & \bullet & \\ & & & & \bullet \\ & & & & F_n(x) \end{vmatrix} > 0 \tag{0-2}$$

where, the blanks in the matrix are all filled with zero or zero matrices.

In the domain of control engineering, the variables of LMI are often taken as matrix form in which a variable of matrix P normally means all elements of P are variables.

Besides the linear combination of variables stated in the LMI problem above, another problem often encountered in control is the convex quadratic inequality as following:

$$R(x) > 0,$$

$$Q(x) - S(x)^T R^{-1}(x) S(x) > 0 \qquad \text{(0-3)}$$

where, $Q(x) = Q(x)^T$, $R(x) = R(x)^T$ and $S(x)$ are of the form of (0-1) and depend affinely on x.

The convex quadratic inequality can be converted to LMI using **Schur Complements** which states the following two expression of matrix inequality are equivalent:

1. The polynomial form:

$$R(x) > 0,$$

$$Q(x) - S(x)^T R^{-1}(x) S(x) > 0 \ ; \qquad \text{(0-4)}$$

2. The matrix form:

$$R(x) > 0,$$

$$\begin{vmatrix} Q(x) & S(x)^T \\ S(x) & R(x) \end{vmatrix} > 0. \qquad \text{(0-5)}$$

Therefore, the nonlinear matrix polynomial in (0-4) can be converted to the standard LMI in form (0-5).

The LMI based optimization extends the problem of solving LMI to an optimization criterion with LMI constraint, normally in the following form:

Minimize $c^T x$

Subject to $F(x) > 0$, $\qquad \text{(0-6)}$

where, x are variables to be solved and $F(x) > 0$ is the linear constraints on x as we described in (0-1).

The basic LMI problem in control engineering is the Lyapunov Inequalities in the following forms:

$$P > 0$$

$$A^T P + PA < 0 \tag{0-7}$$

for continuous time domain; and,

$$P > 0$$

$$A^T PA - P < 0 \tag{0-8}$$

for discrete time domain,

where, P is the matrix to be solved; A is the system matrix for linear system.

The existence of matrix P will guarantee the stability of the linear system since the quadratic Lyapunov function can be built as:

for continuous system with nonzero states:

$$V(t) = x(t)^T P x(t) > 0$$

$$\dot{V}(t) = (Ax(t))^T P x(t) + x(t)^T P (Ax(t)) = x(t)^T (A^T P + PA) x(t) < 0; \tag{0-9}$$

for discrete system with nonzero states:

$$V(k) = x(k)^T P x(k) > 0$$

$$\begin{aligned} & V(k+1) - V(k) \\ & = x(k+1)^T P x(k+1) - x(k)^T P x(k) \\ & = (Ax(k))^T P (Ax(k)) - x(k)^T P x(k) \\ & = x(k)^T (A^T P A - P) x(k) < 0 \end{aligned} \tag{0-10}$$

Different optimization criterion can be applied to meet different performance requirements.